2019-01-01

Energy Management And Control Of Smart Power Distribution Systems

Eric Galvan
University of Texas at El Paso

ENERGY MANAGEMENT AND CONTROL OF SMART POWER DISTRIBUTION SYSTEMS

ERIC GALVAN

Doctoral Program in Electrical and Computer Engineering

APPROVED:

Paras Mandal, Ph.D., Chair

Miguel Velez-Reyes, Ph.D.

Yuanrui Sang, Ph.D.

Tzu-Liang (Bill) Tseng, Ph.D.

Stephen L. Crites, Jr., Ph.D.
Dean of the Graduate School

Dedication

I would like to dedicate this work to my beloved parents Fernando and Leticia, my brother Fernando, my fiancé Maribel, my cousin Salvador and his family, and my aunt Lucila – for all your love and support during this journey.

ENERGY MANAGEMENT AND CONTROL OF SMART POWER DISTRIBUTION SYSTEMS

by

ERIC GALVAN, M.S. in E.E.

DISSERTATION

Presented to the Faculty of the Graduate School of

The University of Texas at El Paso

in Partial Fulfillment

of the Requirements

for the Degree of

DOCTOR OF PHILOSOPHY

Department of Electrical and Computer Engineering

THE UNIVERSITY OF TEXAS AT EL PASO

December 2019

Acknowledgements

First, I thank God for providing endless blessings, health, knowledge, strength, and perseverance to complete my doctoral research and this dissertation. I would like to express my sincere gratitude to my Ph.D. advisor, Dr. Paras Mandal, who provided an excellent and a constructive guidance and mentorship throughout my dissertation period by allowing me to enhance my knowledge in electric power and energy systems, primarily, distribution system/smart grid, renewable energy integration, and energy management and control. I also thank Dr. Mandal for providing me an excellent working environment at the Power and Renewable Energy Systems (PRES) Lab and for encouraging me to attend conferences, publish my research findings in journals, and helping me to become an independent researcher. I am very grateful to Dr. Miguel Velez-Reyes for his continuous advice, encouragement, and support not only as my dissertation committee member but also as the department chair of Electrical and Computer Engineering (ECE). Thank you for all the support with teaching assistantships and fellowships that allowed me to concentrate on my doctoral studies and research. I am also thankful to Dr. Yuanrui Sang and Dr. Bill Tseng for serving as dissertation committee members and providing valuable comments and feedback to improve the quality of the dissertation.

I am very grateful for the love and support of my parents Fernando and Leticia, your example and guidance to never shy away from hard work throughout my life have made me the person I am and has led me to accomplish all the goals I have set upon myself. My brother Fernando, for always being there when I needed advice and words of encouragement, especially in the tough moments. My fiancé Maribel who has stood by me through all my absences, thank you for your patience and unmatched love. To my cousin Sal, Ruth, Paco, and aunt Lucila, no

words are enough to thank you for the love and support I have received from you. I am truly grateful for all your help and especially for making me part of your home.

I also want to recognize Priscilla and the ECE department office personnel for the countless times I received help from them throughout my doctoral studies. To all the ECE department faculty members that I had the opportunity to work with as a teaching assistant, I also thank you for your words of encouragement. To all my friends who supported me during my doctoral studies at UTEP – thank you. Finally, I would like to thank all the members of the PRES Lab. for your valuable support as well as unforgettable friendship.

Abstract

With the development of distributed energy resources (DERs) and advancements in technology, microgrids (MGs) appear primed to become an even more integral part of the future distribution grid. In this transition to the smart power grid of the future, MGs must be properly managed and controlled to allow efficient integration of DERs. Over the past years, there has been rapid adoption of roof-top solar photovoltaic (PV) and battery electric vehicles (BEVs). Although roof-top solar PV and BEVs can provide environmental benefits (e.g., reduction of emissions), they also create various challenges for power system operators. For example, roof-top solar PV generation can create larger valleys in the demand before peak periods leading to high demand ramp rates. Furthermore, BEVs can draw large amounts of power when charging, leading to high demand spikes that may further increase the demand during peak time. As DERs become more prominent at the distribution level, actions must be taken to maximize their benefits and minimize any adverse effects they might impose on the distribution grid. The work described in this dissertation proposes a microgrid energy management system (MGEMS) based on a hybrid control algorithm that combines Transactive Control (TC) and Model Predictive Control (MPC) for efficient management and integration of DERs in prosumer-centric networked MGs. The proposed transactive MGEMS determines a charge schedule for the battery electric vehicle (BEV) and a charge-discharge schedule for the roof-top solar photovoltaic (PV) and a battery energy storage system (BESS). By managing the charge of the BEV and the power output of roof-top solar PV through the use of a BESS, the utility or system operator can prevent overloading of their infrastructure, and residential customers can reduce their costs and improve their overall savings. The proposed networked MGEMS strategy is evaluated under different BEV and solar PV-BESS penetration scenarios to study the potential impacts (e.g., voltage violations, overloading

transformers and feeders) that large amounts of BEVs and solar PV-BESS systems can have on the distribution systems and how different pricing mechanisms can mitigate these impacts. This dissertation also contributes to examining the impact of DERs on the resiliency of the power distribution system to natural disasters. Test results demonstrate that the proposed microgrid energy management and control strategy shows potential to reduce peak load and power losses as well as to enhance customers' savings. Moreover, the results also indicate that, when managed effectively, distributed energy resources can enhance the resiliency of the distribution grid.

The major contributions of this dissertation are the following. Chapter 3 contributes to the development of (i) an efficient strategy to optimally incorporate and locate renewable energy sources in smart distribution networks to reduce overall power losses, peak load, and GHG emissions; (ii) an integrated energy management system that allows the resolution of unit commitment and economic dispatch problems using forecasted and actual data of wind, solar PV, and demand; (iii) an efficient BESS strategy that utilizes the forecasted data of wind power output to determine the optimal charge/discharge cycle of the BESS. Chapter 4 contributes to (iv) the development of a new hybrid TC-MPC mechanism to manage BEVs, solar PV, and BESS of networked MGs; (v) the development of transactive incentive and feedback signals based on distribution locational marginal price; (vi) provide detailed analysis of the impacts on the distribution grid due to an effective use of transactive controls for DERs management, i.e., bus voltage and power loss impacts; (vii) provide detailed cost/savings analysis for consumers/prosumers under different pricing rates when they are equipped with BEVs, roof-top solar, and BESS. Finally, Chapter 5 contributes to the development of (viii) detailed resiliency analysis of realistic case studies that show the potential benefits that DERs managed in networked MGs can provide a power distribution grid; and (ix) calculation of resilience metrics for electrical

service and monetary impacts using DERs, i.e., total customer-hours of outage, total customer energy not served, total and average number of customers experiencing outage, total loss of utility revenue, and total outage costs.

Table of Contents

List of Tables

List of Figures

Nomenclature

a_i, b_i, d_i	Coefficients of the production cost function
C_T	Total production costs
η_j	Round-trip efficiency of ESS *j*
$ESS_{j,t}^{SOC}$	State of charge of ESS *j* at time *t*
$ESS_{j,\max}^{SOC}$	Maximum capacity of ESS *j* in Wh
$ESS_{j,\min}^{SOC}$	Minimum capacity of ESS *j* in Wh
$F_{c,i}$	Production cost function of unit i
$I_{i,t}$	Commitment state of unit i at time t
Nc	Total number of bus combinations
$NESS$	Total number of energy storage systems
Ng	Total number of generating units
Nb	Total number of buses
NPV	Total number of PV aggregates
NW	Total number of wind turbines
$P_{D,t}$	Load demand at time t
$PESS_{i,t}$	Active power of ESS i at time t
$PESS_{j,t}$	Active power output of ESS *j* at time t
$PESS_{j,t}^{ch}$	Charging power of ESS *j* at time *t*
$PESS_{j,t}^{dch}$	Discharging power of ESS *j* at time *t*
$PESS_{j,\max}^{ch}$	Maximum charging limit of ESS *j*
$PESS_{j,\max}^{dch}$	Maximum discharging limit of ESS *j*
$P_{i,t}$	Active power generation of unit i at time t
P_i^{Max}	Maximum active power generation of unit i
P_i^{Min}	Minimum active power generation of unit i
$P_{L,t}$	Active power losses
$PR_{l,t}$	Active power output of RES *l*
$PS_{i,t}$	Active power generation of PV i at time t
$PW_{i,t}$	Active power generation of wind turbine i at time t
RD_i	Ramp-down rate limit of unit i
$R_{i,t}$	Reserve of unit *i* at time *t*
$R_{Si,t}$	Spinning reserve of unit i at time t
$R_{S,t}$	System spinning reserve at time t
$R_{Oi,t}$	Operating reserve of unit i at time t
$R_{O,t}$	System operating reserve at time t
RU_i	Ramp-up rate limit of unit i

$SD_{i,t}$	Shutdown cost of unit i at time t
$SU_{i,t}$	Startup cost of unit i at time t
T	Total number of time periods
T_i^{off}	Minimum up time of unit i
T_i^{on}	Minimum down time of unit i
$u_{j,t}$	ESS j discharging mode decision variable
$u_{j,t}^{c}$	ESS j charging mode decision variable
V_k	Voltage magnitude at bus k
V_k^{Max}	Maximum voltage magnitudes at bus k
V_k^{Min}	Minimum voltage magnitudes at bus k
W_l	Maximum power ramp-down decrement of PR_l
$x_{i(t-1)}^{off}$	OFF time of unit i at time t
$x_{i(t-1)}^{on}$	ON time of unit i at time t
Z_l	Maximum power ramp-up increment of PR_l

Chapter 1: Introduction

1.1 Background and Research Motivation

The increase in demand-side distributed energy resources (DERs), e.g., rooftop solar photovoltaic systems (PV), battery energy storage systems (BESS), and battery electric vehicles (BEVs) make the operation of the distribution grid extremely challenging and highly inefficient under the traditional approach. Hence, new operation and control strategies are required to meet the growing challenges associated with the adoption of DERs that may compromise the efficiency and reliability of the system. Within this context, microgrid (MG) concept can enable a more efficient and reliable operation of the electrical distribution system, this concept considers local generation sources and demand as a smaller system (sub-system) of the main grid [1-3]. An MG, equipped with advanced automation and communication systems, can autonomously manage and power sections of the electrical distribution grid that can range from a building to several buildings or full neighborhoods. A system containing two or more MG should be considered as a multi-MG system. The MG enables local control of the DERs thus, the need for vertical central control is reduced. However, coordination in a multi-MG system is no easy task, without proper coordination, MG energy balancing and connectivity within the distribution system can be compromised causing power quality and stability issues [4]. As a relatively new concept, multi-MG research is important, and as new technology is integrated into the power system, further study is required to meet these new developments. With the increase in DERs, MGs, and continuous transactions or negotiated exchange among the market participants requires the introduction of new electricity market schemes. Transactive energy (TE) is a new approach that combines the use of electricity markets with various control technologies to achieve an optimal and economic operation of the electric power system. combining the use of economic systems such as markets

and the use of control systems technology. TE is defined as "A set of economic and control mechanisms that allows the dynamic balance of supply and demand across the entire electrical infrastructure using value as a key operational parameter" [5].

- The main value drivers for deployment of TE systems are the following:
- Reduce consumer energy cost; increase prosumer energy revenue;
- Enable participation of demand-side capabilities to enhance power system reliability and reduce power system operation costs at the distribution and bulk power system levels respectively;
- Transition energy production and consumption to become more environmentally friendly;
- Provide investment opportunities for clean energy technologies.

The aforementioned points should be achieved within the consumer/prosumer comfort range and with minimal imposition on power system operators (minimal or no additional manual intervention) [6]. TE system utilizes two major transactive signals, i.e., transactive incentive signal (TIS) and transactive feedback signal (TFS). These signals are produced by the distribution system operator (DSO) and are sent through the smart grid infrastructure back and forth between utilities, grid operators, and individual assets, that help communicate the real-time flow and cost of power. These signals propagate through an information network, which is the transactive control (TC) system embedded in the electrical network. A TC structure that combines both the dynamic market transactions at the higher level within a region and unit-level control at the lower levels is becoming more and more important as new time-scales with uncertainties become more prominent [7]. Also, more regular and constant information exchange is required to mitigate costs imposed due to intermittency and uncertainty of the DERs [8]. The TIS represents the actual delivered cost of electric energy ($/kWh) and the TFS the net electric load (kW) at a specific system location known as a transactive node (TN). Both signals include the current value and a forecast of future

values, as forward-looking signals. TCs can be located in different areas of the distribution system, e.g., in an MG. The TN can represent load points, e.g., distribution substation, distribution transformer, prosumer, consumer, and others. TIS and TFS can be communicated to TNs located in the same MG and among other MGs for energy balancing utilizing a transactive coordination system (TCS) [9].

Figure 1.1 illustrates the application of TCs, which is a single, integrated, smart grid incentive signaling approach that combines multiple objectives and constraints (economic and operational) using uniform TIS and TFS. In Figure 1.1, the role of the TC is to respond to system conditions represented by incoming TIS and TFS. Also, in Figure 1.1, each load point (e.g., MG-1 under TC) represents a TN.

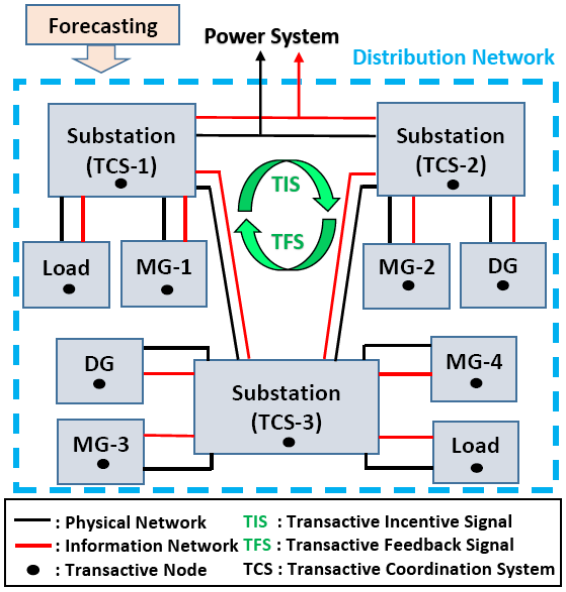

Figure 1.1: Role of transactive energy signals in a multi-MG electrical distribution system.

It has been reported in the Pacific Northwest Smart Grid Demonstration Project (PNWSGD) [10], that in order to better take advantage of transactive system benefits, further work is needed in the following areas:

- Improved load models and forecasting techniques;
- Different methods to monetize system objectives to produce the transactive incentive signals;

- Development of libraries of system models that accurately represent system assets to be used by the transactive algorithms;
- Research that identifies business models and policies that can be utilized by utilities and their customers to enable customer engagement through the use of transactive systems;
- Research on policies that enable the use of a dynamic cost or price signal that incentivizes customer participation;
- Analysis and testing of transactive control systems to verify their stability and convergence.

These findings suggest that TE is an area of great research opportunities to improve smart grid operations.

1.2 PROBLEM STATEMENT AND RATIONALE FOR THE STUDY

Over the past years, technological developments have driven an increase in DERs across the distribution network, particularly at the demand side. DERs are changing the electrical landscape from a conventional demand-driven power grid to a transactive supply following energy system where customers (as electricity consumers and/or producers) are actively engaged in transactions and participating in the operation and management of the power grid [5,11,12]. Although the overall installed capacity of DERs is still significantly low, projections indicate a ramp-up in the coming years. According to the U.S. Energy Information Administration (EIA), solar PV generation at the distribution level (Utility-scale and small-scale) has grown 232% over the past five years (2014-2018) going from a total net generation of 28,925 MWh in 2014 to 96,147 MWh in 2018 [13]. Moreover, the EIA in its 2019 annual energy outlook projects electricity generation from solar PV will reach 15% of total U.S. electricity generation by 2050 [14].

On another front, transportation has also been experiencing important changes around the world. According to the international energy agency (IEA), in 2017 a new milestone was reached

with more than 3 million BEVs on the road worldwide [15]. Furthermore, the same report projects the worldwide BEVs fleet to reach 13 million and 130 million by 2020 and 2030, respectively. Thus, it can be seen that in the next few years, the increase in BEVs and solar PV generation will cause various integration challenges on the electric grid. The current power grid was not designed to host the increase of load caused by BEV charging and power flow fluctuations caused by solar PV generation, especially low voltage distribution networks.

The growing attention for DER, BESS, EVs, and a transactive grid reflects the increase in awareness that the conventional operation and control of the electric system has become outdated and is no longer suitable for the modern, digitized information-driven economy [16]. Several assumptions that have been the drivers for operation and regulation of the electric industry are now outdated, e.g., consumer demand is largely inelastic, centralized power generation and control are the best; reliance on DER will result in higher electricity costs. Another important issue is the gap in price signals between customer-side resources with system costs and benefits. Also, in part due to the centralized approach customer-side generation adds more complexity to the operation and control of the conventional system [16]. Whereas, under the decentralized approach, control decisions are made locally [17].

Although decentralized control of the power system has been studied in the literature, there is still a considerable void in the research of power system control and operations under TE framework. Specifically, at the distribution level where a high penetration of DERs is occurring, a TE approach could ensure an efficient integration to enhance the operation of the power distribution system. Thus, a new transactive-model predictive control approach based on TE framework is introduced to improve the efficiency, reliability, and resilience of power distribution systems.

Furthermore, research is required to design and construct transactive signals as they can result in proper decision-making tools for transactive market participants (e.g., DSO and MGs). Very limited literature is available apart from the work done by the Pacific Northwest National Laboratory (PNNL) in the PNWSGD explaining how to model transactive signals. The PNWSGD

determined TIS and TFS as the total cost per total energy resources and sum of all predicted elastic and inelastic loads, respectively [9]. Where the TFS was calculated at the interface between utility-side nodes and the transmission zone nodes that supply the energy. The transactive signals reported in [9] were developed to allow energy balancing between TNs that shared a TCS in which the energy management system had the transactive controls embedded for local control and decision making.

Hence, the development of a TC based MG energy management system (MGEMS) constituted by DERs and using transactive signals will enable a more effective and efficient operation of the distribution system. As dynamic demand-side management could improve power quality, system cost minimization, generation-load balancing, and load-shaping support for the grid.

1.3 DISSERTATION OBJECTIVES

The main objective of this dissertation is to derive an efficient energy management and control strategy for the economical and resilient operation of the smart power distribution systems that are heavily constituted by DERs. This dissertation also investigates and studies different mechanisms that enable customers owning DERs to become more active participants in the operation of the electric distribution grid, in particular networked microgrids. In order to achieve the main objective of this dissertation, the following specific objectives are carried out.

- **Objective 1: Efficient Integration of Distributed Energy Resources into Power Distribution Systems**

This objective involves the design and development of control models for DERs (specifically BESS and solar PV) to manage their location and power exchange with the distribution grid to allow efficient integration of the DERs into electrical distribution systems. For objective 1, a planning strategy that considers forecasted power outputs of the DERs and their

consideration in unit commitment and economic dispatch is used to determine the number of possible and optimal locations for the DERs in the power distribution system.

- **Objective 2: Develop a Hybrid Control Mechanism for Prosumer-Centric Networked Microgrids**

This objective entails the development of a hybrid Transactive-Model Predictive Control based Microgrid Energy Management System (TC-MPC) MGEMS for the management of DERs. Furthermore, pricing mechanisms are developed and coupled with TC-MPC to enable and incentivize customer-side resource participation in different electricity market programs. For this objective, the TC-MPC MGEMS utilizes different DER penetration levels and a Monte Carlo simulation (MCS) to generate daily driving patterns of BEVs to optimize the charging of the BEVs and account for the stochastic nature of BEV use.

- **Objective 3: Evaluate the Resiliency of Networked Microgrids During Natural Disasters**

The outcome sought for this objective is to evaluate the use of DER management to reduce the extent and duration of power outages during natural disasters (windstorms and thunderstorms) to improve the distribution grid´s resiliency. Objective 3 emphasizes on different disruption levels on the power distribution system and evaluates the impact of DERs by utilizing different resiliency metrics.

1.4 SCOPE AND LIMITATIONS

The major scope of this dissertation is to identify different control and pricing schemes that allow efficient integration of DERs into the power distribution systems. A techno-economic analysis is conducted to determine the impacts that DER integration has on the power distribution systems, i.e., the effects on costs, power losses, bus voltage profiles, and peak load. Furthermore, a resiliency analysis is done to determine the effectiveness of the DERs to improve the overall resiliency of power distribution systems. Resiliency metrics such as total customer-hours of outage, total customer energy not served, total and average number of customers experiencing

outage, total loss of utility revenue, and total outage costs are utilized to determine the possible impacts DERs can have on the resiliency of the power distribution system.

The following are the limitations of this dissertation.

- The forecasted information required for simulation purposes has been acquired from available databases or data generated by existing forecasting tools.
- Battery degradation of BESS and BEV is not studied in this dissertation.
- The purchase and installation costs of DERs are not considered in the cost-benefit analysis.
- Communication systems are not part of the scope of this dissertation, it will be assumed that the system under study has the required communication network to exchange the required data.
- Protection system coordination is not considered while simulating and analyzing the power distribution systems.
- Cybersecurity is not considered while developing the TC+MPC based MGEMS.

1.5 DISSERTATION ORGANIZATION

This dissertation is constituted by 6 chapters and is organized as presented in Figure 1.2. This section presents a brief description of each chapter.

- Chapter 2 presents a literature review, providing an in-depth analysis of literature regarding the integration of DER technologies specifically solar PV, BESS, and BEVs with a focus on residential customers located in MGs. The literature review first describes impacts of location of DERs in the electrical distribution system. Afterwards, a comparison of various transactive control methodologies used to integrate DERs in MGs and networked-MGs is presented, and finally, a summary of previous studies that utilize DERs to improve power distribution systems resiliency is discussed.

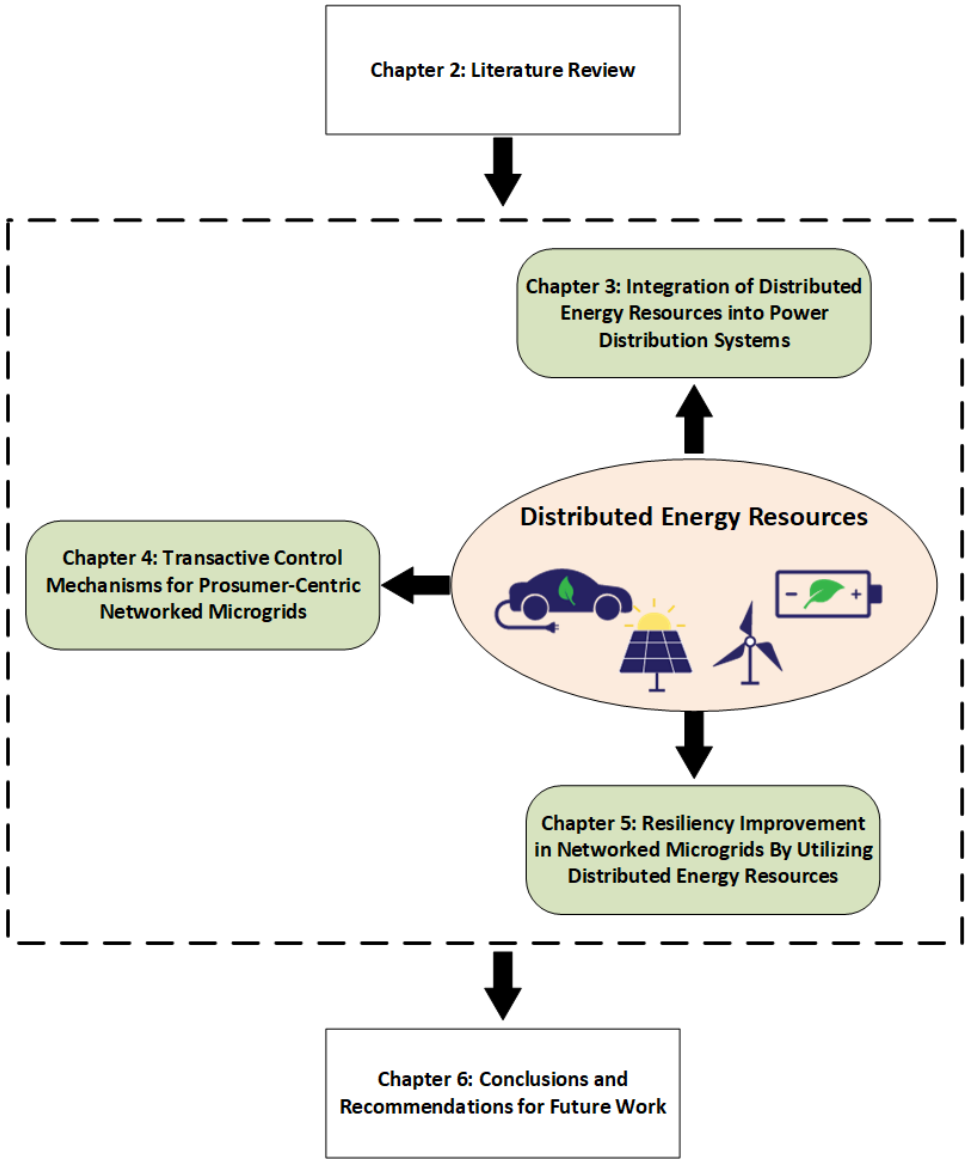

Figure 1.2: Organization of the dissertation.

- Chapter 3 presents a planning strategy to allocate and integrate DERs in electrical distribution networks with a goal of minimizing costs and active power losses. The formulation of the ESS control and its integration in unit commitment and economic dispatch problems are described in this chapter. Different case studies considering various weather scenarios are presented to verify the proposed DER location strategy.

- Chapter 4 describes a proposed MGEMS based on a hybrid control algorithm that combines TC and MPC for efficient management of DERs in prosumer-centric networked MGs. The mathematical formulation of the TC-MPC and an MCS that is utilized to generate daily driving patterns of BEVs are described in detail. An evaluation of the proposed networked MGEMS strategy under different BEV and PV-BESS penetration scenarios to study the potential impact that large amounts of BEV and PV-BESS systems can have on the distribution system and how different pricing mechanisms can mitigate these impacts is also presented in this chapter.
- Chapter 5 is focused on presenting a resiliency analysis process to determine the impacts DERs can have on improving the power distribution system resiliency to natural disasters. The chapter provides the resiliency analysis goals and metrics under different disaster scenarios, as well as, simulated results comparison and discussion.
- Finally, Chapter 6 summarizes the major findings and contributions of the dissertation as well as providing directions for potential future research work.

Chapter 2: Literature Review

2.1 Distributed Energy Resources and Their Impact on Power Distribution Systems

A transition to clean and sustainable energy systems involves various social, economic, environmental, technical, and political factors [18]. With a growing need to cut down on greenhouse gas (GHG) emissions, solutions involve integrating intermittent renewable energy sources (RES), primarily wind and solar. The grid in-feed takes place at the distribution level; however, most power distribution systems were not built to handle multiple, distributed generators, bi-directional power flow, and intermittency issues. Hence, they lack the capacity and technical prerequisites to successfully integrate large amounts of RES and distributed generation (DG).

As we move into the future, it is expected that RES and DG will grow rapidly in distribution networks (DNs). With a large penetration of RES and DG, power utilities will face more challenges to handle integration issues and inherent uncertainty associated with RES. Therefore, power system operators need efficient tools to model and analyze the electric grid with newly added components in order to facilitate their smooth integration within given constraints. Furthermore, as the margin between system load and system capacity decreases, utilities require innovative solutions. To address the aforementioned issues, energy storage systems (ESS) can be a viable solution [19]. A well-designed hybrid energy system consisting of RES and ESS can improve the power system performance and reliability. For example, smart grids, which consist of RES, DG, ESS, demand response (DR) programs and other efficient technologies, are heavily automated. The automation enhances the capability of the smart grids to manage and meet the load in an effective and efficient manner. The role of distributed energy resources in smart grid operations can increase system efficiency, reliability, security, stability, and power quality [20]. To achieve these benefits electric utilities, need to find the optimal location where the units (i.e., RES, DG, and ESS) will be installed to maximize their potential benefits.

The positive and negative impacts of DG in DNs have been discussed in detail in the literature [21]-[27]. While reducing the power losses and increasing the reliability of the power system are the direct benefits of DG installation. It can also benefit the DSO to reduce the congestion of DNs due to growth in load demand as DG can help defer investments [28,29]. Most technical and economic advantages of DG can be achieved by determining its optimal location.

Several papers are available in the literature that discuss the optimal location and sizing of DG in DNs considering different objectives. Loss reduction in a DN is discussed in [30] and [31] where different methods are applied to determine an optimal allocation of DG. An optimization technique based on genetic algorithm (GA) was proposed in [32] to evaluate the optimal sizing and location of DG in radial distribution systems to minimize losses. Multi-objective optimization was also applied in [33] where a single DG was located on various standard DNs to find the optimal location. Moreover, impact indices and a trade-off technique are used for DG location planning as reported in [34]. However, references [30]-[34] considered only controllable or dispatchable generation.

Different optimization algorithms are available in the literature to achieve optimal size and location of RES. A hybrid algorithm between the Chu-Beasly Genetic Algorithm (CBGA) and particle swarm optimization (PSO) is applied to optimally locate wind, PV, and small-scale hydro generation [35]. A constrained discrete PSO technique is reported in [36] to select optimal locations and sizes of PV, wind turbines, and capacitor banks. References [35], [36] considered a fixed power output of the RES. In [37], optimal location of PV is determined by using PSO for loss reduction and frequency control. Pandžić et al. [38] proposed a planning technique to determine the optimal locations and parameters of distributed storage units with wind farms to reduce congestion. Kalkhambkar et al. [39] proposed an analytical method for determining the size of solar PV and battery and concluded that minimization of losses and variable output power of PV are the main parameters to consider when optimally sizing and placing solar PV and battery storage.

A thorough literature review, as presented above, suggests that there is still a great need to consider the unpredictability and intermittency associated with RES while optimally locating them in the DNs. Failing to consider these characteristics of the RES can cause a less efficient operation and unreliable output from these resources.

2.2 TRANSACTIVE ENERGY IN POWER DISTRIBUTION SYSTEMS

As we move into the future, it is expected that DER will be present in most distribution systems, and power utilities will face more challenges as they need efficient tools to model and analyze the electric grid with newly added components to facilitate smooth integration within given constraints [1,10,40,41]. Furthermore, the electric power industry is in the early stages of the adoption of transactive operations. As the deployment of automated intelligent devices increases, the opportunities for transactive energy will also increase. This is illustrated in Figure 2.1.

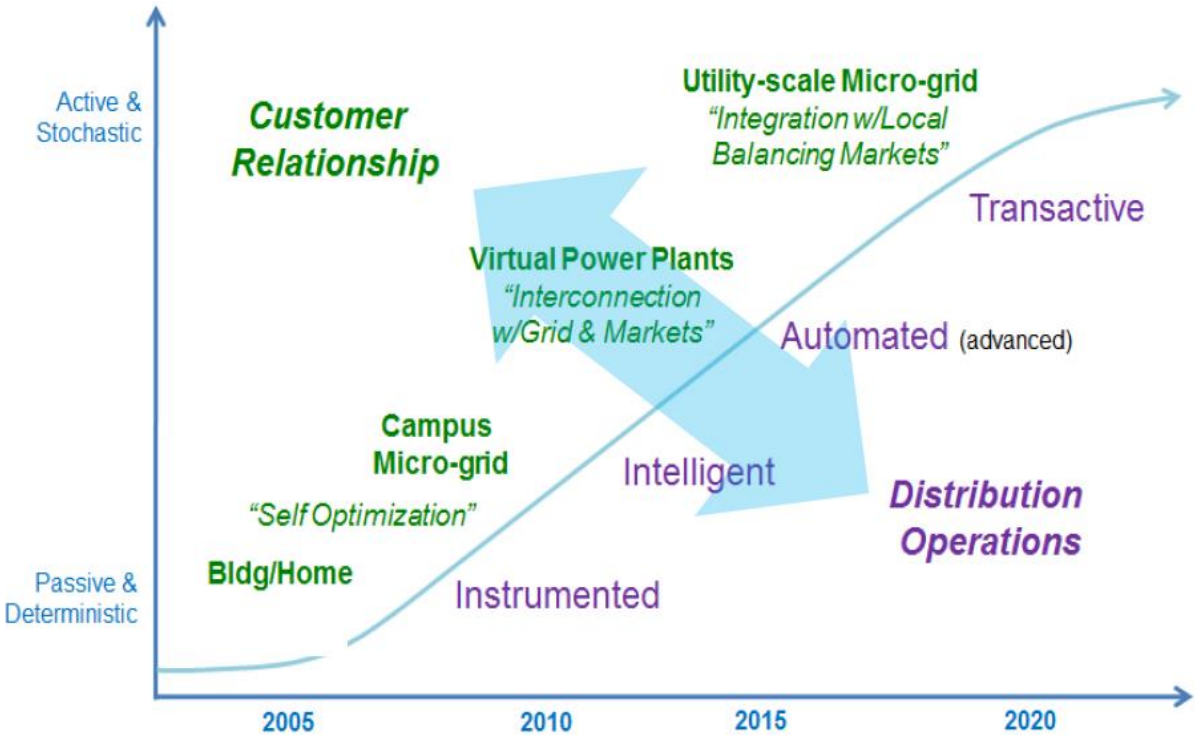

Figure 2.1: Stages of adoption of transactive operations for industry [5].

Under the TE framework, the transactions can take place among prosumers, prosumers, and utilities, between distribution utilities and the power system operators at the wholesale market level. Thus, the development of a new DSO is fundamental to reach the goal of the future grid. The DSO could be an independent entity, or an electric utility [42,43]. The DSO should be able to integrate customer-side assets and consider them during the planning stage of the distribution system and for operation practices, also creating price signals that prosumers can use for investment and operation purposes for long-term and short-term time spans while maintaining the distribution system reliability, efficiency, and security. TE in coordination with TC technology and architecture can elucidate the convergence of technologies, policies, and financial drivers required to evolve the grid's centralized control model to a distributed control architecture [5,6,9,44,45]. The PNNL with the Olympic Peninsula Project One has applied TE framework in the form of a double auction market mechanism utilized to control demand-side assets. This was achieved through the use of two-way communication providing actual demand and price signals; the results indicated that price can be an effective control signal to alleviate congestion in transmission and distribution systems [45]. In [46], a summary of highlights of a five-year PNWSGD is presented where the project's transactive system operated for approximately two years and demonstrated the potential of TCs. Furthermore, findings of the projects showed that research is also needed into the policies to encourage customers to respond to incentive signals. As it is still unclear for large-scale deployment whether to use dynamic cost signals as a dynamic tariff, or an approach based on periodic compensation for which customers agree to respond to the dynamic signal [46]. Other important research that is taking place in the U.S. related to TE is reported in [47]-[49]. The National Institute of Standards and Technology (NIST) through the Transactive Energy Modeling and Simulation Challenge for the Smart Grid ("TE Challenge") plan to develop and demonstrate standardized models and simulation platforms to apply TE [47]. The NYISO is planning to adopt policies toward future energy to maximize the financial benefits of the network where they have studied the benefits and market potential for demand response and future smart grid concept believing that dynamic pricing could be the best strategy to motivate

consumers to participate in the demand response. That is why the NYISO Consumer Advisory recommends that the NYISO should intelligently monitor the emerging TE community of innovation to get a deep insight on how to expand the role of demand response at scale consistent with the New York regulatory environment [48]. TeMix inc. prepared a TE vision for CAISO as an alternative approach. They believe that TE is a more efficient and transparent scheme than centrally distributed models. Moreover, they envision that transactive tariffs will lower the cost of electric power system operations and encourage consumers to buy more DER, helping California reach its clean energy and sustainable goals [49].

In recent years, TC mechanism use in smart grid and MG applications has been studied due to its potential for efficient DER management and the creation of opportunities to engage in transactions between the different entities that constitute the electrical distribution system, e.g., electric utility and customers. A review of the state-of-the-art of transactive energy systems and concepts are presented in [50]. In [51], a transactive bilateral energy trading mechanism is proposed to minimize the costs for individual participants while ensuring the reliability of the power distribution system, where Nash bargaining theory and alternating direction method of multipliers (ADMM) were used to model the problem. A multi-agent transactive energy management framework for networked MGs is presented in [52]. The multi-agent system manages energy imbalances in the MGs using demand response and battery energy storage systems (BESS) with an objective of minimizing the costs for the MG customers. A multi-agent system is also proposed in [53], where an auction-based locational marginal price (LMP) has been used to incentivize energy trading between MGs. In [54], a day-ahead transactive market framework is proposed for DER scheduling to reduce local supply costs. TCs are used for BEV charging in [55-57]. A TC based on model predictive control (MPC) is utilized for real-time scheduling of BEVs in [55], where the MPC is used to clear a day-ahead transactive market. In [56], the charging demand of the BEV is used to manage uncertainties of the building PV generation. Hu et al. [57] implemented a TC with the purpose of minimizing the BEV charging cost as well as preventing grid congestions and voltage violations. A reactive power incentive program to maintain

distribution system reliability is presented in [58]. In [59], A Nash bargaining formulation is proposed for energy trading between networked MGs for MG operation cost reduction. A TC coupled with a pricing rule is proposed for grid-connected, islanded, and congested networked MGs in [60]. DC MGs have also been studied for application of TCs [61-63]. In [61], a framework is proposed for short-term operation of DERs, controllable demands, and MGs in a transactive energy architecture, with a focus on the distributed energy management of hybrid AC/DC microgrids. Jingpeng et al. [62] presented a centralized energy management system approach based on transactive energy to reduce the total operation cost and achieve efficiency in a DC residential system. In [63], a transactive energy management system for supply/demand coordination with demand response programs was implemented to manage rural DC MGs.

Several other models have been proposed for BEVs charging/discharging and pricing scheduling [64-69]. The impact of variable prices on the behavior of BEV users is studied in [64] where the variable prices are based on the distribution locational marginal price (DLMP) and updated continuously based on the users' trips and behavior. In [65], an optimal Time-of-Use (TOU) schedule and a controlled BEV charging algorithm are utilized to maximize both customer and utility benefits and for which, the controlled charging provided voltage profile improvements while taking into account customer preferences. In [66], meta-heuristic techniques are utilized for charging coordination of BEVs with simultaneous operation of capacitor switching to minimize power losses and voltage deviation in a distribution system. Furthermore, a TOU electricity tariff was included in the proposed charging coordination to reduce the PEV charging cost. Cherikad et al. [67] proposed a variable pricing model for BEVs charge/discharge scheduling coupled with an energy management system in an MG. Their model consisted of a cloud-software define networking communication architecture and a linear optimization approach to achieve efficiency in the MG. A model to estimate the cost of BEV charging while considering the impacts of solar PV generation on the charging costs of BEVs is presented in [68]. The model described in [68] estimated the costs considering demand charges and utility loss of revenue and was compared to a TOU tariff. In [69], a two-stage real-time optimization algorithm is proposed to recharge a fleet of

plug-in BEVs to minimize costs, avoid creating new peaks in the demand profile, and improve utilization of power system equipment. The optimization algorithm used a dynamic price signal based on probabilistic models developed utilizing historical price data.

All the aforementioned papers had significant contribution in the matters of energy management using TCs. Nonetheless, there are still gaps in the development of the TE approach, which need to be addressed.

2.3 DISTRIBUTED ENERGY RESOURCES IMPACTS ON RESILIENCY OF POWER DISTRIBUTION SYSTEMS

Today's electricity grid faces challenging issues with aging infrastructure and high concerns regarding cyber and physical system security. As infrastructure ages, many risks arise with it, e.g., increased maintenance and operation costs, equipment failure, inefficient operation, and in severe cases cascading blackouts [70]. While blackouts are considered as low-probability events, the socioeconomic costs and impacts are extensive [71]. Over the past decades hundreds of major blackouts have occurred in the U.S. causing an estimated one billion dollars per event and over one trillion dollars in total damages [72]. Where most of these outages (over 90%) have occurred at the distribution level [73]. As these events become more recurrent in the U.S. (30 weather/climate events where losses exceed 1 billion dollars over the past two years 2017-2018) [72] coupled with a high dependency on electricity in today's society for almost all activities, creates an urgent need to improve the resiliency of the electric power grid to reduce the potential impacts these types of events could have. In recent years, microgrids (MGs) have continued to be developed as different research and pilot projects have shown the potential of MGs to improve resiliency of power distribution grids.

There are various publications that have focused on control strategies for MGs [74-78]. The concept of community MGs where MGs interact with the main grid and among other MGs has also been studied [79,80]. In [81], the coordination of different control levels in a MG was implemented to achieve an economic operation of the MG. The control of DERs within a MG pilot-project at the Illinois Institute of Technology showed to be an effective way to improve the resiliency of the MG under emergency events [82]. In [83], an optimal arrangement of MGs is proposed using graph-related theories based on modularity to quantify the resiliency level of electric distribution systems. A methodology to quantify the resilience improvement in a building MG by adding photovoltaic solar energy and electrochemical storage has been presented in [84]. A two-stage stochastic program for designing resilient distribution grids with networked MGs is proposed in [85]. Where, individual MGs, hardened networks, and a combination (networked MGs) were utilized to evaluate costs of increasing system resiliency. In [86], an MG formation method based on network reconfiguration is proposed for a resilient operation of distribution systems under emergency situations. A software-defined networking (SDN) architecture equipped with event-triggered communication is presented in [87], to transform isolated local MGs into integrated networked MGs capable of power-sharing to improve system efficiency and resiliency. An islanding detection algorithm was used to detect sectioned areas of a distribution system to ensure the system remained operational while experiencing islands [88]. In [89], a detailed literature review of resilience enhancement strategies for power systems is presented. A conceptual framework that considers resiliency during the planning stages of a MG is reported in [90]. In [91], a model to determine the location of MGs for resiliency improvements in a power grid by considering probability of equipment failure was presented. A flood preventive scheduling scheme that isolates vulnerable areas of a MG during floods has been proposed to improve MG resiliency

[92]. In [93], a network reconfiguration algorithm for MGs that considered grid topology and hierarchy of loads (critical and no-critical) was presented and evaluated utilizing different resilience metrics.

Although there are many publications related to the resiliency of power distribution systems, there are still gaps in the literature, specifically in developing realistic case studies and utilizing appropriate resilience metrics.

Chapter 3: Integration of Distributed Energy Resources into Power Distribution Systems

3.1 Introduction

This chapter presents an efficient strategy to optimally allocate RES, primarily wind and solar PV, and ESS in electrical distribution networks with a goal of minimizing costs and active power losses. A planning strategy is used to determine the number of possible and optimal locations for the hybrid RES-ESS system. This chapter also presents a control scheme to optimally dispatch the output of ESS, which increases the effective utilization of RES by reducing their day-ahead forecast errors in order to minimize the deviation between forecasted and actual values. In the proposed strategy, the location that produces the least overall power losses complying with the system constraints is considered as the optimal one. Numerical results and discussion are presented towards the end of the chapter where the effectiveness of the proposed method is evaluated.

3.2 Planning Strategy to Determine the Optimal Location of Distributed Energy Resources

A DSO can reduce overall system costs and losses by coordinating conventional generation with RES. The objectives of DSO are to (i) minimize the power production costs, (ii) determine an efficient operation of DG, (iii) minimize power losses, and (iv) determine the optimal placement of RES. While planning the integration of RES to grids and their expansion, it is of high importance to consider the appropriate location of RES and their impact on the system. Neglecting the optimal siting of the RES can lead to reliability issues and increased real power losses. In addition, by not considering the output power of RES and ESS in the UC and ED problems, it can lead to increased energy costs, which could be due to overcommitting thermal generation or increased operational reserves, and a non-optimal charge/discharge cycle of the ESS.

3.2.1 Battery Energy Storage System Model

The control algorithm for the ESS is embedded in both UC and ED formulation as a sub-problem, which optimizes the scheduling of the ESS by maximizing its power output. The problem is formulated as described below.

$$Max \sum_{t=1}^{T} \sum_{i=1}^{n} \left[PESS_{i,t} \right] \tag{3.1}$$

subject to

$$\sum_{i=1}^{n} PESS_{i,t} = \sum_{j=1}^{ns} (PESS_{j,t}.u_{j,t} - PESS_{j,t}.u_{j,t}^{c}) + \sum_{l=1}^{nr} PR_{l,t} \tag{3.2}$$

$$u_{j,t} + u_{j,t}^{c} \leq 1 \quad \forall j, \forall t \tag{3.3}$$

$$ESS_{j,t}^{SOC} = ESS_{j,t-1}^{SOC} + PESS_{j,t}^{ch}.\eta_j - \quad PESS_{j,t}^{dch}.\eta_j \cdot \left(1 / \eta_j \right) \tag{3.4}$$

$$ESS_{j,\min}^{SOC} \leq ESS_{j,t}^{SOC} \leq ESS_{j,\max}^{SOC} \qquad \forall j, \forall t \tag{3.5}$$

$$0 \leq PESS_{j,t}^{ch} \leq PESS_{j,\max}^{ch}.u_{j,t}^{c} \qquad \forall j, \forall t \tag{3.6}$$

$$0 \leq PESS_{j,t}^{dch} \leq PESS_{j,\max}^{dch}.u_{j,t} \qquad \forall j, \forall t \tag{3.7}$$

$$u_{j,t} = \begin{cases} 1 & if \quad PR_{l,t} - PR_{l,t-1} < W_l \\ 0 & if \quad W_l \leq PR_{l,t} - PR_{l,t-1} \leq Z_l \end{cases} \tag{3.8}$$

$$u_{j,t}^{c} = \begin{cases} 1 & if \quad PR_{l,t} - PR_{l,t-1} > Z_l \\ 0 & if \quad W_l \leq PR_{l,t} - PR_{l,t-1} \leq Z_l \end{cases} \tag{3.9}$$

The objective function (3.1) is the total power output of the ESS. Constraint (3.2) represents

the total available active power, constraint (3.3) is the state of the ESS, (3.4)-(3.5) are the storage balancing constraints, (3.6)-(3.7) are the charge/discharge limits constraints, and (3.8)-(3.9) represent the charge/discharge decision variables.

3.2.2 Day-Ahead Unit Commitment

The day-ahead model determines the UC operational decisions and is used during the ED phase. The objective function of the UC problem is to minimize the energy costs and is described as follows.

$$Min \sum_{t=1}^{Ng}\left[F_{c,i}\left(P_{i,t}\right)I_{i,t} + SU_{i,t} + SD_{i,t}\right] \tag{3.10}$$

subject to

$$\sum_{i=1}^{Ng} P_{i,t}I_{i,t} + \sum_{i=1}^{NW} PW_{i,t} + \sum_{i=1}^{NPV} PS_{i,t} + \sum_{i=1}^{NESS} PESS_{i,t} = P_{D,t} \quad \forall t \in T \tag{3.11}$$

$$\sum_{i=1}^{Ng} R_{Si,t}I_{i,t} \geq R_{S,t} \quad \forall t \in T \tag{3.12}$$

$$\sum_{i=1}^{Ng} R_{Oi,t}I_{i,t} \geq R_{O,t} \quad \forall t \in T \tag{3.13}$$

$$P_{i,t} - P_{i,(t-1)} \leq \left[1 - I_{i,t}\left(1 - I_{i,(t-1)}\right)\right]RU_i + I_{i,t}\left(1 - I_{i,(t-1)}\right)P_i^{Min}$$
$$(i = 1,...,Ng)(t = 1,...,T) \tag{3.14}$$

$$P_{i,(t-1)} - P_{i,t} \leq \left[1 - I_{i,(t-1)}\left(1 - I_{i,t}\right)\right]RD_i + I_{i,(t-1)}\left(1 - I_{i,t}\right)P_i^{Min}$$
$$(i = 1,...,Ng)(t = 1,...,T) \tag{3.15}$$

$$\left[x_{i,(t-1)}^{on} - T_i^{on}\right]\left[I_{i,(t-1)} - I_{i,t}\right] \geq 0 \quad \forall i \in Ng, \forall t \in T \tag{3.16}$$

$$\left[x_{i,(t-1)}^{off} - T_i^{off}\right]\left[I_{i,t} - I_{i,(t-1)}\right] \geq 0 \quad \forall i \in Ng, \forall t \in T \tag{3.17}$$

$$P_i^{Min} \leq R_{i,t} + P_{i,t} \leq P_i^{Max} \quad \forall i \in Ng, \forall t \in T \tag{3.18}$$

$$F_{c,i}\left(P_{i,t}\right) = a_i + b_i P_{i,t} + d_i {P_{i,t}}^2 \tag{3.19}$$

The objective function (3.10) is composed by the thermal generator's operation cost and startup/shutdown costs. (3.11) represents the energy balance constraint. Constraints (3.12)-(3.13) represent the spinning and operating reserves constraints, the generators ramp-up and ramp-down constraints are (3.14) and (3.15), respectively. The generators minimum and maximum up and down times are described by constraints (3.16) and (3.17), constraint (3.18) is the generator maximum/minimum power output limits, and (3.19) is the generator cost function. For these case studies, the UC problem is solved using dynamic programming implemented in MATLAB® 2013.

3.2.3 Real-Time Economic Dispatch

The objective of the ED problem is to minimize the operation cost, the formulation of the ED problem is described as follows.

$$Min\ C_T = \sum_{i=1}^{Ng} F_{c,i}\left(P_{i,t}\right) I_{i,t} \tag{3.20}$$

subject to

$$\sum_{i=1}^{Ng} P_{i,t} I_{i,t} + \sum_{i=1}^{NW} PW_{i,t} + \sum_{i=1}^{NPV} PS_{i,t} + \sum_{i=1}^{NESS} PESS_{i,t} = \sum_{i=1}^{Nb}\left(P_{Di,t} + P_{L,t}\right) \tag{3.21}$$

$$\left|V_k^{Min}\right| \leq \left|V_k\right| \leq \left|V_k^{Max}\right| \quad \forall k \in Nb \tag{3.22}$$

$$P_i^{Min} \leq P_i \leq P_i^{Max} \tag{3.23}$$

The objective function (3.20) is the sum of the thermal generation costs. The energy balance constraint is shown in (3.21), constraint (3.22) represents the bus voltage limits, and (3.23) represents the thermal generators power output limits. In this study, the ED and power flow problems are solved using MATPOWER version 5.1 [94].

Figure 3.1 depicts a flowchart of the proposed strategy to optimally determine the location for RES-ESS. Note that our proposed strategy can be applied to any time scale, e.g., very short-term (5 to 30 minutes-ahead) and short-term (day-ahead to week-ahead).

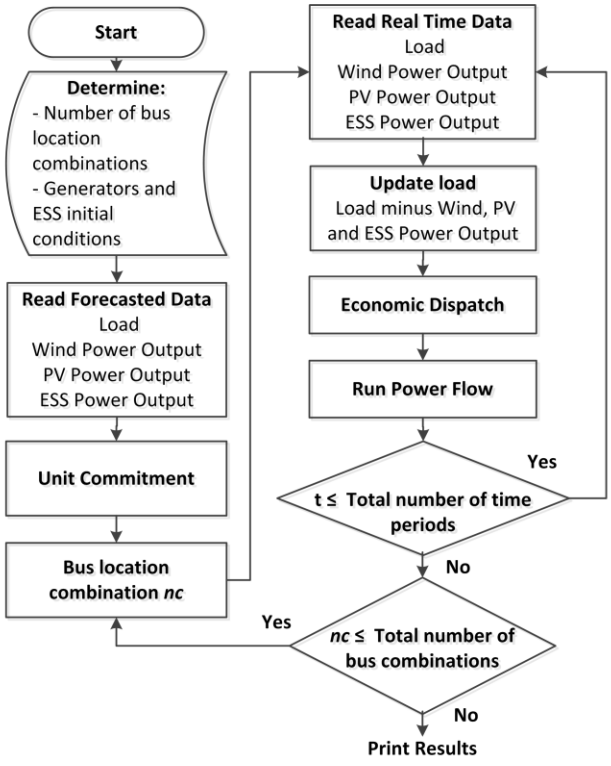

Figure 3.1: The proposed strategy to determine the optimal location of RES-ESS.

The algorithm to solve short-term coordination problems (UC and ED) and then to determine the optimal location of RES and ESS can be described as follows.

1) Forecast day-ahead hourly load, wind power, PV power, and ESS power output. Define the initial conditions for the thermal generators. Determine the total number of bus locations *(nc)* for PV, wind, and ESS.
2) Subtract PV, wind, and ESS power output from the forecasted load.
3) Solve the day-ahead UC problem with the updated load.
4) Determine bus location for PV, wind, ESS, $nc=nc-1$.
5) Update the net real-time load by subtracting the output power of wind, PV, and ESS from the system load.
6) Solve the ED problem with actual data.
7) Run power flow to determine losses, overloads, and bus voltage magnitudes.
8) If this is the last hour period, stop; otherwise, go to step 5.
9) If this is the last bus location, stop; otherwise, go to step 4.

3.3 NUMERICAL RESULTS AND DISCUSSION

3.3.1 Test System and Data

This research study considers a 16-bus test system that represents a small DN. The complete network data is acquired and modified from [95], [96]. There are two thermal units at buses 8 and 15. The thermal generation data is described in [95]. It is considered that buses 1, 2 and 3 are connected to a substation that interconnects with the power grid from where energy is purchased. A 2.5 MW PV installation and a 6 MW wind farm are considered for the study. Interconnected with the wind farm is a 1 MW NaS-ESS, which can operate at its rated power (±1 MW) for extended periods. The NaS-ESS characteristics and attributes are described in detail in [95].

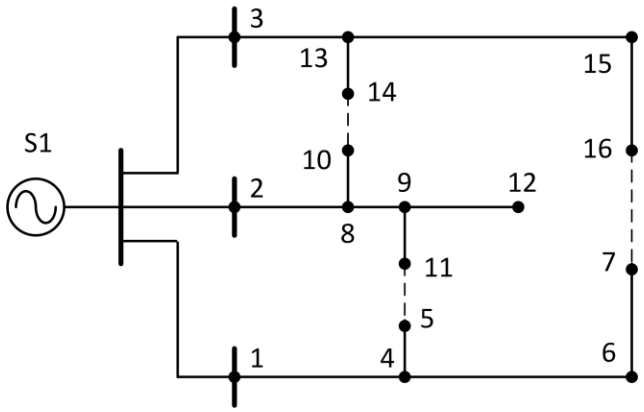

Figure 3.2: A 16-bus test system.

The total installed capacity of RES-ESS (9.5 MW) is 34% of the peak load and is considered the maximum allowable sizing of RES-ESS for this system. Any value above this installed capacity can cause adverse effects on the system, e.g., over-voltages and an increase in the requirement of spinning reserve.

3.3.2 Hybrid Forecasting Models and Forecast Data

In this study, hybrid intelligent algorithms are used for day-ahead hourly forecasts of load, wind power, and solar PV power. Details of the forecast models are presented in [97]-[99] and a brief description is presented below.

Solar PV Power Forecasting

In this study, solar PV output power forecasting was carried out using the combination of a data filtering technique based on wavelet transform (WT) and artificial intelligence technique based on generalized regression neural network (GRNN), which is optimized by a PSO technique [97].

Wind Power Forecasting

For this study, a combination of WT and Fuzzy ARTMAP (FA) network, was used to produce

hourly wind power forecasts. The accuracy of the predictions was tested by comparing the forecast to a persistence method [98].

Load Forecasting

In this study, load demand forecasted data is obtained from a hybrid intelligent model that combines WT and FA where the FA network is optimized by meta-heuristic firefly (FF) optimization algorithm [99]. This combination of algorithms provided more accurate forecasted data.

3.3.3 Case Study Results and Discussion

To carry out simulations, three different PV output power scenarios are considered: (i) scenario 1: sunny day, (ii) scenario 2: cloudy day, and (iii) scenario 3: rainy day. The actual and forecasted data of load, wind power, and PV power are used in these scenarios. In this study, we consider the sunny day, cloudy day, and rainy day based on the data of direct solar radiation [97]. Tables AI.1-AI.5 in Appendix I show the actual and forecasted data used for the simulations.

The following are the assumptions made for simulation purposes.

- Wind-ESS power output and system load are assumed to be the same for all the aforementioned three scenarios.
- The ESS and wind turbine, i.e., hybrid wind-ESS, are assumed to be located at bus 13 for scenario 1, bus 12 for scenario 2, and bus 4 for scenario 3.
- PV panels can be placed at any of the following buses 4, 6, 7, 11, 12, 15, and 16; however, our proposed strategy (see Figure 3.1) will determine its optimal location.

- The RES-ESS are assumed to be owned by independent power producers. Therefore, installation, operation, and maintenance costs are covered by them, and these costs are not considered in these case studies.

The wind farm location must be chosen where wind speeds are strong and constant. On the other hand, PV panels must be placed where they receive direct solar irradiance. Based on the aforementioned assumptions, this study considered certain bus locations in the DNs that meet the requirements for a wind farm and PV siting, e.g., land rights, required area, adequate wind, and direct solar irradiance. Thus, the ESS and wind farm are assumed to be located at bus 13 (scenario 1), bus 12 (scenario 2), and bus 4 (scenario 3). For each scenario, UC and ED problems will utilize the forecasted information and real-time data, respectively, this is described in Figure 3.1. The real-time data is the updated net load data (see Figure 3.1), which is close to the real or target time. Table 3.1 shows the UC results for the considered three scenarios. Test results of the ED problem associated with each scenario are described in forthcoming sub-sections.

Table 3.1 Thermal Generator Status.

Hour		1	2	3	4	5	6	7	8	9	10	11	12	13	14	15	16	17	18	19	20	21	22	23	24
Sc. 1	**G1**	1	1	1	1	1	1	1	1	1	1	1	1	1	1	1	1	1	1	1	1	1	1	1	1
	G2	1	1	1	1	1	1	1	1	1	1	1	0	1	1	1	1	1	1	1	1	1	1	1	1
	G3	1	1	1	1	1	1	1	1	1	1	1	0	1	1	1	1	1	1	1	1	1	1	1	1
Sc.2	**G1**	1	1	1	1	1	1	1	1	1	1	1	1	1	1	1	1	1	1	1	1	1	1	1	1
	G2	1	1	1	1	1	1	1	1	1	1	1	0	1	1	1	1	1	1	1	1	1	1	1	1
	G3	1	1	1	1	1	1	1	1	1	1	1	0	1	1	1	1	1	1	1	1	1	1	1	1
Sc. 3	**G1**	1	1	1	1	1	1	1	1	1	1	1	1	1	1	1	1	1	1	1	1	1	1	1	1
	G2	1	1	1	1	1	1	1	1	1	1	1	0	1	1	1	1	1	1	1	1	1	1	1	1
	G3	1	1	1	1	1	1	1	1	1	1	1	1	1	1	1	1	1	1	1	1	1	1	1	1

3.3.3.1 Optimal location of Distributed Energy Resources Scenario 1-Sunny day

In this scenario, the optimal location problem is solved assuming the weather conditions are those of a sunny day. Figure 3.3 depicts the day-ahead hourly forecasted system load and the

actual load. Figures 3.4 and 3.5 show the forecasted and actual power output of the PV and wind, respectively. As it can be observed in Figures 3-5, our hybrid intelligent models are able to produce forecasted values close to the actual ones for load, PV, and wind power. The maximum system load and PV power are 27.42 MW and 2.24 MW, respectively. The maximum power of the wind-ESS aggregate is 5.85 MW.

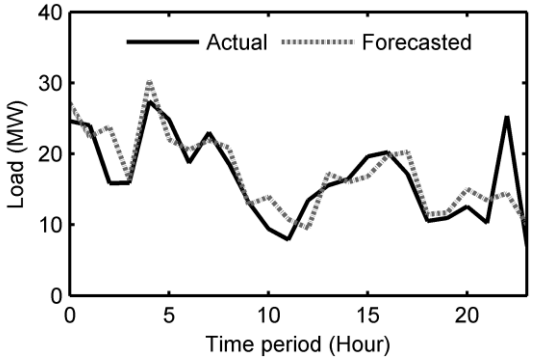

Figure 3.3: Forecasted load vs actual load.

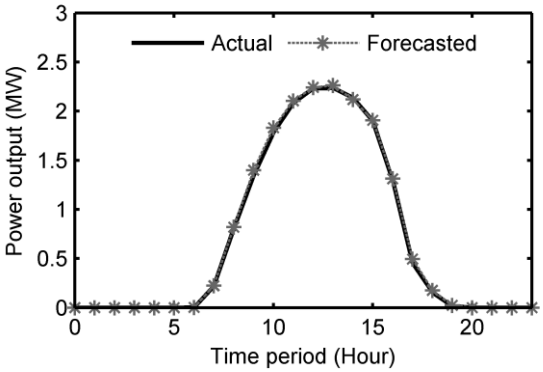

Figure 3.4: Forecasted PV power vs actual PV power (Scenario 1).

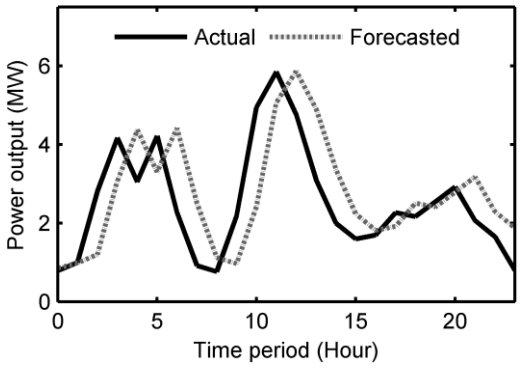

Figure 3.5: Forecasted wind power vs actual wind power.

Figure 3.6 shows the hourly wind-ESS schedule. Positive power corresponds to the hours when ESS is discharged, and negative power corresponds to the charging hours. The wind farm will charge the ESS during early morning hours when the hourly power output of the wind farm is sufficient to charge. This operational scheme provides a lower cost for supplying the hourly load compared with charging the battery when energy prices are high. The ESS will supply the local load during evening peak hours when the wind farm power is low as illustrated in Figure 3.6.

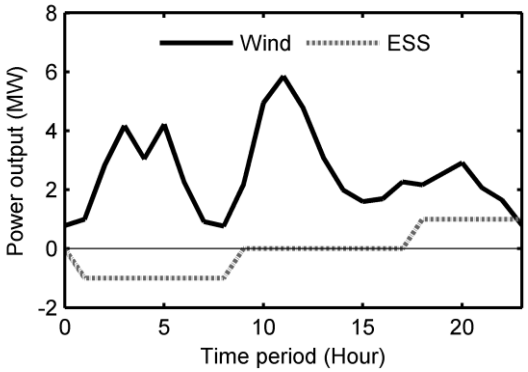

Figure 3.6: Forecasted wind-ESS charge/discharge schedule.

Table 3.2 Sunny Day: Possible Bus Locations for RES-ESS and Optimal Solution

	Wind-ESS	**PV**	**Ploss (MW)**
Bus	13	4	8.50
Bus	13	6	8.47
Bus	13	7	8.47
Bus	13	11	8.31
Bus	**13**	**12**	**8.26**
Bus	13	15	9.37
Bus	13	16	9.37

Table 3.2 presents a summary of the combinations of the bus location (for hybrid wind-ESS and only PV) and the power losses (Ploss) associated with each location. It can be seen from Table 3.2 that there are 7 possible locations for the PV system in the considered DNs. We can observe that the best siting for the PV system, determined by our proposed method, is bus 12 as this bus presents the least power losses (8.26 MW) compared to other bus locations. Moreover, it can be noted that the wind-ESS is located at bus 13 for all the combinations, which are the results of the assumptions made in this study as previously described. Thus, the optimal location for the PV and wind-ESS under the sunny day scenario are buses 12 and 13, respectively.

3.3.3.2 Optimal location of Distributed Energy Resources Scenario 2-Cloudy day

In scenario 2, the optimal location problem is solved assuming the weather conditions are those of a cloudy day. Figure 7 shows the forecasted/actual PV power. The maximum system load is 27.42 MW. The maximum PV power (1.54 MW) is comparatively lower than that of the sunny day (2.24 MW), i.e., there is a reduction of 31% in the maximum PV power output. The maximum power output of the wind-ESS system is 5.85 MW.

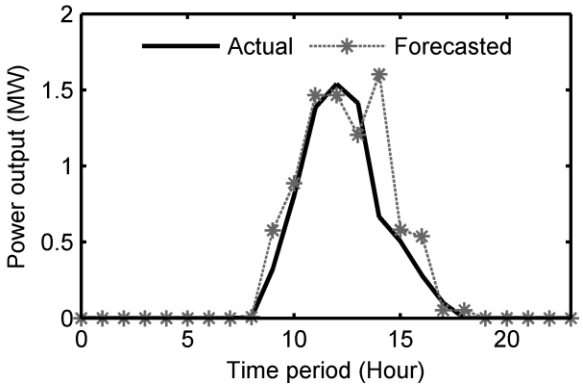

Figure 3.7: Forecasted PV power vs actual PV power (Scenario 2).

Table 3.3 Cloudy Day: Possible Bus Locations for RES-ESS and Optimal Solution.

	Wind-ESS	PV	Ploss (MW)
Bus	12	4	6.94
Bus	12	6	6.92
Bus	**12**	**7**	**6.80**
Bus	12	11	6.96
Bus	12	12	6.98
Bus	12	15	7.16
Bus	12	16	7.16

By analyzing the results presented in Table 3.3, the best siting for PV under the cloudy day scenario is at bus 7 where the least power loss is obtained as 6.80 MW. Thus, under scenario 2 (cloudy day), the optimal locations for the PV and hybrid wind-ESS systems are buses 7 and 12, respectively.

3.3.3.3 Optimal location of Distributed Energy Resources Scenario 3-Rainy day

In scenario 3, the optimal location problem is solved assuming the weather conditions are those of a rainy day. Figure 3.8 shows the forecasted/actual PV power. The maximum system load is 27.42 MW. The maximum PV power is 1.17 MW, which is 47% and 24% less than that of the sunny day (2.24 MW) and the cloudy day (1.54 MW), respectively. The maximum power of the wind-ESS system is 5.85 MW. It can be observed from Table 3.4 that for a rainy day, the best and optimal location for the PV system and wind-ESS systems are buses 12 and 4, respectively. This combination resulted in the least power loss of 7.09 MW.

Table 3.4. Rainy Day: Possible Bus Locations for RES-ESS and Optimal Solution

	Wind-ESS	PV	Ploss (MW)
Bus	4	4	7.38
Bus	4	6	7.37
Bus	4	7	7.36
Bus	4	11	7.28
Bus	**4**	**12**	**7.09**
Bus	4	15	7.59
Bus	4	16	7.59

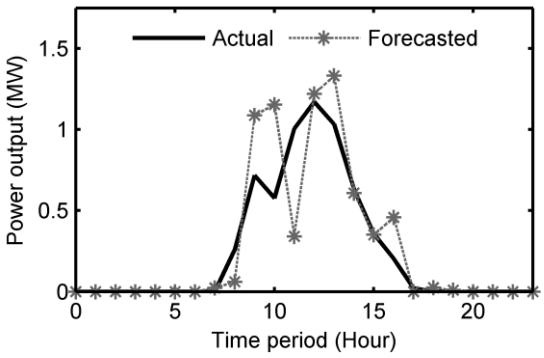

Figure 3.8: Forecasted PV power vs actual PV power (Scenario 3).

Comparing the three scenarios (sunny, cloudy and rainy), the best solution for the optimal location for the PV and wind-ESS systems is the one obtained in scenario 2. In other words, the PV system located at bus 7 and hybrid wind-ESS system located at bus 12 (see Table 3.3) produces the least power loss (6.80 MW), which is comparatively 17% and 4.1% less than those of the optimal solutions obtained in scenarios 1 and 3, respectively. Furthermore, to ensure that the solution obtained in scenario 2 is the optimal one. The optimal location of each scenario is simulated under three weather conditions, i.e., sunny day, cloudy day, and rainy day. Table 3.5 presents the comparison of the simulation results for these weather conditions and also illustrates that the optimal location is the one provided by scenario 2 (cloudy day) as it produces the least overall power losses. With the reduction of the power losses, there is an associated reduction in power generation, this, in turn, will have a significant impact on cutting down energy production costs. Figure 3.9 presents the ED results for the three scenarios. It can be seen from Figure 3.10 that for all the scenarios, there is a reduction in peak load; in particular when it is a sunny day, the PV power production will be higher and it has a significant influence in lowering the peak load. Thus, our proposed planning strategy is able to optimally locate the hybrid RES-ESS system in the DNs efficiently and cost-effectively.

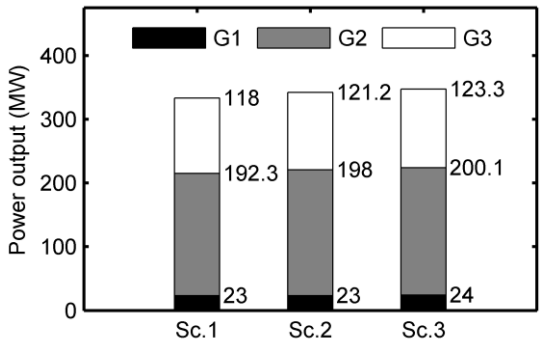

Figure 3.9: Comparison of the ED results for the three scenarios.

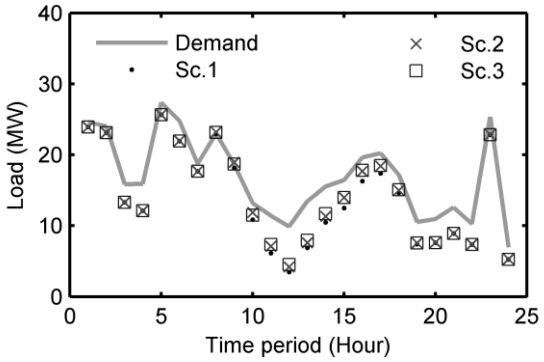

Figure 3.10: Total system demand for the optimal solution of each scenario.

Table 3.5 Comparison of Optimal Locations of RES-ESS for the Three Scenarios.

	Bus location		Sunny day	Cloudy day	Rainy day
	Wind-ESS	PV	Losses (MW)	Losses (MW)	Losses (MW)
Sc. 1	13	12	8.26	8.80	8.84
Sc. 2	**12**	**7**	**6.41**	**6.80**	**6.82**
Sc. 3	4	12	6.68	7.07	7.09

By considering the aforementioned three scenarios, more realistic results are obtained rather than just considering optimal weather conditions, e.g., sunny day or constant wind speed. Furthermore, the proposed approach presented in this chapter allows us to ensure that under any weather condition the given location for the hybrid RES-ESS system will be the optimal one. Thus, this chapter contributed to the efficient planning of the DNs with effective utilization of intermittent RES and ESS. The proposed method can benefit DSOs and utilities during the DN

expansion planning stage, allowing them to determine the optimal site to locate new or future RES-ESS facilities in the most cost-effective manner. The proposed method has been implemented in MATLAB® 2013 and simulated in a personal computer with 2.8 GHz CPU, 4 GB RAM. It should be noted that increasing the size of the test system, i.e., the number of buses, the simulation time will also increase. In this situation, it is necessary to limit the search for possible bus locations. A solution for this problem is to consider locations that meet pre-set requirements, e.g., having the required area for the installation of the wind farm or PV array. This strategy can simplify the size of the networks and reduce the computation cost.

3.4 SUMMARY

This chapter presented an efficient strategy to optimally allocate RES and ESS in electrical distribution networks with a goal of minimizing costs and active power losses. A proposed planning strategy was used to determine the number of possible and optimal locations for the hybrid RES-ESS system. In order to evaluate the effectiveness of the proposed method, a case study of a 16-bus test system constituted by different loads, wind farm, solar PV, and ESS was utilized. The test results demonstrated that by determining the optimal bus location for the RES-ESS system, overall power losses, as well as peak load, can be significantly reduced[1].

[1] Research findings of this chapter have been published in a peer-reviewed journal as indicated below:
E. Galvan, P. Mandal, A. U. Haque, and B. Tseng, "Optimal Placement of Intermittent Renewable Energy Resources and Energy Storage System in Smart Power Distribution Networks," *Electric Power Components and Systems*, Vol. 45, No. 14, pp. 1543-1553, Dec. 2017.

Chapter 4: Transactive Control Mechanisms for Prosumer-Centric Networked Microgrids

4.1 INTRODUCTION

This chapter covers a proposed MGEMS based on a hybrid control algorithm that combines TC and MPC for efficient management of DERs in prosumer-centric networked MGs. This chapter starts with an introduction followed by details of the essential components of the proposed TC+MPC-based MGEMS with the uncertainty modeling and the incentive signal formulation. Afterwards, numerical test results and discussion are presented followed by the summary of the chapter.

Motivated by the promising benefits of using TCs described in Section 2.2 in literature review, in this chapter a hybrid control mechanism based on the combination of TC and MPC for efficient management of DERs in prosumer-centric networked MGs is proposed. Hereinafter, the proposed control approach is termed TC+MPC. This chapter further presents a detailed analysis of the impacts (economical and technical) produced by the TC+MPC within the MGs, and the distribution system as a whole is presented. To carry out this analysis, a Monte Carlo Simulation (MCS) is proposed to consider BEV driving uncertainties and the proposed hybrid TC+MPC management system is used to manage DERs. The hybrid TC+MPC combines the control capabilities and features of the MPC with the TIS–TFS signals of the TC, creating a robust control mechanism that is driven by price signals. The objective of the TC+MPC management system is to produce optimal BEV charge and solar PV-BESS charge/discharge schedules to significantly reduce the residential MG customers' operational cost and to improve their overall savings. The proposed MGEMS is evaluated considering different case studies and scenarios to analyze the impacts that BEV and PV-BESS systems can have on the distribution network.

4.2 TRANSACTIVE CONTROL BASED MICROGRID ENERGY MANAGEMENT SYSTEM

This subsection describes the detailed TC-based MGEMS formulations and comprises the step-by-step procedures followed by several contextual elements required for the optimization

procedure, i.e., the MCS, BEV, and BESS modeling for the MPC, and the schedule optimization process.

4.2.1 Optimization and Control Procedure

The control hierarchy of the distribution system proposed in this chapter is considered to be a hybrid control approach, which is divided into centralized and decentralized control mechanisms. The MG controls are assumed to be decentralized as they use the local information (available solar PV power and state of charge of the BEV and BESS) to optimize and coordinate their schedules. A centralized control mechanism is assumed to be supervised by the distribution system operator (DSO), ensuring generation–demand balance and providing ancillary services for the whole distribution system.

The initial step is the preparation of the input data, i.e., day-ahead electricity price, residential load, solar PV power output, and BEV driving patterns. The initial step also requires the definition of the technical parameters of the DER considered in the case studies, e.g., BEV and BESS battery capacity and charging limits.

Once the input data is prepared, an MCS is conducted to generate a set of BEV driving patterns. This step is explained in detail in Section 4.2.2. The following task is to execute a set of TCs based on MPC to determine the charge schedule of the BEVs and the charge/discharge schedule of the BESS. The mathematical models and MPC formulation are presented in Section 4.2.3. The next task is to assign the load profiles to each bus in the test system and to run a power-flow simulation to calculate the bus voltages, DLMP, power generation, and power losses.

The final step in the procedure is to calculate the costs/savings for the consumers/prosumers, net load, and final BEV and BESS schedules. Figure 4.1 presents a flow chart of the different steps of the optimization and control procedure.

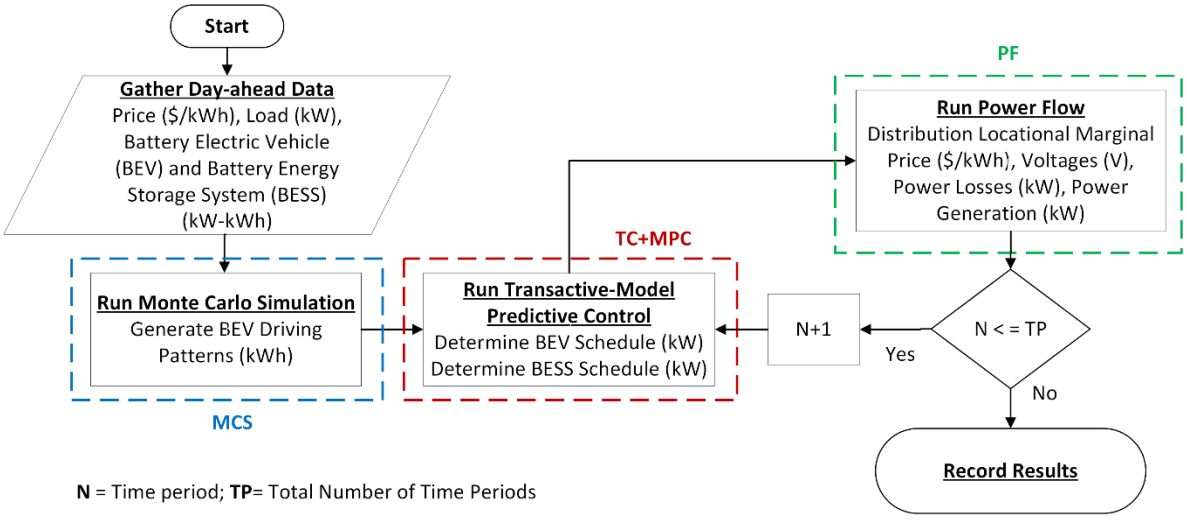

Figure 4.1: Flowchart of the proposed optimization and control procedure.

4.2.2 Monte Carlo Simulation

MCS is an accurate technique to estimate probability density functions (PDFs) using historical data. In this chapter, an MCS is used to consider the uncertainties and stochastic nature of BEV driving patterns. The MCS requires historical BEV driving patterns (δ) to generate a random BEV driving pattern. To consider uncertainties, the underlying stochastic formulation of MCS must include two random components; a uniform distribution (RU) and a normal distribution (RN). The random driving pattern can be formulated as follows [100].

$$d_{n,k}^{i} = (\delta_{k}^{i} + RU_{n,k}^{i}) \cdot (1 + RN_{n,k}^{i}), \tag{4.1}$$

where $d_{n,k}^{i}$ is the stochastic driving pattern of BEV i at time period k, and scenario n. δ_{k}^{i} is the expected energy consumption of BEV i at time period k. This process is repeated for a specified number of scenarios n and ensures convergence over a simulation period t.

Samples of historical data are utilized for the MCS and are constituted by BEV driving patterns in terms of BEV battery energy usage [100]. These BEV driving patterns reflect conventional driving by residential customers and are considered as the base driving patterns.

4.2.3 Transactive Model Predictive Control Formulation

MPC is also known as Receding Horizon Control (RHC) has been developed considerably over the past years and has widely been recognized for its application in academic research and industry. MPC is a control strategy that utilizes current inputs and outputs of a process model to predict future states or outputs [101]. The MPC is solved as an optimization problem with an objective function that considers present and future constraints. The MPC solves the optimization problem in an iterative manner for each time interval of the determined horizon.

In this chapter, the BEV and BESS batteries are formulated as discrete time space models to be utilized in a MPC. The discrete state space model is formulated as follows [101].

$$x_{k+1} = Ax_k + Bu_k + Ed_k \quad \mathrm{k} \in N, \tag{4.2}$$

$$y_k = Cx_k \quad \mathrm{k} \in N, \tag{4.3}$$

$$x(0) = x_0, \tag{4.4}$$

where x_k is the state at time period k, u_k is the input variable, y_k is the output variable, d_k is a random variable acting on the state transition, A is the state transition matrix, B is the input matrix, E is the disturbance matrix, C is the output matrix, and x_0 is the initial state. In (4.2), u_k represents the control variable and the battery state of charge (SOC) is equal to the output variable $y_k = x_k$. In the case of the BEV model, BEV driving usage is represented by d_k as a disturbance of the battery SOC. When modeling the BESS d_k represents the residual solar PV power. The BEV daily usage is modeled using BEV driving patterns generated by the MCS. The state space matrices of the model are the following (4.5)-(4.8).

$$A = 1, \tag{4.5}$$

$$B = (\eta / BEV_{\max})Ts, \tag{4.6}$$

$$C = 1, \tag{4.7}$$

$$E = -(\eta / BEV_{\max})Ts, \tag{4.8}$$

where η is the BEV or BESS efficiency, BEV_{max} is the maximum charging of the BEV or BESS, and Ts is the chosen time sample. The state transition matrix (A) and the output matrix (C) are set to 1 as it is assumed no other factors are affecting the state of charge of the batteries. If other factors were to be considered (e.g., battery degradation, temperature) to affect the state of charge of the batteries, these matrices would be modified. For BESS modeling matrix B is negative and E is positive. The change in signs of matrices B and E for the BESS model, is because the input variable (u_k) is now controlling the discharge of the battery (decreasing the SOC of the battery) and the solar PV power (d_k) is charging the battery (increasing the SOC of the battery).

4.2.3.1 Battery Electric Vehicle Schedule Optimization

Adopting the discrete time space model presented in (4.2)-(4.8), the optimal BEV charge schedule is achieved while minimizing the charging costs as shown in the objective function (4.9), which is subject to constraints (4.10)-(4.13).

$$\min \mathrm{F} = \sum_{k=0}^{N-1} p_k * (u_{BEV,k}), \tag{4.9}$$

subject to

$$x_{BEV,k+1} = Ax_{BEV,k} + Bu_{BEV,k} + Ed_{BEV,k} \qquad k \in N, \tag{4.10}$$

$$y_{BEV,k} = Cx_{BEV,k} \qquad k \in N, \tag{4.11}$$

$$u_{BEV\min} \le u_{BEV,k} \le u_{BEV\max,k} \qquad k \in N, \tag{4.12}$$

$$y_{BEV\min} \le y_{BEV,k} \le y_{BEV\max} \qquad k \in N, \tag{4.13}$$

in (4.9) N is the prediction horizon, p_k is the electricity price, and $u_{BEV,k}$ is the charging power. The discharge constraints are not considered for BEV modelling as the BEV discharge is based on the customer driving patterns and is controlled by the on-board computer of the BEV. From (4.10), $x_{BEV,k+1}$ is the BEV future SOC. $y_{BEV,k}$ is the current battery SOC, u_{BEVmin} and $u_{BEV\,max,k}$ are the battery minimum and maximum charging power, respectively. And constraint (4.13) represents the minimum and maximum SOC of the battery. The optimal BEV charging plan $u_{BEV,k}$ will be solved for the determined prediction horizon N. To carry out the simulations and determine the optimal charging schedule forecasted BEV load $d_{BEV,k}$ and electricity price p_k are used.

4.2.3.2 Battery Energy Storage System Schedule Optimization

Similar to BEV, the BESS is modeled as (4.2)-(4.8). The objective function (4.14) is to maximize the savings of prosumers by optimizing the BESS discharging schedule subject to constraints (4.14)-(4.19). The objective function for the MPC can be formulated as follows [102,103].

$$\max \mathrm{F} = \sum_{k=0}^{N-1} p_k * (u_{BESS,k}) \quad , \tag{4.14}$$

subject to

$$x_{BESS,k+1} = Ax_{BESS,k} + Bu_{BESS,k} + Ed_{BESS,k} \qquad k \in N \quad , \tag{4.15}$$

$$y_{BESS,k} = Cx_{BESS,k} \qquad k \in N \quad , \tag{4.16}$$

$$u_{BESS\min} \le u_{BESS,k} \le u_{BESS\max,k} \qquad k \in N \quad , \tag{4.17}$$

$$d_{BESS\min} \le d_{BESS,k} \le d_{BESS\max,k} \qquad k \in N \quad , \tag{4.18}$$

$$y_{BESS\min} \le y_{BESS,k} \le y_{BESS\max} \qquad k \in N \quad , \tag{4.19}$$

in the above equations $x_{BESS,k+1}$ is the future SOC of the BESS, $y_{BESS,k}$ is the BESS SOC, $u_{BESSmin}$ and $u_{BESS\,max,k}$ are the BESS minimum and maximum discharging power, respectively. In (4.18), $d_{BESSmin}$ and $d_{BESS\,max,k}$ are the minimum and maximum charging power of the BESS and in (4.19) $y_{BESSmin}/y_{BESSmax}$are the minimum and maximum SOC of the BESS. The optimal BESS discharging plan $u_{BESS,k}$ will also be solved for the determined prediction horizon *N*. To determine the optimal discharging schedule, forecasted solar PV power ($d_{BESS,k}$) is considered as the disturbance.

4.2.4 Transactive Control Signals

In this section, DLMP is considered for energy pricing and used for the TC operation. The DLMPs are determined by minimizing the cost of generation considering the physical constraints of the distribution system, thus producing a marginal price at each bus. The DLMP is constructed based on three components: (i) the wholesale locational marginal price (LMP), (ii) system conditions (available generation, load demand, and losses), and (iii) uplift costs (operation and maintenance costs). The LMP is defined as the marginal increase in the overall system costs for the additional per-unit active power consumption at each transmission bus. For simulation purposes, it is assumed that the DSO receives the LMP and determines the DLMP at each bus of the distribution network for the next day and also updates the DLMP in an hourly manner. Equations (4.20) and (4.21) describe the calculations for TIS and TFS, respectively [103]. The TIS is formulated in the following manner.

4.2.4.1 Transactive Incentive Signal

$$TIS_{i,t} = DLMP_t + LC_t + TOC + LOLC_t, \tag{4.20}$$

where $DLMP_t$ is the DLMP at time *t*, LC_t the cost of distribution losses at time *t*, total owning costs (*TOC*) of the transformer, and a penalty cost for transformer loss of life cost (*LOLC*).

The estimated transformer *TOC* considers installation, operation, and maintenance cost over its expected life cycle. The transformer *LOLC* is estimated based on the loading of the transformer.

4.2.4.2 Transactive Feedback Signal

Similarly, TFS signal represents the net load of the customer, and is calculated by.

$$TFS_{i,t} = D_{i,t} + BEVL_{i,t}, \tag{4.21}$$

where $D_{i,t}$ is the demand of customer i at time t and $BEVL_{i,t}$ the BEV charging demand of customer i at time t.

The *TIS* and *TFS* signals are utilized in the MPC formulations presented in subsections 4.2.3.1 and 4.2.3.2 to create a hybrid TC+MPC mechanism. This is achieved by replacing the electricity price p_k with the *TIS* and employing the *TFS* as a disturbance in the MPC discrete time space models.

4.3 NUMERICAL RESULTS AND DISCUSSION

4.3.1 Test System and Data

In this section, case studies are presented to test the proposed hybrid TC+MPC scheduling method on an IEEE 33-bus radial distribution system. For simulation purposes BEV penetration is considered based on the EV30@30 campaign [104]. The EV30@30 campaign was launched at the Eighth Clean Energy Ministerial in 2017, in which the collective goal for all Electric Vehicle Initiative members is to reach a 30% market share for BEVs by 2030. In the case studies a total of 242 households are assumed to be located in three MGs. Data from the US Census Bureau [105], was used to estimate the number of households that own vehicles and assuming a 30% BEV penetration a fleet of 74 BEVs is considered to be distributed among the households located in each MG. Three BEV historical driving patterns are considered for the case studies [100]. Detailed historical BEV driving data expressed in kWh is shown in Table AII.1 in Appendix II. For the

simulation, 1000 scenarios are generated for each BEV type. Table 4.1 shows the BEV parameters utilized to calculate the random components that are needed for generating BEV driving patterns by MCS.

The three MGs considered for the simulations are assumed to be located in a 33-bus radial distribution system as shown in Figure 4.2 The test system data was acquired and modified from [106], by placing three MGs along the feeders of the test system and modifying the load values. Detailed bus load data for the 33-bus distribution system is shown in Table AII.2 in Appendix II. In Figure 4.2, each bus represents a distribution transformer and the dotted lines indicate normally open tie lines. Connected to the transformer are sets of residential customers that are aggregated as CGs or PCGs depending on their classification, i.e., consumer or prosumer.

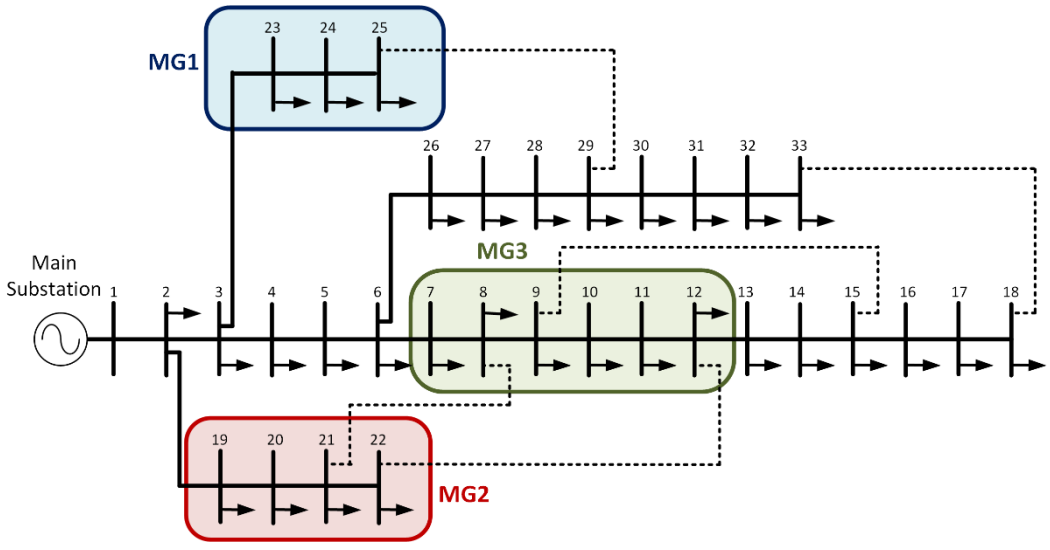

Figure 4.2: Networked microgrids in an IEEE 33-bus distribution network.

Table 4.1 Parameters of Random Components of Residential Customer BEV.

	Parameter	BEV1	BEV2	BEV3
	No. of Scenarios	1000	1000	1000
RN	Stand. Dev (kWh)	2	1	2
	Mean (kWh)	1	0.5	1
Interval RU	(kWh)	0-1	0-1	0-1
Confidence Interval μ	Lower Bound (kWh)	.5668	0.1471	0.3748
	Upper Bound (kWh)	0116	0.8170	1.7552
Confidence Interval σ	Lower Bound (kWh)	1.3297	0.6166	1.2705
	Upper Bound (kWh)	2.3999	1.1128	2.2930

To run the simulations, actual hourly data of load, PV power output, and electricity price have been used. Price data (Fixed and Time of Use rates) was obtained from El Paso Electric, a utility in the U.S. southwest [107,108]. The LMP price data was obtained from PJM market [109]. The load data was obtained from the U.S. Department of Energy Open Data Catalog, residential load at TMY3 locations for the surrounding region of Ashland, Oregon [110]. The specific locations are Klamath Falls, Medford-Rogue Valley, and Redmond, all from Oregon. The individual customer load data for each location is shown in Tables AII.3-5 in Appendix II. The solar PV power output data was obtained from a solar PV system located in Ashland, Oregon. The solar PV power output profile is representative of a sunny summer day. Table AII.6 in Appendix II presents the solar PV data used for the simulations. Figure 4.3 shows the solar PV power output profile considered for each prosumer. The load data was selected for these locations to make the simulation more realistic as the PV power output is considered for the same region. Moreover, by utilizing real load, price, and PV data, the case studies results can better illustrate the potential benefits that can be achieved by using a TC+MPC for BESS and BEV management in residential networked MGs.

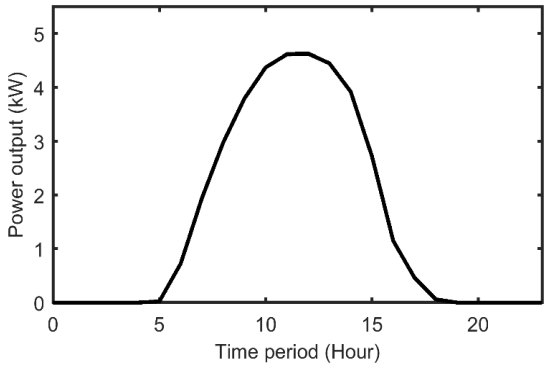

Figure 4.3: Residential solar PV power output profile on a sunny summer day.

Most of the latest BEV models (2019 and newer) that are being produced have driving ranges above 200 miles and are equipped with batteries that have capacities between 60 kWh and 100 kWh [101]. Furthermore, five of the top ten selling BEVs in the U.S. have battery capacities of 60 kWh or higher [112]. Therefore, it is expected that newer BEV models will continue this trend and will become the norm in most distribution systems in the future. Hence, for BEV modeling a Tesla Model S is considered [113]. The Model S offers various battery capacity presentations; we considered the 70 kWh battery. It is assumed that the maximum charging power is 10 kW which is based on a 240 V, 40 A connection. A large scale EV deployment project known as My Electric Avenue was conducted in the United Kingdom between January 2013 and December 2015 [114] in which, one of the major findings was that the likelihood of a BEV being charged when its initial SOC was 16.6% or lower is less than 15%. Another study conducted by the Idaho National Laboratory, U.S.A. found that the average percentage of users who started a commute or a charge with a SOC of 20% or lower is less than 5% [115]. Thus, for the simulation purposes, we assume the minimum/maximum BEV SOC to be 20% and 100%, respectively. The BESS considered for the simulations is a Tesla Powerwall [116]. The PowerWall battery has a capacity of 13.5 kWh and a charging/discharging power of 5 kW. The minimum/maximum BESS SOC are set as 0% and 100%, respectively. The information regarding the BEVs and BESS is

presented in Tables 4.2 and 4.3, respectively. The data used for the case study is summarized in Table 4.4, where households are abbreviated as HHs, Load represents the peak load, PV represents the maximum PV power output, BEV represents the peak BEV load, and BESS – Capacity and Output are the BESS storage capacity and rated power output, respectively.

Table 4.2 Battery Electric Vehicle Data [115].

EV Parameter	**Value**
EV battery size	70 kWh
EV battery efficiency	90%
Maximum charging power	10 kW
Minimum SOC	20%
Maximum SOC	100%

Table 4.3 Battery Energy Storage System Data [116].

BESS Parameter	**Value**
Energy Capacity	13.5 kWh
Operating Voltage	240 V
Operating Current	48 A
Peak Power	7 kW
Continuous Power	5 kW
Round-trip Efficiency	90%
Depth of Discharge	100%

Table 4.4 Case Study Data.

	Bus	**HHs**	**Load (kW)**	**PV (kW)**	**BEV (kW)**	**BESS**	
						Capacity (kWh)	**Output (kW)**
Microgrid 1							
PCG1	23	10	32	50	60	270	50
PCG2	24	12	34	60	50	324	60
CG1	25	15	42	-	50	-	-
Microgrid 2							
PCG3	19	10	28	50	50	270	50
CG2	20	11	30	-	60	-	-
PCG4	21	12	38	60	40	324	60
PCG5	22	12	34	60	30	324	60
Microgrid 3							
CG3	7	40	70	-	50	-	-
CG4	8	40	100	-	60	-	-
PCG6	9	20	48	100	70	540	100
PCG7	10	20	48	100	70	540	100
CG5	11	20	35	-	70	-	-
PCG8	12	25	45	125	80	675	125

The operation of the proposed TC+MPC was analyzed considering five case studies. The following case studies were tested and compared with the base case and among each other. Table 4.5 presents a summary of the different case studies.

1. Case 1: Considering Load and BEV (Without PV and BESS) – Under Fixed Price Signal Scenario
2. Case 2: Considering Load, BEV and PVs (Without BESS) – Under Fixed Price Signal Scenario
3. Case 3: Considering Load, BEV, PV, and BESS – Under Fixed Price Signal Scenario
4. Case 4: Considering Load, BEV, PV, and BESS – Under Time of Use price Signal Scenario
5. Case 5: Considering Load, BEV, PV, and BESS – Under Dynamic Price Signal Scenario

Table 4.5 Case Study Characteristics.

	Load	BEV	PV	BESS	Price Signal
Case 1	✓	✓			Fixed
Case 2	✓	✓	✓		Fixed
Case 3	✓	✓	✓	✓	Fixed
Case 4	✓	✓	✓	✓	Time-of-Use (TOU)
Case 5	✓	✓	✓	✓	Dynamic (DP)

The base case considers only residential and BEV loads. The base case (Case 1) is similar to current electrical distribution systems throughout the United States and around the world. Case 2 is the next step of evolution of the conventional distribution system, where customers also have roof-top solar PV installations. Cases 3, 4, and 5 assume customers have BESS technology which enables them to participate in an electricity retail market and respond to incentives signals generated by the DSO. For all case studies the following assumptions are considered

- It is assumed the consumers/prosumers are equipped with home energy management system (HEMS) in which, the hybrid TC+MPC mechanism is embedded.
- The hybrid TC+MPC mechanism is used for all case studies.

- The BEV charge is analyzed only at the consumer/prosumer household, i.e., charging between 6 am and 6 pm is not available.
- Net metering is considered for cost/savings calculations.
- The BEV SOC must remain at least at 20% throughout the day.

4.3.2 Case 3: Fixed Price Signal Scenario

In this case a fixed cost is utilized [107]. This case can be considered as the conventional case as most residential customers around the world pay the electric utility or DSO a fixed rate for electricity. In the US, normally it is expressed in dollars per kilowatt-hour ($/kWh). Under this pricing rate there is no incentive for customers who own BEVs to charge at different times, e.g., during off-peak hours. Thus, BEV charging is uncontrolled and BEVs are charged at any time. In the case of customers that own PV-BESS systems, the BESS discharge is also uncontrolled and can be discharged at any time as there is no incentive to discharge for example during peak load hours. Figure 4.4 presents a sample of the individual BEV charge/discharge schedules of five BEVs that comprise prosumer group 2 and are located in MG1.

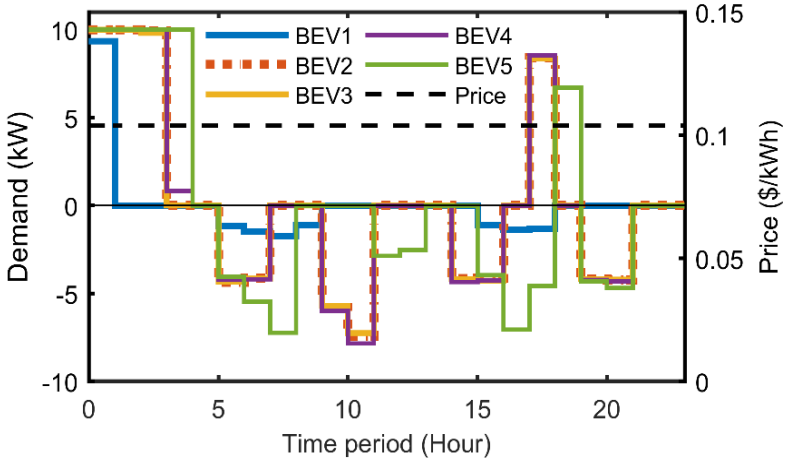

Figure 4.4: Optimal charge schedule and driving pattern of BEVs located in PCG2-MG1 (Case 3).

Table 4.6 presents the numerical values of the BEV charge and usage schedule per MG. The positive values (bold numbers) are the BEVs charging demand and the negative demand represents the BEVs discharging while being driven. Figure 4.5 presents a comparison of the BEVs charge and discharge patterns in each MG. The Figure illustrates the aggregated BEV drive patterns and BEV charge schedules for CGs and PCGs in MG1, MG2, and MG3, respectively. In this case the customer charges the vehicle all night until their departure in the morning (6:00 am), and then another charge is conducted around (7:00 pm) to have enough energy for the commutes between (8:00–9:00 pm). It is clear that since the price is fixed throughout the day the customer doesn't have any incentive to charge at a different time.

Table 4.6 Aggregated BEV Charge Schedule and Driving Pattern (Case 3).

Hour	1	2	3	4	5	6	7	8	9	10	11	12
Price ($/kWh)	0.10	0.10	0.10	0.10	0.10	0.10	0.10	0.10	0.10	0.10	0.10	0.10
BEV-MG1 (kWh)	157	110	110	81	0	-56	-70	-71	-6	-17	-23	-25
BEV-MG2 (kWh)	177	130	126	74	0	-67	-82	-70	-5	-36	-47	-25
BEV-MG3 (kWh)	383	270	259	143	0	-139	-167	-146	-14	-71	-93	-49
Hour	13	14	15	16	17	18	19	20	21	22	23	24
Price ($/kWh)	0.10	0.10	0.10	0.10	0.10	0.10	0.10	0.10	0.10	0.10	0.10	0.10
BEV-MG1 (kWh)	-24	0	-13	-56	-68	-24	48	-49	-53	0	0	0
BEV-MG2 (kWh)	-25	0	-25	-68	-68	-7	54	-63	-67	0	0	0
BEV-MG3 (kWh)	-49	0	-51	-138	-141	-17	113	-125	-132	0	0	0

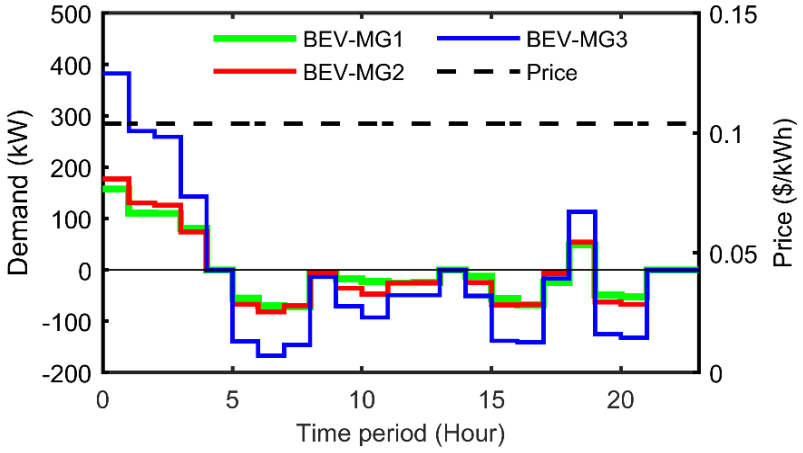

Figure 4.5: Aggregated BEV charge schedule and driving pattern of the three MGs (Case 3).

4.3.3 Case 4: Time-of-Use Price Signal Scenario

In this case a Time-of-Use (TOU) price is considered for a day in Summer. The TOU plans are based on the time of day and the season. By utilizing TOU customers can manage their energy costs. This is achieved by taking advantage of lower rates during off-peak periods and avoiding on-peak periods when energy resources are in high demand. The TOU price that is being tested for this specific case study considers the on-peak period from 12:00 pm through 6:00 pm, Monday through Friday, for the months of June through September. The off-peak period considers all other hours not covered in the on-peak period [108]. Figure 4.6 shows a sample of the individual BEV charge schedules and driving patterns of five BEVs that constitute prosumer group 2 and are located in MG1.

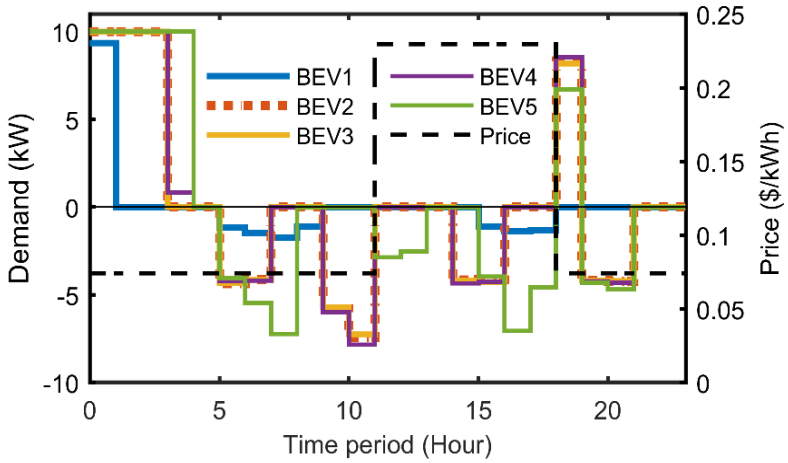

Figure 4.6: Optimal charge schedule and driving pattern of BEVs located in PCG2-MG1 (Case 4).

Table 4.7 presents a numerical summary of the BEV charge schedule and discharge pattern per MG. The TOU price, the aggregated BEV drive pattern, and charge schedule within each MG are depicted in Figure 4.7 The optimal BEVs charge schedule presented in Figure 4.7 is produced by utilizing the TC+MPC. In this case the customer charges the vehicle all night (off-peak period) until their departure in the morning. This is due to the BEV charging taking place during the off-peak period where the price is lowest. Having the price information and an incentive (lower prices) during different periods of the day, allows the customers to charge their BEVs during the low-price periods. Moreover, this process is further optimized with the TC+MPC as it takes in to account the TOU information and BEV driving pattern during the day to produce a least cost schedule. By using the hybrid mechanism, the energy consumption is also minimized as the BEV is charged with the minimum energy required for the daily commute while maintaining a minimum SOC of 20%. Therefore, the customers improve their savings as they charge their vehicle in an optimal manner based on the needs for their commute.

Table 4.7 Aggregated BEV Charge Schedule and Driving Pattern (Case 4).

Hour	1	2	3	4	5	6	7	8	9	10	11	12
Price ($/kWh)	0.07	0.07	0.07	0.07	0.07	0.07	0.07	0.07	0.07	0.07	0.07	0.23
BEV-MG1 (kWh)	157	110	110	81	0	-56	-70	-71	-6	-17	-23	-25
BEV-MG2 (kWh)	177	140	133	64	0	-67	-82	-70	-5	-36	-47	-25
BEV-MG3 (kWh)	383	280	273	133	0	-139	-167	-146	-14	-71	-93	-49
Hour	13	14	15	16	17	18	19	20	21	22	23	24
Price ($/kWh)	0.23	0.23	0.23	0.23	0.23	0.23	0.07	0.07	0.07	0.07	0.07	0.07
BEV-MG1 (kWh)	-24	0	-13	-56	-68	-50	73	-49	-53	0	0	0
BEV-MG2 (kWh)	-25	0	-25	-68	-68	-50	89	-63	-67	0	0	0
BEV-MG3 (kWh)	-49	0	-51	-138	-141	-102	184	-125	-132	0	0	0

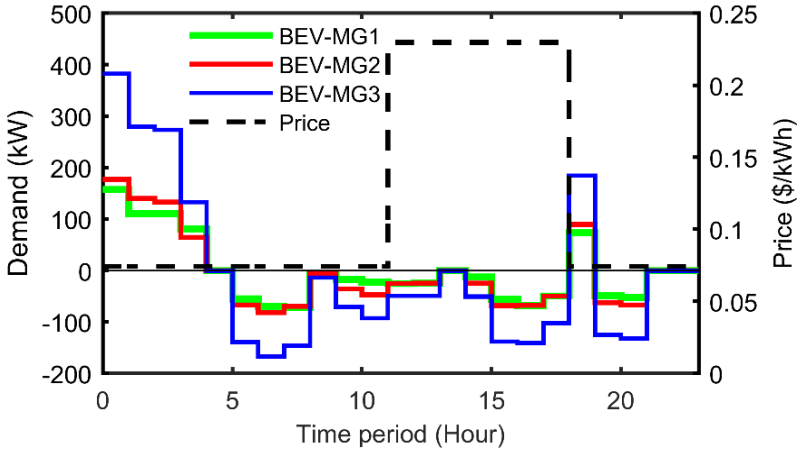

Figure 4.7: Aggregated BEV charge schedule and driving pattern of the three MGs (Case 4).

Comparing the charge schedules with the ones obtained in Case 3, it can be seen that having an incentive (lower price) at different times of the day the TC+MPC increases the charging power (4-8%) between (2:00-3:00 am). The charging power is also increased (52-65%) at 7:00 pm to take advantage of the low price available after 6:00 pm.

4.3.4 Case 5: Dynamic Price Signal Scenario

In the final case a dynamic price signal is considered. The price signal is based on the system DLMP (see section 4.2.4). For this case study the DLMP accounts for marginal costs of generation, marginal costs of losses, and is updated hourly.

Although the customers are receiving the hourly price information it can be difficult and time consuming for a customer to manually be observing the electricity price for that specific hour and decide when to charge their BEV. The HEMS with the embedded TC+MPC can assist the customers by automating the BEV charging. The TC+MPC uses the forecasted DLMP and a forecasted BEV demand pattern to determine the optimal BEV charge schedule that minimizes the customers charging costs. The main differences with the fixed price and TOU is that the DLMP (i) is time varying (in this case hourly) and (ii) it accounts for the system conditions (generation, load, and losses). Figure 4.8 depicts a sample of the individual BEV charge schedules and driving patterns of five BEVs that comprise prosumer group 2 and are located in MG1. A detailed analysis of the numerical values of the aggregated BEV charge schedule and discharge pattern per MG is presented in Table 4.8.

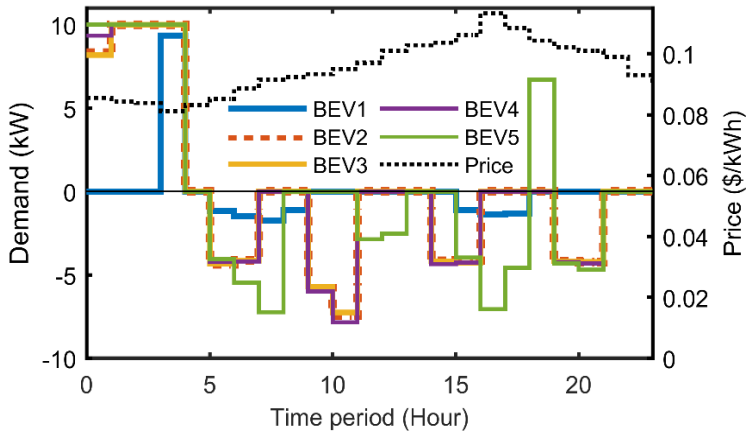

Figure 4.8: Optimal charge schedule and driving pattern of BEVs located in PCG2-MG1 (Case 5).

Table 4.8 Aggregated BEV Charge Schedule and Driving Pattern (Case 5).

Hour	1	2	3	4	5	6	7	8	9	10	11	12
Price ($/kWh)	0.09	0.08	0.08	0.08	0.08	0.09	0.09	0.09	0.09	0.09	0.10	0.10
BEV-MG1 (kWh)	106	110	110	157	0	-56	-70	-71	-6	-17	-23	-25
BEV-MG2 (kWh)	111	140	140	177	0	-67	-82	-70	-5	-36	-47	-25
BEV-MG3 (kWh)	229	280	280	383	0	-139	-167	-146	-14	-71	-93	-49
Hour	13	14	15	16	17	18	19	20	21	22	23	24
Price ($/kWh)	0.10	0.10	0.10	0.11	0.11	0.11	0.10	0.10	0.10	0.10	0.09	0.09
BEV-MG1 (kWh)	-24	0	-13	-56	-68	-50	48	-49	-53	0	0	0
BEV-MG2 (kWh)	-25	0	-25	-68	-68	-50	34	-63	-67	0	0	0
BEV-MG3 (kWh)	-49	0	-51	-138	-141	-102	81	-125	-132	0	0	0

Figure 4.9 shows the aggregated BEVs drive pattern and the optimal charge schedule respectively, for each MG utilizing the TC+MPC. It can be seen from Table 4.8 and Figure 4.9, how the TC+MPC optimizes the BEV charge by selecting the hours where the price is lowest. Specifically, the maximum charging occurs between 2-4 am when the price is lowest and another lower charging period occurs at 7:00 pm. When using the TC+MPC, the BEV is charged with sufficient energy for the daily commute of the customer while minimizing the costs. Comparing the results of this case with Cases 3 there is a decrease between 32-40% at 1:00 am and an increase between 94-168% at 4:00 am. These results explicitly show how the TC+MPC identifies the hours (3:00-4:00 am) with the lowest prices and maximizes the charging at those hours to avoid incurring additional costs during high price hours. When compared to Case 4 there are similarities as both price signals have low price periods. However, for the TOU the low-price periods are fixed regardless of the distribution system conditions.

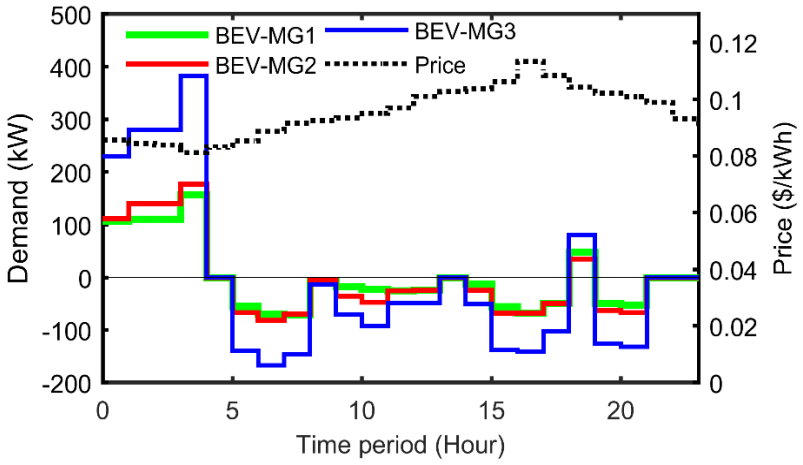

Figure 4.9: Aggregated BEV charge schedule and driving pattern of the three MGs (Case 5).

Figure 4.10 shows the comparison of the overall system net load for each case. Comparing the four cases with the base case (Case 1) it can be seen that the overall system net load is lower for all the cases, which is due to the solar PV power output. It can also be seen from Figure 4.10 that having BESS available allows the prosumers to shift the surplus power production of solar PV (from 7:00 am to 3:00 pm) to peak load periods (between 6:00 and 10:00 pm). Shifting surplus power from off-peak periods can reduce peak load and also avoid steep load ramps. It can also be seen in Figure 4.10 that due to the BESS discharge during the peak period, the demand curve becomes more volatile. Although, compared to the demand ramp rate observed in Case 2 (no BESS), the demand ramp rate created by the BESS discharge in Cases 3-5 is lower. This is an important aspect to consider while setting the BESS discharge constraints in order to minimize negative impacts due to the BESS discharge. Also, incentivizing customers to charge their BEVs during low price periods (off-peak) can reduce peak load and help alleviate steep load ramps.

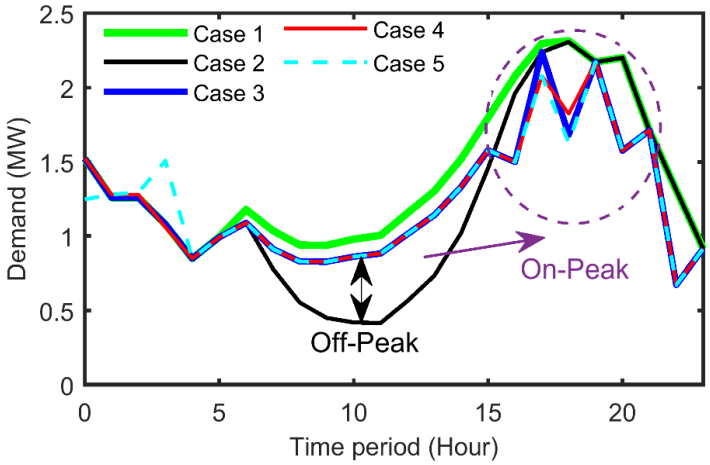

Figure 4.10: Overall system net load comparison for each case.

As it was explained in section 4.2.1, a power flow simulation is conducted to calculate system power losses and bus voltage profiles. The power flow results are obtained using MATPOWER [117]. In MATPOWER, when BEVs and BESS are charging these are treated as load. For every hour, an energy balance is conducted at each bus, i.e., solar PV power is subtracted from the load (household load + BEV and BESS charge). If the net load is negative (i.e., solar PV power generation is greater than the load) then the bus becomes a PV bus. On the other hand, if the net load is positive, the bus remains as a PQ bus. Once the values are assigned for the time period (1-hour), the power flow is executed. This process is repeated for the simulation horizon of 24 hours. Table 4.9 shows a comparison of the total system losses for each case. Comparing the overall system losses of Cases (2-5) with the base Case (Case 1), it can be seen that all the Cases reduce power losses and the highest reduction in losses (11.7%) is achieved in Case 2. Case 2 assumes customers have BEVs and rooftop solar PV installations and any surplus PV power is injected back to the utility grid. Cases 3-5 achieve an overall system power loss reduction of 6.7% compared to the base Case (Case 1). The difference in power loss reduction between Case 2 and Cases 3-5 can be attributed to power losses in storing surplus power in the BESS and the residual

energy that remains stored in the BESS. Although there is a higher power loss reduction in Case 2 compared to Cases 3-5, there are other benefits achieved in Cases 3-5. These benefits are (i) reduction in peak load, (ii) reduction in load ramps, (iii) BEV owners can minimize their charging cost, and (iv) prosumers are able to participate in a retail electricity market and maximize their savings by using the power stored in the BESS during high price periods. Benefit number iv) gives the customers flexibility to utilize the energy for their own use or to sale to other customers when high prices are available.

Table 4.9 Comparison of Total System Power Losses.

	Power Losses (kW)	Reduction (%)
Case 1 (Without PV or BESS)	1788	0%
Case 2 (Without BESS)	1582	11.5%
Case 3 (Fixed Price)	1672	6.5%
Case 4 (TOU Price)	1676	6.3%
Case 5 (Dynamic Price)	1667	6.8%

Voltage profiles are also analyzed to observe the effects produced by the BEVs charging and BESSs discharge schedules for each case. Table 4.10 presents a comparative summary of bus voltage violations (undervoltages) that were recorded when running the simulations as well as improvements to the bus voltage profiles. It should be mentioned that no overvoltages were observed in any of the buses of the test system. The bus voltages that are not shown in Table 4.10 did not present violations (over/under voltages). The comparative analysis summarized in Table 4.10 is done between the base case (Case 1) and Cases 2-5. The values shown in the undervoltage column indicate the number of hours an undervoltage has been recorded in the corresponding case. The values presented in the difference column indicate the difference in number of hour(s) the corresponding case recorded an undervoltage compared to the base case (Case 1). A negative sign (-) indicates a reduction in hour(s), positive sign (+) indicates an increase in hour(s), and a zero (0) indicates no difference.

Table 4.10 Summary of Bus Voltages Improvements.

Bus	Case	Hours Under Voltage (<0.95 p.u.)	Hour Difference	Bus	Case	Hours Under Voltage (<0.95 p.u.)	Hour Difference
9	1	4	0	17	1	11	0
	2	4	0		2	7	-4
	3	2	-2		3	6	-5
	4	1	-3		4	6	-5
	5	1	-3		5	6	-5
10	1	5	0	18	1	11	0
	2	4	-1		2	7	-4
	3	2	-3		3	6	-5
	4	2	-3		4	6	-5
	5	2	-3		5	6	-5
11	1	6	0	28	1	5	0
	2	4	-2		2	4	-1
	3	2	-4		3	2	-3
	4	2	-4		4	2	-3
	5	2	-4		5	2	-3
12	1	7	0	29	1	8	0
	2	5	-2		2	5	-3
	3	3	-4		3	5	-3
	4	3	-4		4	5	-3
	5	3	-4		5	5	-3
13	1	8	0	30	1	10	0
	2	5	-3		2	6	-4
	3	4	-4		3	5	-5
	4	6	-2		4	5	-5
	5	6	-2		5	5	-5
14	1	9	0	31	1	12	0
	2	6	-3		2	7	-5
	3	6	-3		3	7	-5
	4	6	-3		4	7	-5
	5	6	-3		5	7	-5
15	1	9	0	32	1	13	0
	2	6	-3		2	8	-5
	3	6	-3		3	9	-4
	4	6	-3		4	9	-4
	5	6	-3		5	8	-5
16	1	11	0	33	1	13	0
	2	7	-4		2	8	-5
	3	6	-5		3	9	-4
	4	6	-5		4	9	-4
	5	6	-5		5	9	-4

By further analyzing the results presented in Table 4.10, it can be stated that having rooftop solar PV installations (Case 2) can improve bus voltage profiles from 20% and up to 42% compared to the base case (Case 1). However, having a hybrid PV-BESS system (Cases 3-5) can improve voltage profiles between 25% and 75% compared to the base case. In all but one bus (Bus 33), the cases where BESS is present render a higher voltage profile improvement. Thus, having controllable demand-side DER can protect the system from overvoltages that can be incurred in the uncontrolled case (Case 2) while also providing the benefits that have been previously discussed.

Finally, a cost/savings analysis is carried out to compare the total daily costs and savings for the PCGs and CGs located in each MG. The daily costs and savings data is presented in Tables 4.11 and 4.12. In Table 4.11, the Costs ($) refer to the amount paid for the daily energy consumption and Savings ($) refer to energy cost reduction associated to the use of rooftop solar PV and BESS.

Comparing the results of the five cases (see Table 4.11), we can observe that the highest overall savings are achieved by PCGs in Cases 4 (TOU) and 5 (DP). Also, Cases 3-5 produced greater savings then Cases 1 and 2. Specifically, the savings difference were between 52%-76% (Case 3), 128%-144% (Case 4), and 95%-123% (Case 5). When comparing the costs of Cases 2-5 to those of Case 1 (base case) they all achieve a cost reduction. The total cost reductions compared to Case 1 are Case 2 (29%), Case 3 (45%), Case 4 (57%), and Case 5 (37%). The results comparison demonstrates that by having the BESS, the reduction in total costs for Cases 3-5 is improved. This is more noticeable in Case 5 as the demand during high price periods is fulfilled by the energy stored in the BESS. With the reduction of the peak demand between 6:00 pm and 9:00 pm (see Figure 4.10), there is an associated reduction in electricity price, which in turn has a

significant impact on the total costs of the CGs and PCGs. We can clearly observe that by shifting the surplus PV generation with BESS (controlled by TC) to peak load hours, PCGs can reduce their total energy costs.

Table 4.11 Total Daily Costs ($) and Savings ($) Comparison per Microgrid.

		Case 1 Total Costs	Total Savings	Case 2 Total Costs	Total Savings	Case 3 Total Costs	Total Savings
MG1	PCG1	54.66	0.00	40.96	13.70	31.36	23.30
	PCG2	70.65	0.00	51.90	18.75	37.60	33.05
	CG1	52.99	0.00	52.99	0.00	52.99	0.00
MG2	PCG3	51.79	0.00	36.17	15.62	27.32	24.47
	CG2	43.84	0.00	43.84	0.00	43.84	0.00
	PCG4	55.85	0.00	39.41	16.44	29.93	25.92
	PCG5	43.54	0.00	30.91	12.64	23.88	19.66
MG3	CG3	108.42	0.00	108.42	0.00	108.42	0.00
	CG4	165.86	0.00	165.86	0.00	165.86	0.00
	PCG6	89.73	0.00	62.33	27.40	46.09	43.64
	PCG7	92.15	0.00	60.90	31.25	44.63	47.52
	CG5	72.44	0.00	72.44	0.00	72.44	0.00
	PCG8	91.00	0.00	64.67	26.33	50.99	40.01

		Case 4 Total Costs	Total Savings	Case 5 Total Costs	Total Savings
MG1	PCG1	25.50	31.90	39.79	29.63
	PCG2	33.15	45.76	45.73	41.98
	CG1	53.29	0.00	65.07	0.00
MG2	PCG3	21.52	36.59	34.44	29.19
	CG2	42.65	0.00	55.63	0.00
	PCG4	23.72	38.19	35.04	32.01
	PCG5	18.54	24.92	27.15	24.66
MG3	CG3	118.57	0.00	134.84	0.00
	CG4	202.87	0.00	209.43	0.00
	PCG6	37.72	63.07	71.20	56.12
	PCG7	36.74	71.29	62.49	62.32
	CG5	25.50	31.90	39.79	29.63
	PCG8	33.15	45.76	45.73	41.98

Table 4.12 presents the comparison of net costs and the difference between each case and the base case. In Table 4.12, Net Costs are the Costs minus Savings (Costs – Savings), and the percentage column indicates an increase (Inc.) if it is positive and a reduction (Red.) if negative

Further analysis of the net costs results (see Table 4.12) shows that Case 4 achieves the highest net cost reduction percentages for both CGs and PCGs followed by Case 5, which produces a higher net cost reduction for PCGs. Also, CGs achieve more net cost reduction under Fixed and TOU pricing schemes (Cases 3 and 4) compared to a DP scheme (Case 5). These results are reasonable as CGs do not possess alternative sources of generation to fulfill their own demand and can only participate by deferring or shifting load to low price periods.

Therefore, it can be inferred that a DP scheme is better suited for PCGs that are able to respond to price signals via BESS or other controllable distributed generation sources. It should be noted that for simulation purposes in Case 2-5 the price signal is considered the same for buying and selling power (net metering). In different electricity markets, utilities and DSOs have lower paying costs for selling power to the grid. Consequently, the total savings for Cases 2-4 could be lower under these pricing schemes when compared to Case 5, thus adding more value to TC+MPC and BESS for customers under those pricing schemes.

It should be noted that the test results are only representatives and are obtained under simulated conditions for the considered test system. More case studies could be further conducted for longer time horizons (e.g., weeks and months) with different scenarios, test systems, and MG locations in order to be able to conclude that the benefits mentioned in the case studies will be achieved with high certainty.

Table 4.12 Net Costs ($) Comparison Per Microgrid.

		Case 1 Net Costs ($)	Inc. / Red. (%)	Case 2 Net Costs ($)	Inc. / Red. (%)	Case 3 Net Costs ($)	Inc. / Red. (%)
MG1	PCG1	54.66	0.00	27.26	-50.13	8.06	-85.25
	PCG2	70.65	0.00	33.15	-53.07	4.55	-93.57
	CG1	52.99	0.00	52.99	0.00	52.99	0.00
MG2	PCG3	51.79	0.00	20.54	-60.33	2.85	-94.50
	CG2	43.84	0.00	43.84	0.00	43.84	0.00
	PCG4	55.85	0.00	22.97	-58.87	4.01	-92.81
	PCG5	43.54	0.00	18.27	-58.05	4.22	-90.31
MG3	CG3	108.42	0.00	108.42	0.00	108.42	0.00
	CG4	165.86	0.00	165.86	0.00	165.86	0.00
	PCG6	89.73	0.00	34.93	-61.07	2.44	-97.28
	PCG7	92.15	0.00	29.66	-67.82	-2.90	-103.14
	CG5	72.44	0.00	72.44	0.00	72.44	0.00
	PCG8	91.00	0.00	38.34	-57.87	10.97	-87.94

		Case 4 Net Costs ($)	Inc. / Red. (%)	Case 5 Net Costs ($)	Inc. / Red. (%)
MG1	PCG1	-6.40	-111.7	10.17	-81.40
	PCG2	-12.61	-117.8	3.75	-94.69
	CG1	53.29	0.57	65.07	22.79
MG2	PCG3	-15.06	-129.1	5.26	-89.85
	CG2	42.65	-2.73	55.63	26.89
	PCG4	-14.47	-125.9	3.03	-94.58
	PCG5	-6.38	-114.6	2.49	-94.28
MG3	CG3	118.57	9.37	134.84	24.37
	CG4	202.87	22.31	209.43	26.27
	PCG6	-25.35	-128.2	15.08	-83.20
	PCG7	-34.55	-137.5	0.17	-99.82
	CG5	72.33	-0.14	103.88	43.41
	PCG8	-14.18	-115.6	40.30	-55.71

The TC+MPC formulation presented in this chapter has been implemented in MATLAB R2017a and solved with YALMIP and GUROBI (Gurobi Optimization, LLC., Beaverton, OR, USA). MATLAB (The MathWorks Inc., Natick, MA, USA) is used as the programming environment, while YALMIP structures the optimization problem into matrices with the objective function, the optimization variables, and the equality and inequality constraints [118]. GUROBI is

used as an external solver to find the optimal solution of the problem [119]. All simulations were conducted using a personal computer with 2.8 GHz CPU, 4 GB RAM.

4.4 SUMMARY

In this chapter, a MGEMS based on a hybrid control algorithm that combines TC and MPC for an efficient management of DERs in prosumer-centric networked MGs has been presented. The proposed hybrid TC+MPC combines the control capabilities and features of the MPC and the TC, creating a robust control mechanism that is driven by transactive incentive signals, and thus, also providing the MGEMS capability to deal with the stochastic nature of BEV driving by using a MCS to generate the BEV driving patterns. The proposed TC+MPC was able to effectively generate the BEV-charge and BESS-discharge schedules for the CGs/PCGs located in each MG. Test results demonstrated the potential of using pricing mechanisms for demand-side management of DERs[2].

[2] Research findings of this chapter have been published in a peer-reviewed journal as indicated below:
E. Galvan, P. Mandal, S. Chakraborty, and T. Senjyu, "Efficient Energy Management System Using A Hybrid Transactive-Model Predictive Control Mechanism for Prosumer-Centric Networked Microgrids," *Sustainability*, Vol. 11, No. 19, Sep. 2019.

Chapter 5: Resiliency Improvement in Networked Microgrids by Utilizing Distributed Energy Resources

5.1 Introduction

This chapter considers the advantages and challenges of having sections of a power distribution system constituted by networked MGs to manage DERs to improve distribution system resiliency to natural disasters. A detailed resiliency analysis process is presented with two case studies that are tested under different scenarios and evaluated utilizing different resiliency metrics. This chapter contributes to provide realistic case studies that show the potential benefits that DERs managed in networked MGs can provide a power distribution grid.

5.2 System Modeling and Resiliency Metrics

To evaluate the resiliency of the distribution grid with networked MGs and DERs, an analysis based on the Resilience Analysis Process (RAP) is conducted. The RAP was developed at SANDIA national laboratories to provide a means and a set of metrics to analyze the resiliency of energy systems [120]. Frequently, resiliency and reliability are confused as being similar although they account for different types of events and use different metrics, i.e., resiliency analysis considers low probability, high consequence events and the resiliency metrics focus on the impacts on humans. Contrary to the resiliency analysis, reliability analysis considers high probability, low impact events and the focus is on system impacts [120].

The main goal of this chapter is to analyze and evaluate potential improvements of a power distribution systems resiliency to natural disasters using solar PV and BESS. The specific goals are (1) evaluate the impact of outages to the system loads when utilizing MGs and DERs and (2) the monetary impacts the utility or system operator will experience due to the natural disaster.

5.2.1 Classification of Consequences and Resiliency Metrics

For the present study, the consequences and resiliency metrics that are considered for the case studies are described in Table 5.1. The metrics shown in Table 5.1 are based on consequences and resiliency metrics reported in [26].

Table 5.1 Consequence Categories and Resilience Metrics

Consequence Class	**Resiliency Metric**
Electrical Service	Total customer-hours of outages (h) Total customer energy not served (kWh) Total and average number of customers experiencing outage during the specified time period
Monetary	Total loss of utility revenue ($) Total outage costs ($) Total avoided outage cost ($)

5.2.2 Definition of Hazards and Level of Disruption of the Distribution System

The potential hazards that are considered for simulation purposes are storms of different intensities, i.e., moderate intensity and high intensity. The level of damage the grid assets are anticipated to suffer under the storm scenarios are based on the hazard's intensity, i.e., similar damages will be considered (moderate damage and high damage). Specifically, the damages that are anticipated to occur in the distribution grid are downed distribution lines and feeders. The consequence data of the hazards for the case studies is obtained through the execution of power flow in the distribution system [117]. When running the power flow analysis, the bus voltages and power outputs of the DERs are calculated to estimate which loads would be unserved during the outage. In this case, power flow will be executed for the case studies time period (1-day) under the different scenarios that are described in subsection 5.3.1. These simulations will allow to determine and quantify the effects of the hazards on the customers being served in the distribution system and the ability of the utility or system operator to deliver electrical energy to its customers.

5.2.3 Consequences and Resiliency Metrics Calculations

The consequence and resiliency metrics that have been evaluated are listed in Table 5.1. Each metric is calculated as follows.

5.2.3.1 Electrical Service Class

Total customer-hours of outage

$$\sum_{t=1}^{n}\sum_{i=1}^{k} x_i \cdot (t) \tag{5.1}$$

where $x_i \cdot (t)$ is the number of customer-hours without power of customer i for the duration of event n, for all customers k experiencing an outage..

Total customer energy not served

$$\sum_{t=1}^{n}\sum_{i=1}^{k} E_i \cdot (t) \tag{5.2}$$

where $E_i \cdot (t)$ is the total energy not served per customer i for the duration of event n, for all customers k experiencing an outage..

Total and average number of customers experiencing outage during the specified time period

$$\overline{X} = \frac{\sum_{s=1}^{T_s}\sum_{i=1}^{k} x_{i,s}}{T_s} \tag{5.3}$$

where $\overline{X}$ is the average number of customers experiencing an outage during scenario s, k the total number of customers experiencing an outage, and T_s the total number of scenarios.

5.2.3.2 Monetary Class

Total loss of utility revenue

$$C_{LUR,s} = C_e * \left(\sum_{t=1}^{n} \sum_{i=1}^{k} E_{i,s} \cdot (t) \right) \tag{5.4}$$

where $C_{LUR,s}$ is the loss of utility revenue (\$) of scenario s, C_e is the cost of energy (\$/kWh), $E_{i,s} \cdot (t)$ is the total energy not served for the duration of event n, during scenario s, for all customers k experiencing an outage.

Total outage costs

$$C_{out,s} = C_o * \left(\sum_{t=1}^{n} \sum_{i=1}^{k} x_{i,s} \cdot (t) \right) \tag{5.5}$$

where $C_{out,s}$ is the total outage cost (\$) of scenario s, C_o is the outage cost per hour (\$/h), $x_{i,s} \cdot (t)$ the number of customer-hours without power for the duration of event n, during scenario s, for all customers k experiencing an outage.

Total avoided outage cost

$$C_{avd,s} = C_{out-base} - C_{out,s} \tag{5.6}$$

Where $C_{avd,s}$ are the avoided costs (\$) of scenario s, $C_{out-base}$ is the total outage cost (\$) of the base scenario, and $C_{out,s}$ is the total outage cost (\$) of scenario s.

5.3 NUMERICAL RESULTS AND DISCUSSION

In this section, case studies are presented to evaluate the resiliency metrics proposed in the previous subsections. For the proposed research study two cases are considered, (1) case where moderate damage affects the power distribution system and (2) a case where heavy damage occurs to the system. For both cases, it is assumed groups of residential customers own roof-top solar PV.

A 33-bus test system with three MGs is considered to run the simulations [121]. The simulations are carried out for each case and then a comparison of the statistics of each case with a base case that has no DERs is shown. This process is modeled for a day (24 hours) with outages occurring over a three-hour period following the natural disaster event. To estimate the cost of energy not served a fixed energy rate is assumed [107]. In the case of outage costs, a value of 3 $/h is utilized to calculate the total costs [122]. The following assumptions are made for the case studies:

- There are sufficient repair crews to attend all damaged lines
- The estimated time for line repairs is 3 hours
- All lines are repaired simultaneously
- BESS units are utility-owned

5.3.1 Test System and Data

The IEEE 33-bus radial distribution system with three MGs presented in section 4.3 is used for simulation purposes with minor changes made to the system data. Table 5.2 shows the data utilized in the test system. The differences between the test data used for the case studies in this chapter with those of chapter 4 is that in these case studies BEVs are not considered and the BESS is assumed to be utility owned. The solar PV power output data used in simulations for the sunny-day scenarios is presented in Appendix II, Table AII.6. For the rainy-day scenarios, the data is shown in Table III.1 in Appendix III.

For the proposed resiliency analysis, two case studies and five scenarios for each case study are considered. The case studies that were tested and compared with the base scenario and among each other are the following.

Case 1: Moderate Damage

1.1. Base scenario no DERs

1.2. Sunny day preceding the event and all load supplied

1.3. Sunny day preceding the event and only critical loads are supplied

1.4. Rainy day preceding the event and all load supplied

1.5. Rainy day preceding the event and only critical loads are supplied

Case 2: Heavy Damage

2.1. Base scenario no DERs

2.2. Sunny day preceding the event and all load supplied

2.3. Sunny day preceding the event and only critical loads are supplied

2.4. Rainy day preceding the event and all load supplied

2.5. Rainy day preceding the event and only critical loads are supplied

The base scenarios consider there are no DERs interconnected with the power distribution system. For the rest of the scenarios DERs are considered to be interconnected to the distribution grid.

5.3.2 Resiliency Analysis of Distribution Grid-Moderate Damage Case

For this case, three MGs are assumed to be located in a 33-bus radial distribution system as shown in Figure 5.1. In Figure 5.1, each bus represents a distribution transformer and the dotted lines indicate normally open tie lines. Connected to the transformer are sets of residential customers that are aggregated as consumer groups (CG) or prosumer groups (PCG) depending on their classification, i.e., consumer or prosumer. To evaluate the impact of the MGs and the DERs to the resiliency of the distribution system to natural disasters it is assumed a storm occurred and created moderate damage to the feeders of the system. Specifically, to branches 2-19, 3-23, and 6-7, as shown in Figure 5.1. The event is assumed to have occurred at 17:00 hrs. (5:00 pm) and the duration of the outage is 3 hours (17:00 hrs. to 19:00 hrs.). The 3-hour time period is based on the

estimated time it takes a crew of linemen to reestablish the service of the branch that has been damaged. To alleviate the impact of the damaged branches, the normally-open tie lines 8-21, 12-22, 18-33, and 25-29 are connected. The use of tie-lines during failure or damage to branches of the distribution grid is a common practice in most power distribution systems, when available.

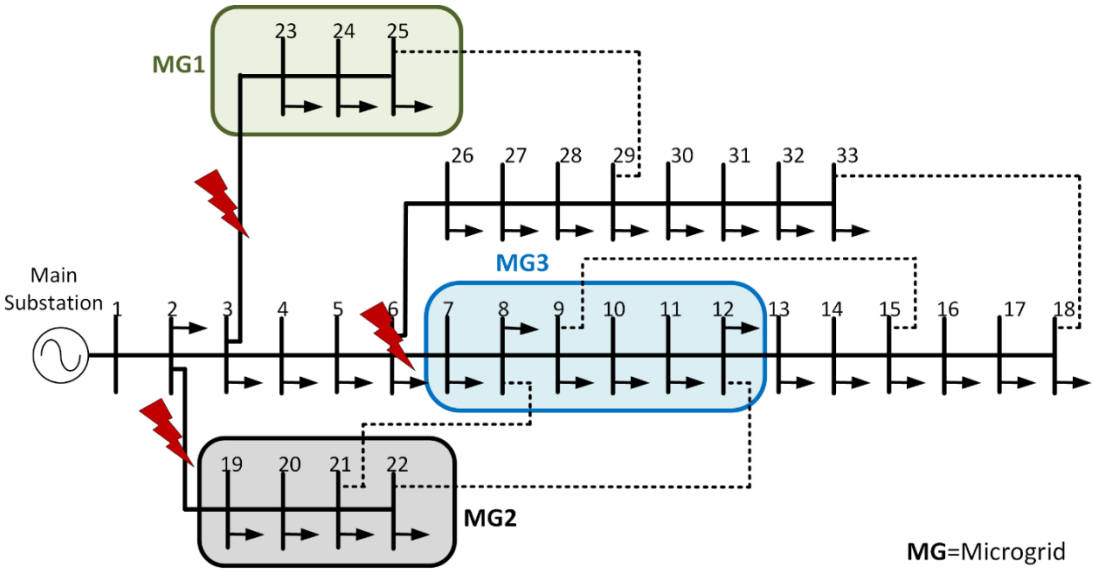

Figure 5.1: Networked microgrids in an IEEE 33-bus distribution network – moderate damage case.

To test the system under failure, five scenarios are considered. The base scenario 1.1 would be the representation of a conventional power distribution system that utilizes available tie-lines to maintain the service of their customers when a high impact event occurs. Scenarios 1.2-1.5 assume DERs are available in the MGs. For scenario 1.2 it is considered a sunny day proceeded the event and as soon as the branches are lost the BESS located in MGs are dispatched to supply the local demand of each MG. Scenario 1.3 also assumes a sunny day proceeded the event and similar to scenario 1.2 the BESS are dispatched after the event occurs. However, in this scenario it is assumed only critical loads (50% of the customers) are met and the rest of the loads are curtailed.

Table 5.2 Resiliency Analysis Case Study Data.

	Bus	**HHs**	**Load (kW)**	**PV (kW)**	**BEV (kW)**	**BESS**	
						Capacity (kWh)	**Output (kW)**
Microgrid 1							
PCG1	23	10	32	50	-	270	50
PCG2	24	12	34	60	-	324	60
CG1	25	15	42	-	-	-	-
Microgrid 2							
PCG3	19	10	28	50	-	270	50
CG2	20	11	30	-	-	-	-
PCG4	21	12	38	60	-	324	60
PCG5	22	12	34	60	-	324	60
Microgrid 3							
CG3	7	40	70	-	-	-	-
CG4	8	40	100	-	-	-	-
PCG6	9	20	48	100	-	540	100
PCG7	10	20	48	100	-	540	100
CG5	11	20	35	-	-	-	-
PCG8	12	25	45	125	-	675	125
Rest of System							
CG6	2	15	48	-	-	-	-
CG7	3	20	56	-	-	-	-
CG8	4	48	120	-	-	-	-
CG9	5	24	60	-	-	-	-
CG10	6	24	60	-	-	-	-
CG11	13	24	60	-	-	-	-
CG12	14	48	120	-	-	-	-
CG13	15	24	60	-	-	-	-
CG14	16	24	60	-	-	-	-
CG15	17	24	60	-	-	-	-
CG16	18	36	90	-	-	-	-
CG17	26	24	60	-	-	-	-
CG18	27	24	60	-	-	-	-
CG19	28	24	60	-	-	-	-
CG20	29	48	120	-	-	-	-
CG21	30	80	200	-	-	-	-
CG22	31	60	150	-	-	-	-
CG23	32	84	210	-	-	-	-
CG24	33	24	60	-	-	-	-

Scenario 1.4 observes the same operation of scenario 1.2 with the difference that a rainy day proceeded the event. Similarly, scenario 1.5 considers the same operation as scenario 1.3 under

rainy day conditions before the event. These scenarios were chosen to represent the various operational strategies that could be considered as well as varying weather. The weather aspect is of fundamental importance as this will affect how much energy is produced by the roof-top solar generators and at the same time how much energy can be stored in the BESS to dispatch when events like the ones considered here occur.

Once the damage to the system and the contingency measures have been set, the distribution system operation is simulated. For all simulations in this chapter power flow is utilized to resemble the operation of the distribution system. When power flow is executed, the power outputs of the roof-top solar and BESS are determined as well as the bus voltages of the distribution network. For simulation purposes it is assumed that the load at any bus with a voltage under 0.9 p.u. will be curtailed. This assumption is made because loads cannot operate under normal conditions with voltages below this value. Figure 5.2 shows the bus voltages for the full day under study. It can be seen that from 5:00 pm to 7:00 pm the voltage at buses 7-22 and 31-33 are below 0.9 p.u. and therefore would be curtailed.

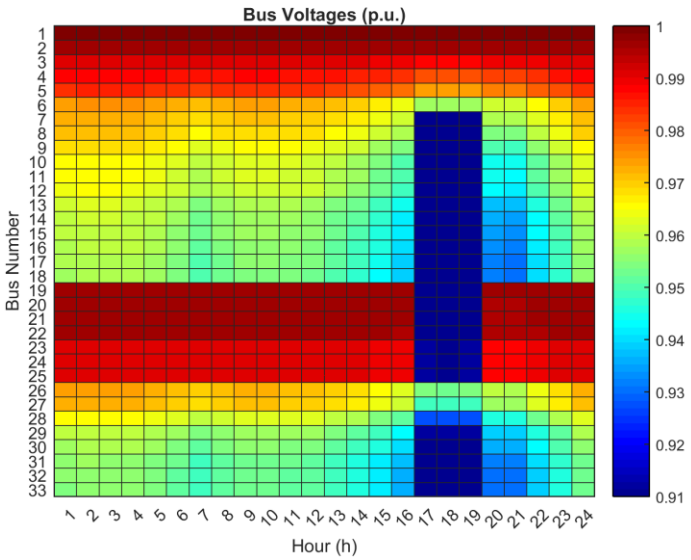

Figure 5.2: Bus voltage profiles base scenario 1.1 – moderate damage case.

Analyzing Figure 5.3 (scenario 1.2) it is noticeable that all bus voltages are above 0.9 p.u. This is achieved by having the MGs supply their local demand through the energy stored in BESSs. Under this scenario no load has to be curtailed during the duration of the outage.

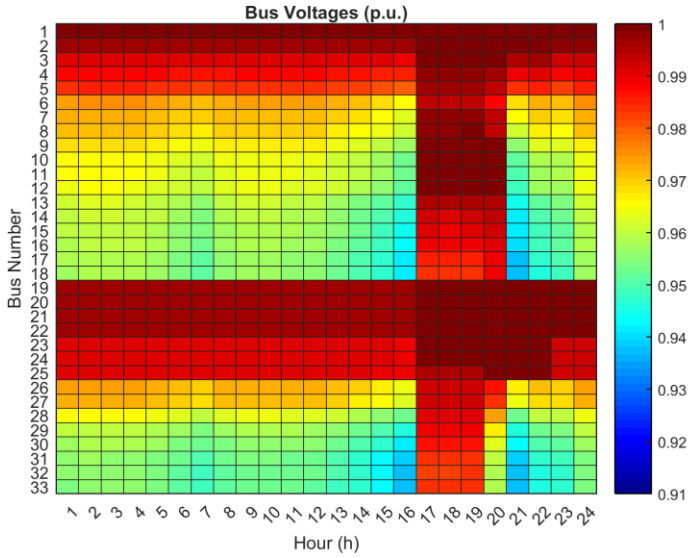

Figure 5.3: Bus voltage profiles sunny day scenario 1.2 – moderate damage case.

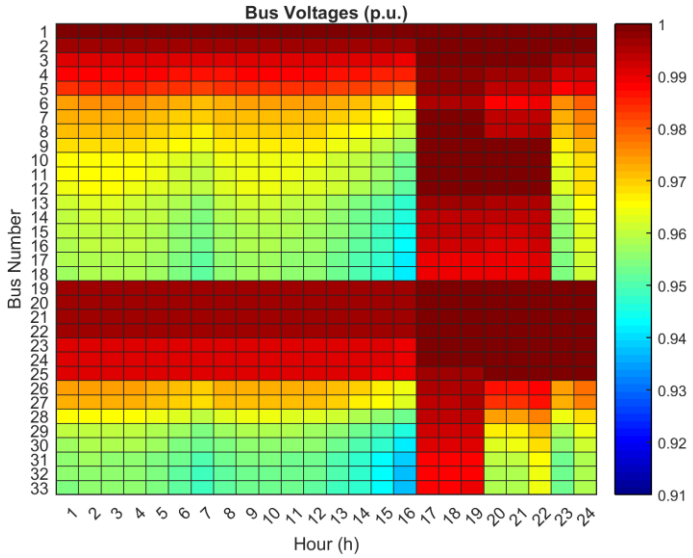

Figure 5.4: Bus voltage profiles sunny day scenario 1.3 – moderate damage case.

In the case of scenario 1.3 (Figure 5.4), only critical loads (50% of loads) remain connected and the rest are curtailed. Having to supply only critical loads ensures that all bus voltages remain above 0.9 p.u. during the duration of the outage. Furthermore, the BESS units can supply the local

demand of each MG for longer periods of time. Figures 5.5 and 5.6, depict the bus voltages for scenarios 1.4 and 1.5, respectively. These scenarios assume a rainy day proceeds the outage. In scenario 1.4, it is observed that from 6:00 pm to 7:00 pm the voltage at buses 7-22 and 31-33 are below 0.9 p.u., therefore loads connected to those buses would be curtailed. Another observation is that due to the outage being proceeded by a rainy day the BESSs can only provide support for 1 hour compared to 3 hours when the outage occurs after a sunny day.

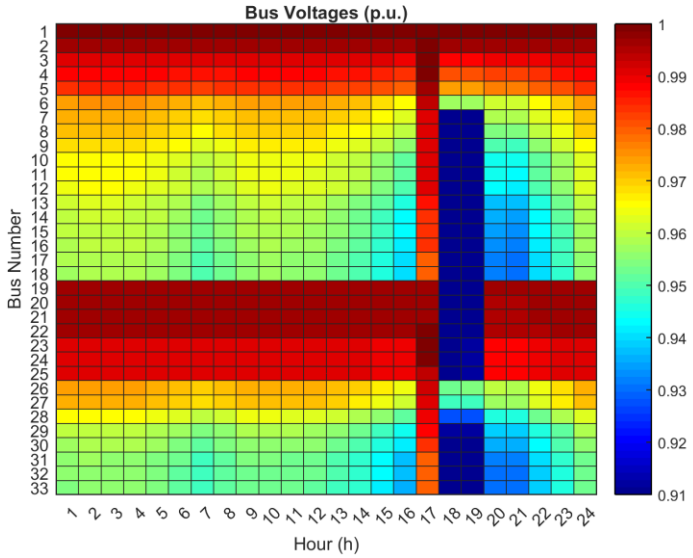

Figure 5.5: Bus voltage profiles rainy day scenario 1.4 – moderate damage case.

For scenario 1.5, critical loads are met by the BESS and the demand is supplied at the MGs for 2 hours (17:00 hrs. to 18:00 hrs.). Afterwards, the loads at buses 7-14 and 19-22 have to be curtailed at 19:00 hrs. as the BESSs can no longer supply the demand of the MGs. These two scenarios clearly show the impact weather has on the support capabilities the BESS can provide as it is dependent on the power that is being produced by the roof-top solar generators. Tables 5.4 and 5.5 present a summary of the two resilience metrics categories that are used to measure the resiliency impacts that DERs can have.

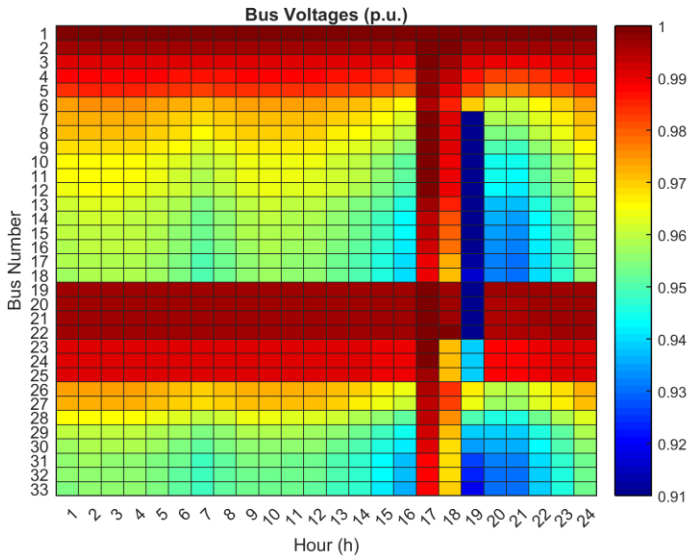

Figure 5.6: Bus voltage profiles rainy day scenario 1.5 – moderate damage case.

Table 5.3 shows the resiliency metrics for the electrical service consequence category. The metrics for this category are cumulative customer-hours of outage, cumulative customer energy demand not served, number and percentage of customers experiencing outage, and average number of customers experiencing outage. Comparing the scenarios, scenario 1.2 had the best performance out of all the scenarios for all resilience metrics, i.e., no customer service was interrupted and therefore no energy demand was unserved. Scenario 1.4 also had a good performance and averaged with scenario 1.2 under these conditions the number of customers experiencing an outage is reduced 30% when compared to the base scenario. Scenarios 1.3 and 1.5, had a much lower improvement compared to the base scenario only a 10% difference in the average number of customers experiencing outage. However, it should be noted that the outage was a low duration outage (3 hours) and that in cases where the outage spans a longer time frame the supply of only critical loads could be more beneficial.

Table 5.3 Resiliency Metrics for Electrical Service Impact: Case 1 Moderate Damage.

Total Customer-Hours of Outage (h)				
Base Scenario 1.1	Scenario 1.2	Scenario 1.3	Scenario 1.4	Scenario 1.5
1,674	0	1,389	1,116	1,668
Total Customer Energy Not Served (kWh)				
Base Scenario 1.1	Scenario 1.2	Scenario 1.3	Scenario 1.4	Scenario 1.5
3,415	0	2,796	2,277	3,196
Total Number and Percentage of Customers Experiencing Outage				
Base Scenario 1.1	Scenario 1.2	Scenario 1.3	Scenario 1.4	Scenario 1.5
558 (60%)	0 (0%)	463 (50%)	558 (60%)	463 (50%)
Average Number and Percentage of Customers Experiencing Outage				
Base Scenario 1.1	Scenarios 1.2 and 1.4		Scenarios 1.3 and 1.5	
558 (60%)	279 (30%)		463 (50%)	

Table 5.4 Resiliency Metrics for Monetary Impact: Case 1 Moderate Damage.

Total Loss of Utility Revenue ($)				
Base Scenario 1.1	Scenario 1.2	Scenario 1.3	Scenario 1.4	Scenario 1.5
355	0	290	236	332
Total Outage Costs ($)				
Base Scenario 1.1	Scenario 1.2	Scenario 1.3	Scenario 1.4	Scenario 1.5
5,022	0	4,167	3,348	5,004
Total Avoided Outage Costs ($)				
Base Scenario 1.1	Scenario 1.2	Scenario 1.3	Scenario 1.4	Scenario 1.5
0	5,022	855	1,674	18

From a monetary consequence perspective (Table 5.4), a similar outcome is observed, scenarios 1.2 and 1.4 obtained the best performance as their average avoided outage cost is $3,348

or a 67% reduction compared to the base scenario. In the case of loss of utility revenue, the best outcome was obtained by scenario 1.2. An interesting observation are the great differences between the loss of utility revenue and outage costs, i.e., it provides a good context of the financial impacts that are created when electric energy is lost.

5.3.3 Resiliency Analysis of Distribution Grid-Heavy Damage Case

In this case, three MGs are also assumed to be located in a 33-bus radial distribution system as shown in Figure 5.7. To evaluate the impact of the MGs and the DERs to the resiliency of the distribution system to natural disasters it is assumed a storm occurred and created heavy damage to the feeders of the system. Specifically, to the main feeder branch 1-2 as shown in Figure 5.7. The event is assumed to have occurred at 17:00 hrs. (5:00 pm) and the duration of the outage is 3 hours (17:00 hrs. to 19:00 hrs.). To test the system under failure, five scenarios are considered. The base scenario 2.1 would be the representation of a conventional power distribution system. In this case, the use of tie lines is not sufficient to reestablish the power distribution system as the main feeder guides power to the whole distribution system. Scenarios 2.2-2.5 assume DERs are available in the MGs. For scenario 2.2 it is considered a sunny day proceeded the event and that as soon as the main branch is lost the BESS located in MGs are dispatched to supply the local demand of each MG. Scenario 2.3 also assumes a sunny day proceeded the event and similar to scenario 2.2 the BESS are dispatched after the event occurs. However, in this scenario it is assumed only critical loads (50% of the customers) are met and the rest of the loads are curtailed. Scenario 2.4 observes the same operation of scenario 2.2 with the difference that a rainy day proceeded the event. Scenario 2.5 considers the same operation as scenario 2.3 under rainy day conditions before the event.

Once the damage to the system and the contingency measures have been set, the distribution system operation is simulated. In the same manner as case 1, for simulation purposes, it is assumed that the load at any bus with a voltage under 0.9 p.u. will be curtailed.

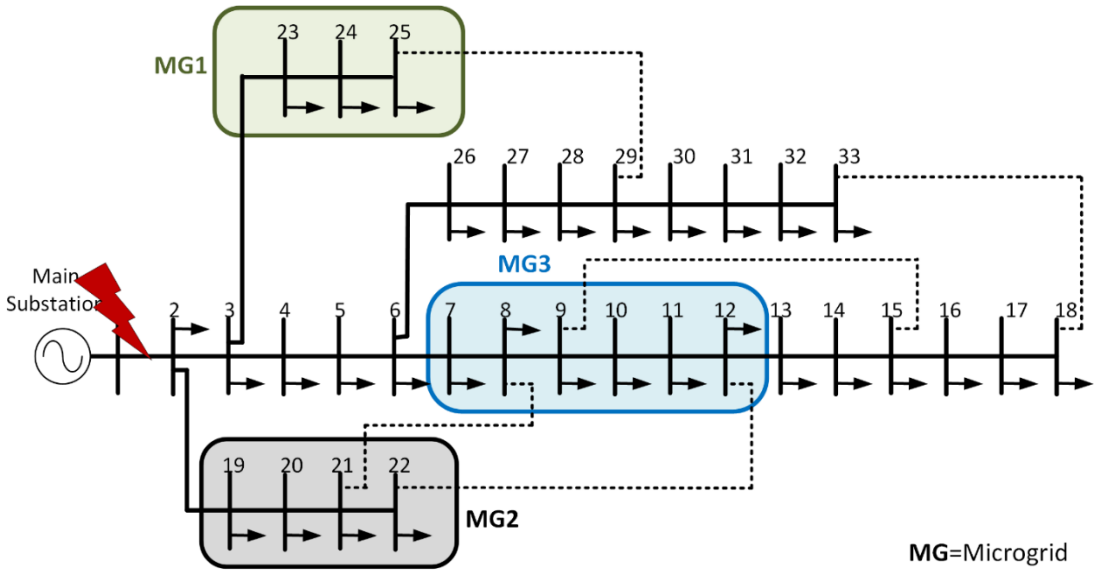

Figure 5.7: Networked microgrids in an IEEE 33-bus distribution network – heavy damage case.

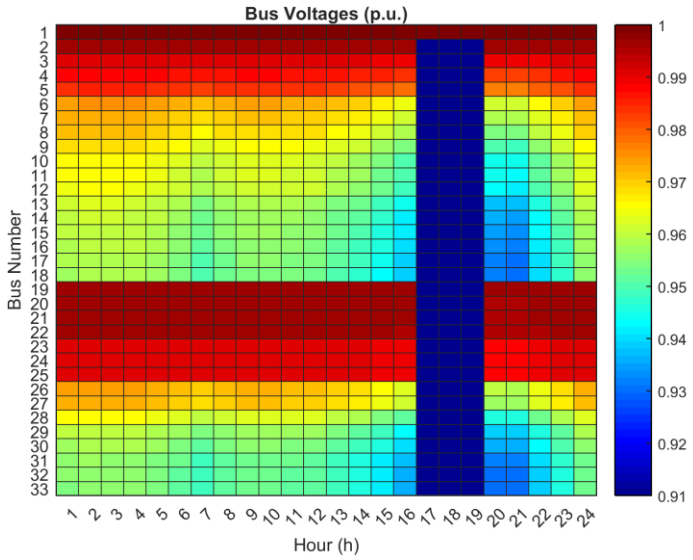

Figure 5.8: Bus voltage profiles base scenario 2.1 – heavy damage case.

Figure 5.8 shows the bus voltages for the full day under study. It can be seen that from 17:00 hrs. to 19:00 hrs. the voltage at buses 2-33 is below 0.9 p.u. and therefore would be curtailed.

Analyzing Figure 5.8 (scenario 2.1) it is noticeable that due to the damage suffered to the main branch 1-2 the whole system goes into a blackout. For scenario 2.2 (Figure 5.9) only the MGs buses 7-12 and 19-25 remain energized through the use of the roof-top solar and the BESSs for the duration of the outage (3 hours).

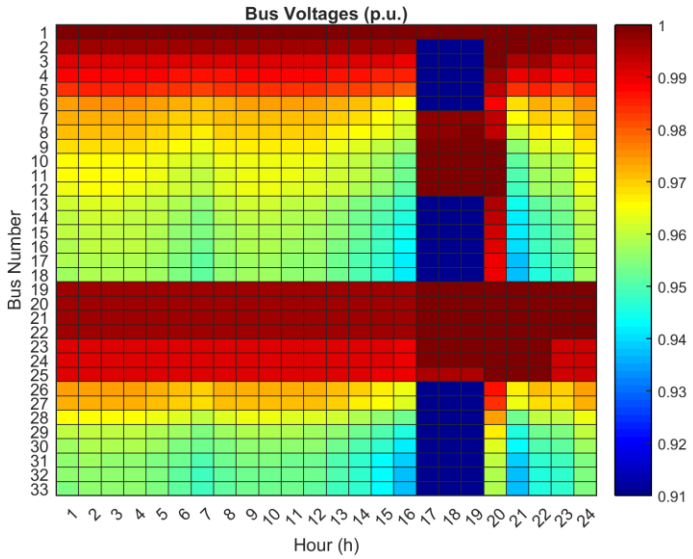

Figure 5.9: Bus voltage profiles sunny day scenario 2.2 – heavy damage case.

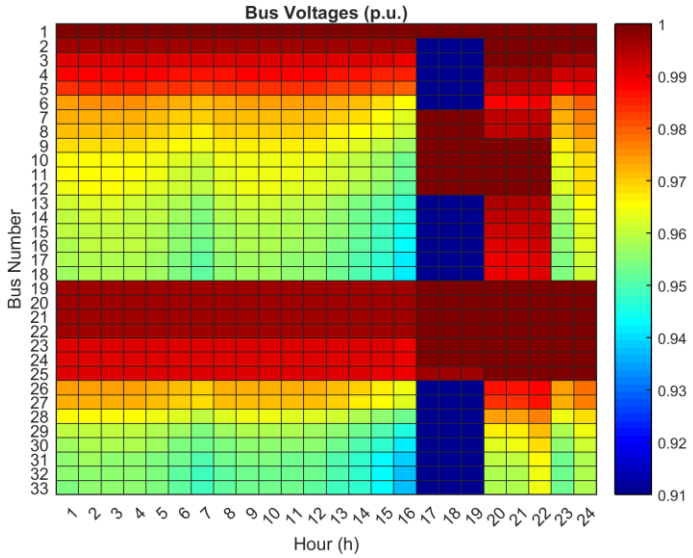

Figure 5.10: Bus voltage profiles sunny day scenario 2.3 – heavy damage case.

When supplying only critical loads and curtailing the remaining 50% of the loads (scenario 2.3) the MGs are also the only buses of the distribution system that remain operational. This can be seen in Figure 5.10. In the scenario where a rainy day precedes the outage (Figure 5.11), only buses 23-25 can remain operational for the time frame of the outage (3 hours), with buses 7-12 and 19-22 remaining online for only 1 hour, and the rest of the buses being under complete blackout. And finally, for scenario 2.5 (rainy day and only critical loads supplied) only buses 23-25 can remain operational for the 3-hour outage, buses 7-12 and 19-22 remaining online for 2 hours, and the rest of the buses are under outage (Figure 5.12).

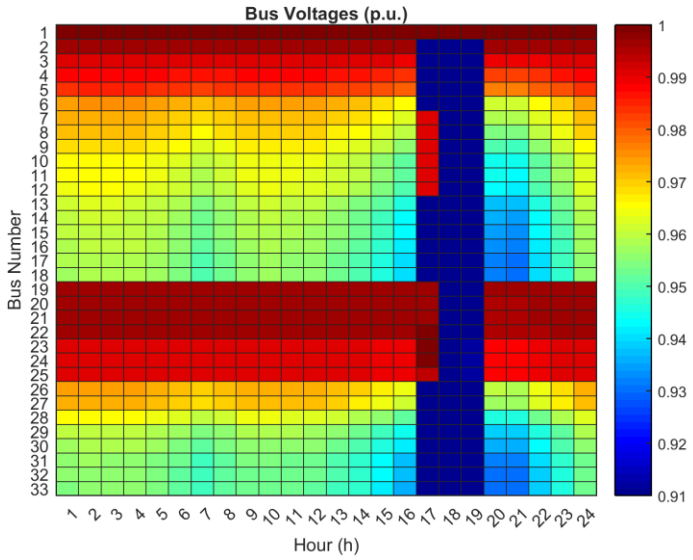

Figure 5.11: Bus voltage profiles rainy day scenario 2.4 – heavy damage case.

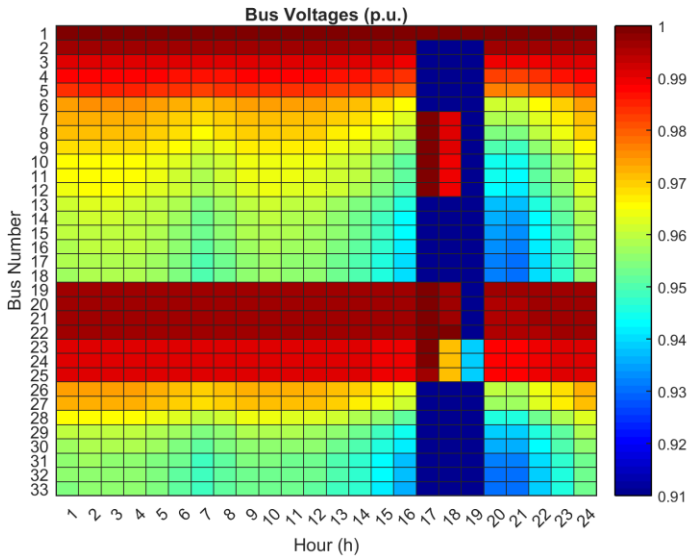

Figure 5.12: Bus voltage profiles rainy day scenario 2.5 – heavy damage case.

One of the interesting observations from scenario 2.5 is that curtailing load and only supplying critical loads extends the period of time for which the BESSs could provide energy. As is seen when comparing Figures 5.11 and 5.12, buses 7-12 and 19-22 went from only being supplied for 1-hour to 2-hours. This reinforces what has been mentioned in sub-section 5.3.2, that in certain situations especially, for long-duration outages or when limited energy is stored in the BESS curtailing the load can allow sections of the distribution system to remain online instead of all being under blackout. When analyzing the resiliency metrics for electrical service (Table 5.5), it is shown that scenarios 2.2 and 2.4 had the best performance by having on average 33% fewer customers under outage. Compared to case 1 (moderate damage) the tie lines are not sufficient to maintain the system under operation as the main feeder was lost and all customers would be lost if no DERs were present.

Table 5.5 Resiliency Metrics for Electrical Service Impact: Case 2 Heavy Damage.

Total Customer-Hours of Outage (h)				
Base Scenario 2.1	Scenario 2.2	Scenario 2.3	Scenario 2.4	Scenario 2.5
2,778	2,037	2,408	2,457	2,513
Total Customer Energy Not Served (kWh)				
Base Scenario 2.1	Scenario 2.2	Scenario 2.3	Scenario 2.4	Scenario 2.5
5,955	4,614	5,103	5,368	5,419
Total Number and Percentage of Customers Experiencing Outage				
Base Scenario 2.1	Scenario 2.2	Scenario 2.3	Scenario 2.4	Scenario 2.5
926 (100%)	349 (38%)	803 (87%)	889 (96%)	803 (87%)
Average Number and Percentage of Customers Experiencing Outage				
Base Scenario 2.1	Scenario 2.2 and 2.4		Scenario 2.3 and 2.5	
926 (100%)	619 (67%)		803 (87%)	

Table 5.6 Resiliency Metrics for Monetary Impact: Case 2 Heavy Damage.

Total Loss of Utility Revenue ($)				
Base Scenario 2.1	Scenario 2.2	Scenario 2.3	Scenario 2.4	Scenario 2.5
618	479	530	557	563
Total Outage Costs ($)				
Base Scenario 2.1	Scenario 2.2	Scenario 2.3	Scenario 2.4	Scenario 2.5
8,334	6,111	7,223	7,371	7,538
Total Avoided Outage Costs ($)				
Base Scenario 2.1	Scenario 2.2	Scenario 2.3	Scenario 2.4	Scenario 2.5
0	2,223	1,112	963	797

Looking into the resiliency metrics for monetary impact (Table 5.6), scenarios 2.2 and 2.3 achieve the highest avoided outage cost which are 27% and 13% less than the base scenario 2.1.

In this specific case, where there is a major failure to the distribution system, outage costs and loss of utility revenue are high for all scenarios. Showing that although DERs can provide support to the power distribution system, the support is dependent on the weather (solar irradiance availability) and the BESS capacity, i.e., a low capacity BESS can only provide limited support to the distribution grid.

5.4 SUMMARY

This chapter provided a detailed analysis of the impacts DERs can have on the resiliency of a power distribution system to natural disasters. A resiliency analysis process was presented with two case studies that are tested under different scenarios and evaluated utilizing different resilience metrics. This chapter contributed to providing realistic case studies that show the potential benefits that DERs managed in networked MGs can provide a power distribution grid. Test results indicated that DERs can provide support to the power distribution system by scheduling the discharge of BESS during outages. For the specific case studies presented in this chapter having roof-top solar and BESS managed by networked MGs on an average can reduce the number of customers experiencing an outage between 38%-58% on a sunny day and 8%-9% on a rainy day when compared to the base scenarios that do not consider DERs. Also, on an average the avoided outage costs during sunny days can be between 20%-58% and between 11%-17% on a rainy day. It should be emphasized that these results were obtained for specific case studies; hence more case studies with different components and a larger test system could provide further solid conclusions. Nonetheless, it is shown that DERs can improve the resiliency of power distribution systems.

Chapter 6: Conclusions and Recommendations for Future Work

6.1 INTRODUCTION

The final chapter of this dissertation is divided into three major sections (1) summary and conclusions, (2) contributions, and (3) recommendations for future work. The summary and conclusions section presents the findings of the study to justify the objectives of this dissertation. The contributions section outlines the major contributions of this dissertation and the final section provides recommendations for future research.

6.2 SUMMARY AND CONCLUSIONS

A summary of this dissertation is outlined as follows.

Chapter 2 presented a literature review of various DER integration methodologies. Issues with control and management of DERs were described. The emerging transactive framework and the smart grid of the future coupled with MG energy management methodologies were discussed. The urgent need to enhance the resilience of the electric power grid and vulnerabilities of existing infrastructure were presented as well.

Chapter 3 presented an efficient strategy to optimally incorporate and locate RES-ESS in smart DNs. The proposed planning strategy allows the resolution of the UC and ED problems and optimally determines the best bus location to integrate PV and wind-ESS systems. A comparison of the test results demonstrated that power losses and peak loads are significantly reduced, achieving increased savings and a reduction in GHG emissions. Another benefit is that wind power becomes more dispatchable by using the day-ahead forecasted information with efficient utilization of ESS. This efficient charge/discharge of the ESS leads to a reduction in forecast error freeing-up thermal capacity and avoiding the commitment of expensive thermal units. Moreover, savings can be increased if other benefits are taken into consideration, such as reliability

improvement and the mitigation of power quality problems. The proposed method can be applied to larger networks and for different time scales; however, the computation time may slightly increase.

In Chapter 4, a new hybrid TC+MPC control mechanism for residential prosumer-centric networked MGs was presented. The proposed hybrid TC+MPC combined the control capabilities and features of the MPC and the TC, creating a robust control mechanism that is driven by transactive incentive signals, and thus, also providing the MGEMS capability to deal with the stochastic nature of BEV driving by using an MCS to generate the BEV driving patterns. The proposed TC+MPC was able to effectively generate the BEV-charge and BESS-discharge schedules for the CGs/PCGs located in each MG. Test results demonstrated the potential of using pricing mechanisms for demand-side management of DERs. The results can be summarized as follows: (i) reduction in peak load (between 21–30%) by shifting surplus PV power from off-peak hours using BESS; (ii) reduction in load ramp rates between 39–58%; (iii) reduction in power losses between 6.3–6.8%; (iv) bus voltage improvements between 25–75% for busses that present undervoltages; and (v) total cost reductions between 29–57% and savings between 52–144%. Therefore, the main objectives of the MGEMS are met by allowing CGs/PCGs to minimize their costs as well as to maximize their savings. It can also be inferred from the results that the incentives provided by the pricing mechanisms can encourage customers to not only reduce peak demand but also to install more demand-side energy resources (e.g., but not limited to BESS and rooftop solar). Moreover, the DSO or utility operators can benefit from controlled customer participation by reducing their system power losses, by improving bus voltage profiles, and by reducing overloading system components. An important finding of the case studies is that the BESS-discharging operation can create steep load ramp rates when discharging during peak periods. This

aspect should be considered high priority when defining the discharge constraints to avoid incurring negative impacts on the grid. For the case studies presented in this chapter, we assumed full BESS discharging (SOC = 0%). It should be noted that this discharging operation could impact the expected life of the BESS.

Chapter 5 provided a detailed analysis of the impacts DERs can have on the resiliency of a power distribution system to natural disasters. A resiliency analysis process was presented with two case studies that are tested under different scenarios and evaluated utilizing different resilience metrics. The results indicate that DERs can provide support to the power distribution system by scheduling the discharge of BESS during outages. For the specific case studies presented in this chapter having roof-top solar and BESS managed by networked MGs on average can reduce the number of customers experiencing an outage between 38%-58% on a sunny day and 8%-9% on a rainy day when compared to the base scenarios that don't have DERs. Also, on average the avoided outage costs on sunny days can be between 20%-58% and between 11%-17% on rainy days.

6.3 CONTRIBUTIONS

In contrast to the existing literature, the major contributions of this dissertation to the state-of-the-art are the following.

- An efficient strategy to optimally incorporate and locate RES-ESS in smart DNs to reduce overall power losses and peak load;
- An integrated energy management system that allows the resolution of UC and ED problems using the forecasted and actual data of wind, PV, and load. This prevents the over commitment of thermal generation and increases in spinning reserve;

- An efficient ESS control strategy that utilizes the forecasted data of wind power output for its operation. Thus, our ESS control strategy determines the optimal charge/discharge cycle of the ESS.
- Development of a new hybrid TC+MPC control mechanism to manage DERs (BEVs, solar PV, and BESS) of networked MGs constituted by consumer groups and prosumer groups and detailed study of their behavior while being incentivized by different price signals;
- Development of TIS and TFS signals where TIS is based on DLMP and distribution system conditions, whereas TFS development is based on CGs/PCGs net load and BEV driving patterns generated by MCS.
- Detailed analysis of the impacts on the distribution grid due to the use of TCs for DER management, i.e., bus voltage and power loss impacts.
- Detailed Cost/Savings analysis for consumers/prosumers under different pricing rates when they are equipped with BEVs, solar PV, and hybrid solar PV-BESS systems.
- Development of a detailed resiliency analysis of realistic case studies that show the potential benefits that DERs managed in networked MGs can provide a power distribution grid.
- Calculation of resilience metrics for electrical service and monetary impacts using DERs, i.e., total customer-hours of outage, total customer energy not served, total and average number of customers experiencing outage, total loss of utility revenue, and total outage costs.

6.4 RECOMMENDATIONS FOR FUTURE WORK

There are different aspects that have not been considered in this dissertation. Following are the potential areas or topics that could be addressed in future research.

- Future work would be interesting to study the depth of discharge impacts on the BESS life cycle for larger time frames (e.g., months and years) to analyze the effects of continuous BEV and BESS charge/discharge cycles.
- It would also be interesting to carry out energy trading in local MG and among MGs and study the effects on power flows and voltage levels.
- From an economic perspective, different TOU and dynamic tariffs could also be tested to further verify the capabilities of the TC. Costs associated with DER purchase and installation could be included to better reflect the net costs/savings.
- From a resiliency perspective, random duration faults could be considered to test the ability of the DERs to support the distribution system during longer periods of time. Other resiliency metrics could also be considered, e.g., time of recovery and restoration costs.

References

[1] EPRI, "Vision for a holistic power supply and delivery chain," *Technical report:* 1018587, 2009.

[2] F.D. Wattjes and J.G. Slootweg, "Design considerations for smart microgrids," in *Proc. Power Engineering Conference (UPEC),* pp. 1-6. Sep. 2013.

[3] M. Parvizimosaed, A. Anvari-Moghaddam, A. Ghasemkhani, and A. Rahimi-Kian, "Multi-objective dispatch of distributed generations in a gridconnected micro-grid considering demand response actions," in *Proc. Electricity Distribution (CIRED),* Jun. 2013.

[4] Q. Wang and P. Zhang, "Energy management system for multi-microgrid," in *Proc. China International Conference on Electricity Distribution (CICED),* Sep. 2014.

[5] GridWise Architecture Council. GridWise transactive energy framework, *Technical report*, 2017.

[6] F. Rahimi, "Valuation of transactive energy systems," in *Proc. of Valuation of Transactive Energy Systems Technical Meeting,* Jul., 2015.

[7] A. K. Bejestani, A. Annaswamy, and T. Samad "A Hierarchical transactive control architecture for renewables integration in smart grids: analytical modeling and stability," *IEEE Transactions on Smart Grid*, vol. 5, no. 4, Jul. 2014.

[8] D. Jin, X. Zhang, and S. Ghosh, "Simulation models of network design and hierarchical transactive control mechanisms in smart grids," in Proc. IEEE PES GM 2012, Jan. 2012.

[9] Transactive Coordination Signals, U.S. Department of Energy, August 2013 [Online]. Available: http://www.pnwsmartgrid.org/docs/Transactive_Coordination_Signals.pdf.

[10] Pacific Northwest Smartgrid Demonstration Project, "Technology performance report highlights," April, 2015.

[11] Cazalet, E., De Martini, P., Price, J., Woychik, E., and Caldwell, J. "Transactive energy models," *NIST Transactive energy challenge: business and regulatory models, White Paper,* 2016.

[12] GridWise Architecture Council, "Transactive energy systems research, development and deployment roadmap," *White paper*, 2018.

[13] U.S. Energy Information Administration, "Electricity Data Browser Net Generation by Energy Source: 2001 – 2018," 2019. [ONLINE] Available online: https://www.eia.gov/electricity/annual/html/epa_03_01_a.html (accessed on April 2019).

[14] U.S. Energy Information Administration, "Annual Energy Outlook 2019 with projections to 2050," 2019. [ONLINE] Available online: www.eia.gov/aeo (accessed on January 2019).

[15] International Energy Agency-IEA, "Global EV Outlook 2018," *Technical report*, 2018.

[16] A. Zibelman, "REVing up the energy vision in New York," *IEEE Power and Energy Magazine*, vol. 14, pp. 18-24, May 2016.

[17] K. Kok and S. Widergren, "A society of devices: integrating intelligent distributed resources with transactive energy," *IEEE Power and Energy Magazine*, vol. 14, no. 3, pp. 34-45, May. 2016.

[18] Wang, Y., Zhou, S., and Huo, H. “Cost and CO2 reductions of solar photovoltaic power generation in China: Perspectives for 2020,” *Renewable and Sustainable Energy Reviews*, vol. 39, pp. 370–380, November 2014.

[19] Tan, M., Serrano, B., and Mohammed, O. "Fuzzy logic based power and thermal management system design for multi-cell lithium-ion battery bank protection and operation," in *Proc. Power Systems Conference (PSC)*, Clemson University, pp.1-5, March 2014.

[20] Al-Muhaini, M., and Heydt, G.T. “A novel method for evaluating future power distribution system reliability,” *IEEE Trans. on Power Systems,* Vol. 28, No. 3, pp. 3018–3027, August 2013.

[21] El-Khattam, W., and Salama, M. M. A. “Distributed generation technologies, definitions and benefits,” *Elect. Power Syst. Res.*, Vol. 71, No. 2, pp. 119–128, October 2004.

[22] G. Pepermans, J. Driesen, D. Haeseldonckx, R. Belmans, and W. D’Haeseleer, “Distributed generation: Definition, benefits and issues,” *Energy Policy*, Vol. 33, pp. 787–798, 2005.

[23] D. H. Popovi´c, J. A. Greatbanks, M. Begovi´c, and A. Pregelj, “Placement of distributed generators and reclosers for distribution network security and reliability,” *Int. J. Elect. Power & Energy Syst.*, vol. 27, no. 5–6, pp. 398–408 June–July 2005.

[24] D. Zhu, R.P. Broadwater, K.S. Tam, R. Seguin, and H. Asgeirsson, “Impact of DG placement on reliability and efficiency with time-varying loads,” *IEEE Transactions on Power Systems*, vol. 21, no. 1, pp. 419 - 427, January 2006.

[25] P. Chiradeja and R. Ramakumar, “An approach to quantify the technical benefits of distributed generation,” *IEEE Transactions on Energy Conversion*, vol. 19, no. 4, pp. 764–773, December 2004.

[26] D.M. Cao, D. Pudjianto, G. Strbac, A. Martikainen, S. Karkkainen, and J. Farin, “Costs and benefits of DG connections to grid system—studies on the UK and finish systems,” *DG-GRID Project—European Commission*, December 2006.

[27] L.F. Ochoa, A. Padilha-Feltrin, and G.P. Harrison, “Evaluating distributed generation impacts with a multiobjective index,” *IEEE Transactions on Power Delivery*, vol. 21, no. 3, pp. 1452–1458, July 2006.

[28] H.A. Gil and G. Joos, “On the quantification of the network capacity deferral value of distributed generation,” *IEEE Transactions on Power Systems,* vol. 21, no. 4, pp. 1592–1599, November 2006.

[29] G.P. Harrison, A. Piccolo, P. Siano, and A.R. Wallace, “Exploring the trade-offs between incentives for distributed generation developers and DNOs,” *IEEE Transactions on Power Systems*, vol. 22, no. 2, pp. 821–828, May 2007.

[30] V.V.S.N. Murthy and A. Kumar, “Comparison of optimal DG allocation methods in radial distribution systems based on sensitivity approaches,” *Int. J. Elect. Power Energy Syst.*, vol. 53, pp. 450–467, December 2013.

[31] S. Ghosh and S.P. Ghoshal, “Two analytical approaches for optimal placement of distributed generation unit in power systems,” in *Proc. International Conference on Power Systems (ICPS)*, pp. 1–6, December 2009.

[32] T.N. Shukla, S.P. Singh, V. Srinivasarao, and K.B. Naik, "Optimal sizing of distributed generation placed on radial distribution systems," *Electric Power Components and Systems,* vol. 38, no. 3, pp. 260–274, January 2010.

[33] S. Ghosh, S.P. Ghoshal, and S. Ghosh, "Optimal sizing and placement of distributed generation in a network system," *Int. J. Elect. Power Energy Syst.*, vol. 32, no. 8, pp. 849–856, October 2010.

[34] R.K. Singh and S.K. Goswami, "Multi-objective optimization of distributed generation planning using impact indices and trade-off technique," *Electric Power Components and Systems*, vol. 39, no. 11, pp. 1175–1190, August 2011.

[35] L.F. Grisales, A. Grajales, O.D. Montoya, R.A. Hincapié, and M. Granada, "Optimal location and sizing of distributed generators using a hybrid methodology and considering different technologies," in *Proc. IEEE 6th Latin American Symposium on Circuits & Systems (LASCAS)*, pp. 1-4, February 2015.

[36] P. Kayal, T. Ashish, and C.K. Chanda, "Simultaneous placement and sizing of renewable dgs and capacitor banks in distribution network," in *Proc. International Conference on Circuit, Power and Computing Technologies (ICCPCT)*, pp. 607-611, March 2014.

[37] H. Keshtkar, J. Solanki, and S.K. Solanki, "Analyzing multi-microgrid with stochastic uncertainties including optimal PV allocation," in *Proc. Int. Conf. on Smart Cities and Green ICT Systems (SMARTGREENS)*, pp. 1-9, May 2015.

[38] H. Pandžić, Y. Wang, T. Qiu, Y. Dvorkin, and D.S. Kirschen, "Near-optimal method for siting and sizing of distributed storage in a transmission network," in *IEEE Transactions on Power Systems*, vol. 30, no. 5, September 2015.

[39] V. Kalkhambkar, R. Kumar, and R. Bhakar, "Optimal sizing of PV-battery for loss reduction and intermittency mitigation," in *Proc. IEEE Int. Conference on Recent Advances and Innovations in Engineering (ICRAIE)*, pp. 1-6, May 2014.

[40] EPRI, "Methodological approach for estimating the benefits and costs of smart grid demonstration projects," *Technical report*: 1020342, 2010.

[41] The US Department of Energy, "The smart grid: an introduction," 2008.

[42] P. Zhang, F. Li and N. Bhatt, "Next-Generation Monitoring, Analysis, and Control for the Future Smart Control Center," *IEEE Transactions on Smart Grid*, vol. 1, no. 2, pp. 186-192, September 2010.

[43] F. Rahimi, A. Ipakchi, and F. Fletcher, "The changing electrical landscape," *IEEE Power and Energy Magazine*, vol. 14, pp. 52-62, May 2016.

[44] L. Kristov, P. De Martini, and J.D. Taft, "A tale of two visions: designing a decentralized transactive electric system," *IEEE Power and Energy Magazine*, vol. 14, no. 3, pp. 63-69, May 2016.

[45] D. J. Hammerstrom, R. Ambrosio, J. Brous, T. A. Carlon, D. P. Chassin, J. G. DeSteese, R. T. Guttromson, G. R. Horst, O. M. Järvegren, R. Kajfasz, and S. Katipamula, "Pacific northwest gridwise testbed demonstration projects - Part I" *Olympic Peninsula Project*, October 2007.

[46] Battelle Memorial Institute, "Pacific Northwest Smartgrid Demonstration Project: technology performance report," *Technical report*, vol. 1, Jun. 2015.
[47] National Institute of Standards and Technology (NIST), "Transactive Energy Modeling and Simulation Challenge for the Smart Grid", [Online]. Available http://www.nist.gov/smartgrid/techallenge.cfm
[48] Recommendations of the NYISO Consumer Advisory Council to the NYISO Board of Directors, Final Report. [Online]. Available: http://www.nyiso.com/public/webdocs/markets_operations/committees/consumer_advisory_council/Final%20NYISO%20CAC%20Report%20Nov%2011%202013.pdf
[49] Energy Storage and Distributed Energy Resources Enhancements Phase 2 Issue Paper, Comments of TeMix Inc., CAISO. [Online]. Available: https://www.caiso.com/Documents/TeMixIncComments-EnergyStorageandDistributedEnergyResourcesPhase2-IssuePaper.pdf
[50] Z. Liu, Q. Wu, S. Huang, and H. Zhao, "Transactive energy: a review of state of the art and implementation," *Proc. IEEE PowerTech Manchester*, pp. 1-6, 2017.
[51] J. Li, C. Zhang, Z. Xu, J. Wang, J. Zhao, and Y.J.A. Zhang, "Distributed transactive energy trading framework in distribution networks," *IEEE Transactions on Power Systems,* vol. 33, no. 6, pp. 7215–7227, 2018.
[52] H.S.V.S.K. Nunna and D. Srinivasan, "Multiagent-based transactive energy framework for distribution systems with smart microgrids," *IEEE Transactions on Industrial Informatics,* vol. 13, no. 5*,* pp. 2241–2250, 2017.
[53] Y. Amanbek, Y. Tabarak, H.S.V.S.K. Nunna, and S. Doolla, "Decentralized transactive energy management system for distribution systems with prosumer microgrids," i*n Proc. 19th Int. Carpathian Control Conf.,* pp. 553–558, 2018.
[54] Y.K. Renani, M. Ehsan, and M. Shahidehpour, "Optimal transactive market operations with distribution system operators," *IEEE Transactions on Smart Grid,* vol. 9, no. 6, pp. 6692–6701, 2018.
[55] Z. Liu, Q. Wu, K. Ma, M. Shahidehpour, Y. Xue, and S. Huang, "Two-stage optimal scheduling of electric vehicle charging based on transactive control," *IEEE Transactions on Smart Grid,* vol. 10, no. 3, pp. 2948–2958, 2019.
[56] Z. Liu, Q. Wu, M. Shahidehpour, C. Li, Huang, S.; Wei, W. "Transactive real-time electric vehicle charging management for commercial buildings with pv on-site generation," *IEEE Transactions on Smart Grid,* 2018, *(Early Access)*.
[57] J. Hu, G. Yang, and H.W. Bindner, "Network constrained transactive control for electric vehicles integration," *in Proc. 2015 IEEE PESGM,* 2015, pp. 1-5, 2015.
[58] R. Shigenobu, M. Kinjo, P. Mandal, A. Howlader, and T. Senjyu, "Optimal operation method for distribution systems considering distributed generators imparted with reactive power incentive", *Applied Sciences,* vol. 8, no. 8, 2018.
[59] H. Wang and J. Huang, "Incentivizing energy trading for interconnected microgrids, *IEEE Transactions on Smart Grid*," vol. 9, no. 4, pp. 2647–2657, 2018.

[60] W. Liu, J. Zhan, and C.Y. Chung, "A novel transactive energy control mechanism for collaborative networked microgrids," *IEEE Transactions on Power Systems, vol. 34, no. 3,* pp. 2048 – 2060, 2019.

[61] M.E. Khodayar, S.D. Manshadi, and A. Vafamehr, "The short-term operation of microgrids in a transactive energy architecture". *The Electricity Journal*, vol. 29, no. 10, pp. 41–48, 2016.

[62] Y. Jingpeng, H. Zhijian, L. Chendan, J.C. Vasquez, and J.M. Guerrero, "Economic power schedule and transactive energy through an intelligent centralized energy management system for a dc residential distribution system," *Energies*, vol. 10, 2017.

[63] G. Prinslooa, A. Mammolib, and R. Dobsona, "Customer domain supply and load coordination: A case for smart villages and transactive control in rural off-grid microgrids," *Energy*, vol.135, pp. 430-441, 2017.

[64] B. Canizes, J. Soares, A. Costa, T. Pinto, F. Lezama, P. Novais, and Z. Vale "Electric vehicles' user charging behavior simulator for a smart city," *Energies,* vol. 12, no. 8, 2019.

[65] A. Dubey and S. Santoso, "Electric vehicle charging on residential distribution systems: impacts and mitigations," *IEEE Access, vol. 3,* 2015.

[66] H. Suyono, M.T. Rahman, H. Mokhlis, M. Othman, H. Azil Illias, and H. Mohamad, "Optimal scheduling of plug-in electric vehicle charging including time-of-use tariff to minimize cost and system stress," *Energies,* vol. 12, no. 8, 2019.

[67] D.A. Chekired, L. Khoukhi, and H.T. Mouftah, "Decentralized cloud-SDN architecture in smart grid: a dynamic pricing model," *IEEE Transactions on Industrial Informatics,* vol. 14, no. 3, pp. 1220-1231, 2018.

[68] M. Pasetti, S. Rinaldi, A. Flammini, M. Longo, and F. Foiadelli, "Assessment of electric vehicle charging costs in presence of distributed photovoltaic generation and variable electricity tariffs," *Energies,* vol. 12, no. 3, 2019.

[69] S. Liu and A.H. Etemadi, "A dynamic stochastic optimization for recharging plug-in electric vehicles," *IEEE Transactions on Smart Grid,* vol. 9, no. 5, pp. 4154-4161, 2018.

[70] R. E. Brown, C. S. Wilson, and H. van Nispen, "Becoming the utility of the future," *IEEE Power and Energy Magazine*, pp. 57-65, September-October 2016.

[71] A. Golami, F. Aminifar, and M. Shahidehpour, "Front lines against the darkness," *IEEE Electrification Magazine*, vol. 4, no. 1, pp. 18-24, March 2016.

[72] Office for Coastal Management, National Oceanic and Atmosperic Administration, "Weather Disasters and Costs," Available online: https://coast.noaa.gov/states/fast-facts/weather-disasters.html.

[73] L. Ren, Y. Qin, B. Wang, P. Zhang, P. B. Luh, and R. Jin, "Enabling resilient microgrid through programmable network," *IEEE Transactions on Smart Grid*, vol. 8, no. 6, pp. 2826 – 2836, November 2017.

[74] P. C. Loh, L. Ding. Y. Chai, and F. Blaabjerg, "Autonomous operation of hybrid microgrid with AC and DC subgrids," *IEEE Transactions on Power Electronics*, vol. 28, No. 5, pp. 2214–2223, May 2013.

[75] R. Majumder, "A hybrid microgrid with DC connection at back to back converters," *IEEE Trans. Smart Grid*, vol. 5, No. 1, pp. 251–259, January 2014.

[76] N. Eghtedarpour and E. Farjah, "Power control and management in a hybrid AC/DC microgrid," *IEEE Transactions on Smart Grid*, vol. 5, No. 3, pp. 1–12, April 2014.

[77] M. Pipattanasomporn, H. Feroze and S. Rahman, "Securing critical loads in a PV-based microgrid with a multi-agent system," *Renewable Energy*, vol. 39, no. 1, pp. 166-174, March 2012.

[78] R. Zamora and A.K. Srivastava, "Controls for microgrids with storage: Review, challenges, and research needs," *Renewable and Sustainable Energy Reviews*, vol. 14, pp. 2009-2018, 2010.

[79] E. J. Ng and R. A. El-Shatshat, "Multi-microgrid control systems (MMCS)," *in Proc. IEEE PESGM 2010*, pp. 1–6, July 2010.

[80] L. Mariam, M. Basu, and M. F. Conlon, "Development of a simulation model for a community microgrid system," *in Proc. 49th Int. Univ. Power Eng. Conf. (UPEC)*, pp. 1–6, September 2014.

[81] L. Che, M. Shahidehpour, A. Alabdulwahab, and Y. Al-Turki, "Hierarchical coordination of a community microgrid with AC and DC microgrids," *IEEE Transactions on Smart Grid*, vol. 6, no.6, pp. 3042 – 3051, March 2015.

[82] L. Che and M. Shahidehpour, "DC Microgrids: Economic Operation and Enhancement of Resilience by Hierarchical Control," *IEEE Transactions on Smart Grid*, vol. 5, No. 5, pp. 2517- 2526, September 2014.

[83] S. Mousavizadeha, T. Ghanizadeh Bolandib, M. R. Haghifama, M. Moghimic, and J. Luc, "Resiliency analysis of electric distribution networks: a new approach based on modularity concept," *Electrical Power and Energy Systems*, vol. 117, May 2020.

[84] E. Rosales-Asensio, M. S. Martín, D. Borge-Diez, J.J. Blanes-Peiro, and A. Colmenar-Santos, "Microgrids with energy storage systems as a means to increase power resilience: An application to office buildings," *Energy*, vol. 172, pp.1005-1015, February 2019.

[85] A. Barnes, H. Nagarajan, E. Yamangil, R. Bent, and S. Backhaus, "Resilient design of large-scale distribution feeders with networked microgrids," *Electric Power Systems Research*, vol. 171, pp. 150–157, February 2019.

[86] J. Zhua, Y. Yuana, and W. Wang, "An exact microgrid formation model for load restoration in resilient distribution system," *Electrical Power and Energy Systems*, vol. 116, October 2019.

[87] L. Ren, Y. Qin, Y. Li, P, Zhang, B. Wang, P.B. Luh, S. Han, T. Orekan, and T. Gong, "Enabling resilient distributed power sharing in networked microgrids through software defined networking," *Applied Energy*, vol. 210, pp. 1251–1265, June 2017.

[88] M.U. Shahida, M. Mansoor Khan, K. Hashmi, R. Boudina, A. Khana, J. Yuning, and H. Tang, "Renewable energy source (RES) based islanded DC microgrid with enhanced resilient control," *Electrical Power and Energy Systems*, vol. 113, pp. 461–471, May 2019.

[89] A. Hussain, V.H. Bui, and H.M. Kim "Microgrids as a resilience resource and strategies used by microgrids for enhancing resilience," *Applied Energy*, vol. 240, pp. 56–72, February 2019.

[90] M. S. S. Danish, H. Matayoshi, H.R. Howlader, S. Chakraborty, P. Mandal, and T. Senjyu, "Microgrid planning and design: resilience to sustainability," *in Proc. 2019 IEEE PES GTD Grand International Conference and Exposition Asia (GTD Asia)*, March 2019.

[91] R. Eskandarpour, H. Lotfi, and A. Khodaei, "Optimal microgrid placement for enhancing power system resilience in response to weather events," *in Proc. 2016 North American Power Symposium*, pp. 1-6, November 2016.

[92] M.H. Amirioun, F. Aminifar, and H. Lesani, "Towards proactive scheduling of microgrids against extreme floods," *IEEE Transactions on Smart Grid*, vol. 9, no. 4, pp. 3000-3902, July 2018.

[93] S. Chanda and A.K. Srivastava, "Defining and enabling resiliency of electric distribution systems with multiple microgrids," *IEEE Transactions on Smart Grid*, vol. 7, no. 6, pp. 2859- 2868, November 2016.

[94] Zimmerman, R. D., Murillo-Sánchez, C. E., and Thomas, R. J. "MATPOWER: steady-state operations, planning and analysis tools for power systems research and education," *IEEE Trans. on Power Systems*, vol. 26, no. 1, pp. 12-19, February 2011.

[95] E. Galvan and G. Gutierrez-Alcaraz, "Two-phase short-term scheduling with renewable energy resources and storage," in *Proc. 2013 North American Power Symposium (NAPS),* pp. 1-6, September 2013.

[96] S. Civanlar, J.J. Grainger, and S.H. Lee, "Distribution feeder reconfiguration for loss reduction," *IEEE Transactions on Power Delivery*, vol. 3, no. 3, pp. 1217-1223, July 1988.

[97] D.I. AlHakeem, P. Mandal, A.U. Haque, A. Yona, T. Senjyu, and B. Tseng, "A new strategy to quantify uncertainties of Wavelet-GRNN-PSO based solar PV power forecasts using bootstrap confidence intervals," *in Proc. 2015 IEEE PES GM,* pp. 1-5, July 2015.

[98] A.U. Haque, P. Mandal, J. Meng, A.K. Srivastava, T.L. Tseng, and T. Senjyu, "A novel hybrid approach based on wavelet transform and Fuzzy ARTMAP networks for predicting wind farm power production," *IEEE Transactions on Industry Applications*, vol. 49, no. 5, pp. 2253-2261, September/Octctober 2013.

[99] A.U. Haque, P. Mandal, J. Meng, and R.L. Pineda, "Performance evaluation of different optimization algorithms for power demand forecasting applications in a smart grid environment," *Complex Adaptive Systems, Procedia Computer Science,* vol. 12, pp. 320 – 325, 2012.

[100] M. Pantos, "Exploitation of electric-drive vehicles in electricity markets," *IEEE Transactions on Power Systems,* vol. 27, no. 2, pp. 682 – 694, 2012.

[101] E.F. Camacho and C. Bordons, "*Model Predictive Control*," 2nd ed.; Publisher: Springer-Verlag, London, pp. 1–30, 2007.

[102] E. Galvan, P. Mandal, A.U. Haque, and B. Tseng, "Optimal placement of intermittent renewable energy resources and energy storage system in smart power distribution networks," *Electric Power Components and Systems,* vol. 45, no. 14, pp. 1543-1553, 2017.
[103] E. Galvan, P. Mandal, S. Chakraborty, and A.Y. Saber, "Efficient transactive control for energy storage management system in prosumer-centric networked microgrids," *in Proc. North American Power Symposium (NAPS),* pp. 1 – 6, January 2019.
[104] International Energy Agency (IEA). Global EV outlook: towards cross-modal electrification, *Technical Report*, 2018.
[105] United States Census Bureau. Comparative housing characteristics. Available online: https://factfinder.census.gov/faces/tableservices/jsf/pages/productview.xhtml?pid=ACS_17_5YR_CP04&prodType=table (accessed on 15 January 2019).
[106] M.E. Baran and F.F. Wu, "Network reconfiguration in distribution systems for loss reduction and load balancing," *IEEE Transactions on Power Delivery*, vol. 4, no. 2, pp. 1401-1407, 1989.
[107] El Paso Electric Company. Residential service rate 2018. Available online: https://www.epelectric.com/files/html/Rates_and_Regulatory/Docket_46831_Stamped_Tariffs/03_-_Rate_01_Residential_Service_Rate.pdf. (accessed on 15 January 2019).
[108] El Paso Electric Company. Electric vehicle charging rate 2018. Available online: https://www.epelectric.com/files/html/Rates_and_Regulatory/Docket_46831_Stamped_Tariffs/36_-_Rate_EVC_Electric_Vehicle_Charging_Rate.pdf. (accessed on 15 January 2019).
[109] PJM. Price data. Available online: http://www.pjm.com/markets-and-operations/energy.aspx (accessed on 15 January 2019).
[110] U.S. Department of Energy, Office of Energy Efficiency & Renewable Energy (EERE) Open Data Catalog. Residential load at TMY3. Available online: https://openei.org/datasets/files/961/pub/. (accessed on 15 January 2019).
[111] InsideEVs.com. Available online: https://insideevs.com/reviews/344001/compare-evs/ (accessed on 30 August 2019).
[112] Edison Electric Institute (EEI) https://www.eei.org. Electric vehicle sales: facts & figures Available online: https://www.eei.org/issuesandpolicy/electrictransportation/Documents/FINAL_EV_Sales_Update_April2019.pdf (accessed on 30 August 2019).
[113] Tesla Motors. Tesla charging, 2019. Available online: https://www.tesla.com/models-charging#/basics. (accessed on 30 May 2019).
[114] J. Quiros-Tortos, L.F. Ochoa, and T. Butler, "How electric vehicles and the grid work together: lessons learned from one of the largest electric vehicle trials in the world," *IEEE Power and Energy Magazine,* vol. 16, no. 6, pp. 64-76, 2018.
[115] Idaho National Laboratory, U.S. Department of Energy Office of Energy Efficiency and Renewable Energy. Plug-in electric vehicle and infrastructure analysis, *Technical Report*, 2015.

[116] Tesla Motors. Tesla powerwall, 2019. Available online: https://www.tesla.com/powerwall. (accessed on 15 January 2019).
[117] R.D. Zimmerman, C.E. Murillo-Sánchez, R.J. Thomas, "MATPOWER: steady-state operations, planning and analysis tools for power systems research and education," *IEEE Transactions on Power Systems, vol. 26, no. 1,* pp. 12-19, 2011.
[118] YALMIP. Available online: https://yalmip.github.io/ (accessed on 15 January 2019).
[119] GUROBI. Available online: https://www.gurobi.com/ (accessed on 15 January 2019).
[120] J.P. Watson, R. Guttromson, C. Silva-Monroy, et al., "Conceptual Framework for Developing Resilience Metrics for the Electricity, Oil, and Gas Sectors in the United States," *Technical Report SAND2014-18019*, Sandia National Laboratories, September 2015. Available online: http://energy.gov/sites/prod/files/2015/09/f26/EnergyResilienceReport_Final_SAND2014-18019.pdf
[121] E. Galvan, P. Mandal, S. Chakraborty, and T. Senjyu, "Efficient Energy Management System Using A Hybrid Transactive-Model Predictive Control Mechanism for Prosumer-Centric Networked Microgrids," *Sustainability*, vol. 11, no. 19, September 2019.
[122] L. Lawton, M. Sullivan, K. Van Liere, A. Katz, and J. Eto "A Framework and Review of Customer Outage Costs: Integration and Analysis of Electric Utility Outage Cost Surveys," Lawrence Berkeley National Laboratory, *Technical report*, November 2003.

Appendix I: Data Utilized in Case Studies of Chapter 3

Table AI.1 Actual and Forecasted Wind Power Output.

Hour (h)	Actual Power (MW)	Forecasted Power (MW)	Hour (h)	Actual Power (MW)	Forecasted Power (MW)
1	0.53	0.58	13	3.25	4.01
2	0.68	0.67	14	2.12	3.35
3	1.92	0.82	15	1.36	2.30
4	2.85	2.10	16	1.09	1.52
5	2.08	2.99	17	1.16	1.24
6	2.88	2.26	18	1.55	1.31
7	1.55	3.02	19	1.48	1.71
8	0.63	1.71	20	1.74	1.64
9	0.52	0.76	21	1.99	1.91
10	1.49	0.66	22	1.41	2.17
11	3.38	1.65	23	1.13	1.57
12	4.00	3.46	24	0.55	1.28

Table AI.2 Actual and Forecasted Load.

Hour (h)	Actual Power (MW)	Forecasted Power (MW)	Hour (h)	Actual Power (MW)	Forecasted Power (MW)
1	24.62	27.15	13	13.46	9.50
2	24.03	22.37	14	15.54	17.19
3	15.85	23.81	15	16.43	16.03
4	15.90	16.30	16	19.63	16.82
5	27.42	30.34	17	20.23	19.72
6	24.80	22.02	18	17.16	20.27
7	18.73	20.54	19	10.53	11.47
8	23.02	21.90	20	10.94	11.68
9	18.64	20.87	21	12.58	15.03
10	13.18	12.82	22	10.25	13.43
11	11.42	15.95	23	25.33	14.45
12	9.88	12.76	24	6.99	10.05

Table AI.3 Actual and Forecasted PV Power – Sunny Day.

Hour (h)	Actual Power (MW)	Forecasted Power (MW)	Hour (h)	Actual Power (MW)	Forecasted Power (MW)
1	0.00	0.00	13	2.23	2.24
2	0.00	0.00	14	2.24	2.26
3	0.00	0.00	15	2.14	2.12
4	0.00	0.00	16	1.90	1.91
5	0.00	0.00	17	1.29	1.31
6	0.00	0.00	18	0.45	0.49
7	0.00	0.00	19	0.15	0.18
8	0.22	0.22	20	0.02	0.02
9	0.80	0.82	21	0.00	0.00
10	1.34	1.40	22	0.00	0.00
11	1.78	1.83	23	0.00	0.00
12	2.08	2.11	24	0.00	0.00

Table AI.4 Actual and Forecasted PV Power – Cloudy Day.

Hour (h)	Actual Power (MW)	Forecasted Power (MW)	Hour (h)	Actual Power (MW)	Forecasted Power (MW)
1	0.00	0.00	13	1.54	1.47
2	0.00	0.00	14	1.41	1.20
3	0.00	0.00	15	0.67	1.60
4	0.00	0.00	16	0.50	0.58
5	0.00	0.00	17	0.28	0.54
6	0.00	0.00	18	0.10	0.05
7	0.00	0.00	19	0.00	0.05
8	0.00	0.00	20	0.00	0.00
9	0.01	0.01	21	0.00	0.00
10	0.32	0.58	22	0.00	0.00
11	0.80	0.89	23	0.00	0.00
12	1.38	1.47	24	0.00	0.00

Table AI.5 Actual and Forecasted PV Power – Rainy Day.

Hour (h)	Actual Power (MW)	Forecasted Power (MW)	Hour (h)	Actual Power (MW)	Forecasted Power (MW)
1	0.00	0.00	13	1.17	1.22
2	0.00	0.00	14	1.03	1.33
3	0.00	0.00	15	0.63	0.61
4	0.00	0.00	16	0.36	0.35
5	0.00	0.00	17	0.20	0.46
6	0.00	0.00	18	0.02	0.00
7	0.00	0.00	19	0.00	0.02
8	0.00	0.02	20	0.00	0.01
9	0.26	0.06	21	0.00	0.00
10	0.72	1.09	22	0.00	0.00
11	0.58	1.15	23	0.00	0.00
12	1.01	0.34	24	0.00	0.00

Appendix II: Data Utilized in Case Studies of Chapter 4

Table AII.1 Historical BEV Daily Driving Patterns.

BEV Driving Patterns (kWh)							
Hour (h)	BEV1	BEV2	BEV3	Hour (h)	BEV1	BEV2	BEV3
1	0.0	0.0	0.0	13	1.6	0.0	0.0
2	0.0	0.0	0.0	14	0.0	0.0	0.0
3	0.0	0.0	0.0	15	0.0	0.0	2.7
4	0.0	0.0	0.0	16	2.7	1.3	2.7
5	0.0	0.0	0.0	17	4.8	1.6	0.0
6	2.7	1.3	2.7	18	3.2	1.6	0.0
7	3.8	1.9	2.7	19	0.0	0.0	0.0
8	4.8	2.4	0.0	20	2.7	0.0	2.7
9	0.0	1.3	0.0	21	3.0	0.0	2.7
10	0.0	0.0	4.0	22	0.0	0.0	0.0
11	0.0	0.0	5.4	23	0.0	0.0	0.0
12	1.6	0.0	0.0	24	0.0	0.0	0.0

Table AII.2 Load Data for the 33-Bus Distribution System.

Bus	Pd (kW)	Qd (kVAR)	Bus	Pd (kW)	Qd (kVAR)
2	97	60	18	64	40
3	80	40	19	24	40
4	117	80	20	19	40
5	43	30	21	29	40
6	58	20	22	21	40
7	71	100	23	24	50
8	97	100	24	29	200
9	49	20	25	27	200
10	48	20	26	58	25
11	35	30	27	58	25
12	44	35	28	58	20
13	58	35	29	85	70
14	117	80	30	195	600
15	43	10	31	145	70
16	58	20	32	204	100
17	58	20	33	58	40

Table AII.3 Load Data for Klamath Falls, Oregon.

Hour (h)	Power (kW)	Hour (h)	Power (kW)
1	1.35	13	1.29
2	1.18	14	1.23
3	1.12	15	1.22
4	1.11	16	1.37
5	1.11	17	1.91
6	1.19	18	2.74
7	1.47	19	3.19
8	1.91	20	3.00
9	1.80	21	2.87
10	1.50	22	2.67
11	1.42	23	2.18
12	1.37	24	1.76

Table AII.4 Load Data for Medford-Rogue Valley, Oregon.

Hour (h)	Power (kW)	Hour (h)	Power (kW)
1	1.07	13	1.30
2	0.94	14	1.27
3	0.87	15	1.28
4	0.86	16	1.41
5	0.87	17	1.79
6	0.95	18	2.45
7	1.21	19	2.79
8	1.64	20	2.60
9	1.55	21	2.48
10	1.35	22	2.27
11	1.33	23	1.87
12	1.33	24	1.49

Table AII.5 Load Data for Redmond, Oregon.

Hour (h)	Power (kW)	Hour (h)	Power (kW)
1	1.12	13	1.34
2	0.96	14	1.31
3	0.89	15	1.32
4	0.88	16	1.44
5	0.89	17	1.83
6	0.96	18	2.50
7	1.21	19	2.83
8	1.64	20	2.63
9	1.58	21	2.51
10	1.39	22	2.29
11	1.37	23	1.89
12	1.36	24	1.52

Table AII.6 Solar PV Power for Ashland, Oregon Sunny-Day.

Hour (h)	Power (kW)	Hour (h)	Power (kW)
1	0.00	13	4.63
2	0.00	14	4.45
3	0.00	15	3.92
4	0.00	16	2.72
5	0.00	17	1.15
6	0.02	18	0.46
7	0.72	19	0.06
8	1.94	20	0.00
9	2.97	21	0.00
10	3.80	22	0.00
11	4.38	23	0.00
12	4.62	24	0.00

Appendix III: Data Utilized in Case Studies of Chapter 5

Table AIII.1 Solar PV Power for Ashland, Oregon Rainy-Day.

Hour (h)	Power (kW)	Hour (h)	Power (kW)
1	0.00	13	2.31
2	0.00	14	2.04
3	0.00	15	1.25
4	0.00	16	0.70
5	0.00	17	0.40
6	0.00	18	0.04
7	0.00	19	0.00
8	0.00	20	0.00
9	0.51	21	0.00
10	1.42	22	0.00
11	1.14	23	0.00
12	1.99	24	0.00

Appendix IV: List of Publications

List of publications that were generated during my Ph.D. studies at UTEP.

Peer-reviewed Journal Papers

*: my Ph.D. advisor and corresponding author of the paper

1. **E. Galvan**, P. Mandal*, S. Chakraborty, and T. Senjyu, "Efficient Energy Management System Using A Hybrid Transactive-Model Predictive Control Mechanism for Prosumer-Centric Networked Microgrids," *Sustainability*, Vol. 11, No. 19, Sep. 2019.
2. **E. Galvan**, P. Mandal*, A. U. Haque, and B. Tseng, "Optimal Placement of Intermittent Renewable Energy Resources and Energy Storage System in Smart Power Distribution Networks," *Electric Power Components and Systems*, Vol. 45, No. 14, pp. 1543-1553, Dec. 2017.

Peer-reviewed Manuscript Under Review

3. **E. Galvan**, P. Mandal*, and Y. Sang, "Resiliency Analysis of Networked Microgrids in Power Distribution Systems," *International Journal of Electrical Power & Energy Systems (Submitted in December 2019)*

Peer-reviewed Conference Papers

1. **E. Galvan**, P. Mandal*, S. Chakraborty, and A. Y. Saber, "Efficient Transactive Control for Energy Storage Management System in Prosumer-Centric Networked Microgrids," in *Proc. North American Power Symposium (NAPS 2018)*, Sep. 2018.
2. **E. Galvan,** P. Mandal*, M. Velez-Reyes, and S. Kamalasadan, "Transactive Control Mechanism for Efficient Management of EVs Charging in Transactive Energy Environment," in *Proc. North American Power Symposium (NAPS 2016)*, Sep. 2016.
3. **E. Galvan,** P. Mandal*, T. L. Tseng, and M. Velez-Reyes, **"**Energy Storage Dispatch Using Adaptive Control Scheme Considering Wind-PV in Smart Distribution Network," in *Proc. North American Power Symposium (NAPS 2015)*, Oct. 2015.

Symposium Papers

4. **E. Galvan** and P. Mandal*, “Transactive Control for Energy Storage Dispatch in Microgrids,” in *Proc. Southwest Emerging Technology Symposium,* Apr. 2018.
5. **E. Galvan** and P. Mandal*, “Smart Microgrid Energy Management System and Control,” *UTEP Graduate Student Research Expo,* Nov. 2017.
6. **E. Galvan** and P. Mandal*, “Transactive Energy Systems,” in *Proc. Southwest Emerging Technology Symposium,* Apr. 2016.
7. **E. Galvan** and P. Mandal*, “Optimal Placement of Intermittent Renewable Energy Resources and Energy Storage Systems in Smart Power Distribution Network,” *UTEP Graduate Student Research Expo,* Nov. 2015.
8. **E. Galvan** and P. Mandal*, “Optimal Operation Strategy for Grid Connected WIND/PV and Energy Storage System,” in *Proc. Southwest Energy Science and Engineering Symposium,* Apr. 2015.

Vita

Eric Galvan was born in Kansas City, Kansas, USA. He received his Bachelor of Science and Master of Science degrees in Electrical Engineering from the Instituto Tecnológico de Morelia, Morelia, Michoacán, Mexico in 2010 and 2013, respectively. In January 2015, he joined the Department of Electrical and Computer Engineering (ECE) at the University of Texas at El Paso (UTEP) to pursue Doctor of Philosophy in Electrical and Computer Engineering (Ph.D. in ECE). His doctoral research career started in January 2015 when he joined the Power and Renewable Energy Systems (PRES) Lab within the ECE Department and started his doctoral research under the direct supervision of PRES Lab's director Dr. Paras Mandal who guided and mentored him throughout his dissertation period in the area of Smart Power Distribution Systems. During his doctoral studies, he was a recipient of (i) Kenneth R. Heitz/El Paso Electric Company Endowed Scholarship, (ii) Fellowship of the Hispanic Alliance for the Professoriate in Environmental Sciences and Engineering, and (iii) UTEP Graduate Student Travel Award (which he received three times in order to present his research findings at IEEE conferences). He has presented his research findings at several meetings, symposiums, and international conferences. His work has appeared in the proceedings of these conferences as well as in peer-reviewed journals. A list of publications that he generated from his Ph.D. period is provided in Appendix IV. While pursuing his Ph.D. degree at UTEP, he worked as a Teaching Assistant for the ECE department and also as an Assistant Instructor for the College of Engineering. In Summer 2019, he obtained a full-time position at the El Paso Electric Company in El Paso, Texas where he is currently working as a researcher at the Economic Research Department.

Contact Information: egalvan4@miners.utep.edu

This dissertation was typed by Eric Galvan.